

Theoretical examinations of interface mediated interactions between colloidal particles

**Diplomarbeit
von
Martin Michael Müller**

angefertigt am Max-Planck-Institut
für Polymerforschung, Mainz

vorgelegt dem Fachbereich Physik der
Johannes Gutenberg-Universität, Mainz

Dezember 2004

1. Gutachter: Prof. Dr. Kurt Kremer
Max-Planck-Institut für Polymerforschung, Mainz

2. Gutachter: Prof. Dr. Rolf Schilling
Johannes Gutenberg-Universität, Mainz

Für meine Familie

Zusammenfassung:

Weiche Grenzflächen können Wechselwirkungen zwischen Teilchen vermitteln, die an sie gebunden sind. Dies geschieht beispielsweise mit Proteinen in einer Lipidmembran. Der traditionelle Ansatz zur Bestimmung der auftretenden Kräfte ist folgender: Die Gesamtenergie des Teilchen-Grenzfläche-Systems wird als Funktion der Teilchenpositionen berechnet. Kräfte zwischen den gebundenen Teilchen ergeben sich dann durch geeignete Ableitungen. Leider zwingt einen die inhärente Nichtlinearität dieses Problems fast immer, sich auf lineare Näherungen der Energetik zu beschränken.

Es ist jedoch stattdessen auch möglich, einen anderen, kovarianten Ansatz zu wählen, der Ergebnisse liefert, die auch im nichtlinearen Regime gültig sind: Die Kräfte zwischen den Teilchen werden durch die Grenzfläche vermittelt und sind daher in ihrer Geometrie kodiert. In Analogie zur klassischen Elastizitätstheorie lassen sie sich durch Integrale über den Oberflächenspannungstensor ausdrücken. Dieser wiederum hängt auf bekannte Weise von der Energiedichte der Grenzfläche ab. Für den Fall einer symmetrischen Zweiteilchen-Konfiguration liefert dieser Ansatz exakte analytische Formeln für die Kraft in Abhängigkeit von der Geometrie an der Mittelebene. Manchmal ergibt sich daraus bereits das Vorzeichen der Kraft, d.h. ob Anziehung oder Abstoßung auftritt, kann auch für starke Oberflächenverformungen vorausgesagt werden.

Abstract:

Soft interfaces can mediate interactions between particles bound to them. One example is the interaction of protein inclusions in a lipid membrane. Traditionally, this phenomenon is treated by calculating the total energy of the particle-interface system as a function of particle positions. The forces between the bound particles can then be obtained via appropriate derivatives. Unfortunately, the intrinsic nonlinearity of the problem generally forces one to restrict to linear approximations of the energetics.

It is, however, possible to choose a different, covariant approach and gain some results that are also valid in the nonlinear regime: the forces between the particles are mediated through the interface and are thus encoded in its geometry. In analogy to classical elasticity theory one can write them as integrals over the surface stress tensor, which itself depends in a transparent way on the interfacial energy density. For standard symmetric two-particle situations this approach yields exact formulas for the force in terms of the midplane geometry. Sometimes the sign of the force is evident, *i. e.* the occurrence of attraction or repulsion can be predicted even for large interface deformations.

Contents

| | |
|---|-----------|
| Introduction | 1 |
| 1 The energetics of interfaces | 3 |
| 1.1 Surface tension | 4 |
| 1.1.1 The origin of surface tension | 4 |
| 1.1.2 Soap and soap-like molecules | 6 |
| 1.2 Bending | 10 |
| 1.2.1 Curvature energy | 10 |
| 1.2.2 Self-assembly of amphiphiles | 11 |
| 1.2.3 Membranes in cell biology | 13 |
| 1.3 Other interfaces | 16 |
| 2 Stresses in interfaces | 17 |
| 2.1 The stress tensor in three-dimensional elasticity theory and its analog for surfaces | 17 |
| 2.2 Derivation of the surface stress tensor | 19 |
| 2.2.1 Approach 1: Variation in the embedding functions | 19 |
| 2.2.2 Approach 2: Using auxiliary variables | 24 |
| 2.3 The surface stress tensor of special interfaces | 27 |
| 3 One colloidal particle at an interface | 31 |
| 3.1 The three-phase boundary solid/liquid/gas | 31 |
| 3.1.1 The Young-Dupré equation | 31 |
| 3.1.2 Force balance for a colloidal particle floating on a liquid | 34 |
| 3.1.3 Pinning of the contact line | 38 |
| 3.2 Colloidal particle bound to a fluid membrane | 39 |
| 3.2.1 Adhesion | 39 |
| 3.2.2 Membrane inclusions | 42 |
| 4 Forces between interface-bound particles | 45 |
| 4.1 Interface mediated interactions | 45 |
| 4.2 Forces via the energy | 47 |
| 4.3 Example: Two quadrupoles on a soap film | 49 |

| | | |
|----------|--|-----------|
| 5 | Forces via the stress tensor | 51 |
| 5.1 | General approach | 51 |
| 5.2 | Explicit force formulas | 53 |
| 6 | Comparison between the approaches | 57 |
| 6.1 | Soap film type | 57 |
| 6.2 | Fluid Membrane type | 60 |
| 6.2.1 | Adhering cylinders | 61 |
| 6.2.2 | Discoidal inclusions | 63 |
| 7 | Conclusions | 67 |
| A | Conventions and used symbols | 69 |
| B | Classical differential geometry of two-dimensional surfaces | 75 |
| B.1 | Basic definitions | 75 |
| B.2 | Gauss-Bonnet theorem | 82 |
| B.3 | Monge parametrization | 84 |
| C | Surface variations | 87 |
| | List of Tables | 91 |
| | List of Figures | 93 |
| | Acknowledgements | 95 |
| | Bibliography | 97 |

Introduction

Forces between particles that are bound to an interface can be either of *direct* or *indirect* origin. The former are, for instance, electrostatic or Van der Waals' interactions; the latter are mediated by the interface and caused by the deformations the particles induce in its shape.

One example of such an *interface mediated interaction* can easily be given in a little experiment: take two sewing needles and a bowl filled with water. Let the needles slide carefully onto the water surface and you will see that they attract as soon as the deformations of the surface start to overlap (see Fig. 1).¹

Apart from this, interface mediated interactions play an important and more serious role in technological processes such as ore flotation or foam stabilization [RSS89, NS03]. Other research has been dedicated to the possibilities of such forces to induce the self-assembly of small-scale structures: one of the hopes at present is, for instance, to find easy ways of manufacturing components of micro-electromechanical systems [VM04].

Interface mediated forces are also relevant for biological systems: cell membranes carry a large variety of molecular devices such as membrane proteins. It was discovered that these proteins can form domains [SI97]. Equivalent observations have also been made in studies with artificial fluid membranes [KIH98]. One possible explanation for the experimental findings are membrane mediated interactions.

Unfortunately, theoretical considerations of such interactions are mathematically rather involved due to the fact that the relevant field equations are typically nonlinear differential equations. Present calculations therefore mostly yield approximative results for the forces.

In this thesis, a new geometrical ansatz is introduced that avoids to solve the field equations explicitly. It is thus clear that this approach, which does not intend to determine the exact shape of the interface for a given particle attachment, will also not provide numerical values for the force without further work. However, exact analytical results for the force in terms of the geometric interface properties can be obtained, which are valid in the nonlinear regime. In some cases they enable one to predict the sign of the interaction [MDG04].

¹ One of course has to make sure that the needles are neither magnetized nor electrically charged if one really wants to observe *interface mediated interactions*.

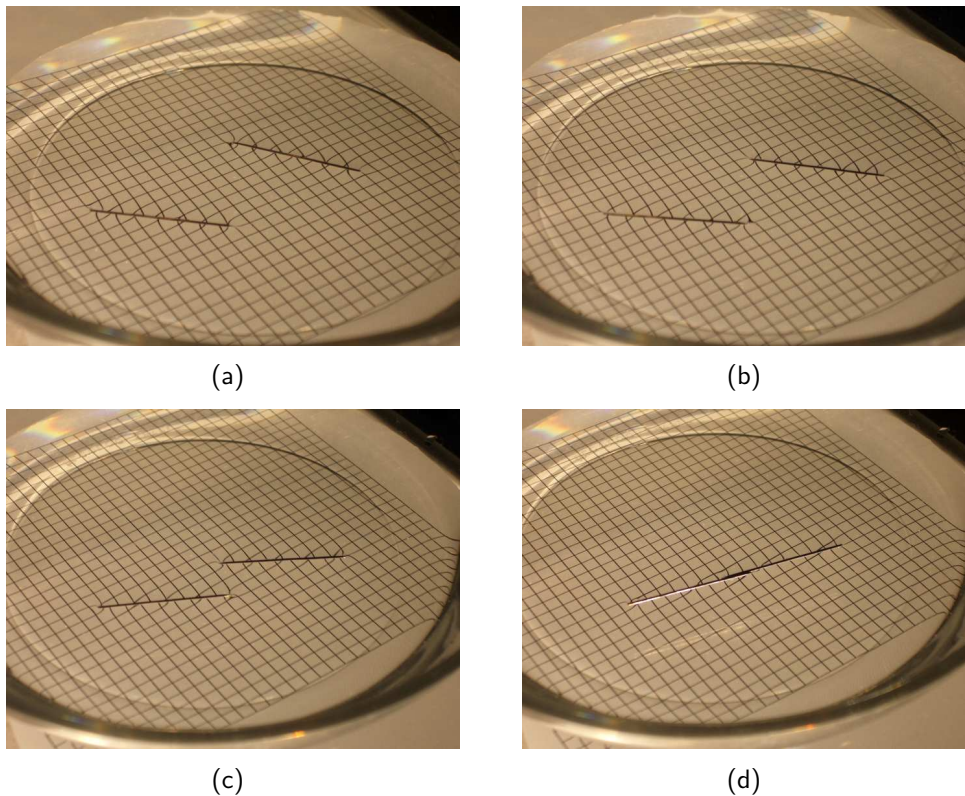


Figure 1: Attraction of two sewing needles floating on water as one example of interface mediated interactions (see also [GS71]). The whole process proceeds on a timescale of a few seconds, becoming increasingly faster from (a) to (d).

For that final purpose this thesis starts with the introduction of different interface energetics in the first chapter. We will only discuss interfaces in their ground state. Thermal fluctuations around that state or dynamical phenomena will not be taken into account.

The second chapter provides a mathematical approach to stresses in interfaces, showing how forces, that are transmitted through the interface, can be obtained via a line integral over the surface stress tensor. This fact is the key to the new approach. Before introducing it, however, we will discuss how one traditionally determines the shape and the energy of the interface when either one or two particles are bound to it and how thereby interface mediated forces can be obtained (see Chaps. 3 and 4). Chapter 5 presents the key results of this thesis where the stress tensor is exploited in order to find nontrivial exact results for interface mediated interactions. Finally, it is demonstrated in Chap. 6 that the two approaches are in fact consistent. With this general outline in mind, let us now start to discuss free interfaces.

1 The energetics of interfaces

Two phases that do not mix with each other are physically separated by an interface or surface. Such a system can, for example, consist of a liquid and its vapor phase or a membrane between two domains of water.

In this thesis, the dividing boundary layer will be called an *interface* if reference is made to the physical quantity; however, the mathematical concept will be referred to as a *surface*.¹

An interface is usually not a sharp discontinuity between two phases but a continuous transition on molecular length scales (see for instance [BM93, p. 2 et seq.]). It is nevertheless possible to consider it to be two-dimensional as long as one is interested in a *mesoscopic* point of view. This is applicable when the lateral extension of the interface (and the size of all other objects and deformations of interest) is much larger than its width. The interface can then be treated as a two-dimensional surface embedded in three-dimensional Euclidean space \mathbb{R}^3 which is described locally by its position $\mathbf{X}(\xi^1, \xi^2) \in \mathbb{R}^3$, where the ξ^a are a suitable set of local coordinates. The surface is not flat in general and therefore requires for its characterization tools from differential geometry. The underlying basics of that approach are summarized in App. B.1.

The creation of an interface costs free energy because molecules have to be removed from their bulk environment and brought to the boundary between the two phases. This energy (per area) is called *surface tension* σ . In Sec. 1.1 we will focus on interfaces that can be completely described energetically by a Hamiltonian including surface tension only.

More general Hamiltonians may also contain terms that penalize other features of the surface. Section 1.2 will deal with *bending* as the dominant part in the energetics. Further possible characteristics of interfaces will be briefly discussed in Sec. 1.3. In the present work, the focus will generally be on interfaces whose energetics can be described by a Hamiltonian which is a surface integral over a local Hamiltonian density \mathcal{H} . This density shall depend only on scalars constructed from local sur-

¹ Other authors do not distinguish between surfaces and interfaces or use different definitions, such as Ref. [Saf94, p. 2 et seq.]: If the system consists of a “semi-infinite, bulk system or vacuum (or its own dilute, vapor phase) ... [the separating boundary layer] is generally referred to as a surface. When this semi-infinite material coexists with another condensed phase, the separating surface is referred to as an interface. An interface can be composed of a material that is different from the two bulk phases.”

face tensors², such as the metric g_{ab} , the extrinsic curvature K_{ab} , or its covariant derivatives $\nabla_a K_{bc}$, etc.:

$$H_\Sigma[\mathbf{X}] = \int_\Sigma dA \mathcal{H}(g_{ab}, K_{ab}, \nabla_a K_{bc}, \dots) \quad , \quad a, b \in \{1, 2\} \quad , \quad (1.1)$$

where dA is the infinitesimal area element and Σ the potentially curved surface domain one is interested in. Note also that Hamiltonian (1.1) shall be invariant under surface reparametrization. This means that no energy penalty is associated with shearing deformations of the interface [CG02b].

This rather general definition will be illustrated in the following by the two cases of surface tension and bending energy.

1.1 Surface tension

1.1.1 The origin of surface tension

Consider a system consisting of water and its vapor: under zero gravity the water minimizes its area in equilibrium and thus forms a perfect sphere. An explanation of this circumstance can be found if one considers the energetics of the system [Isr92]: molecules at the interface are in a state of higher energy than those in the bulk. This is due to the fact that the former particles are missing bonds compared to the latter (see Fig. 1.1). A positive (free) energy per area, σ , can therefore be associated with the interface. It is minimal if the interfacial area is minimized, which leads to the explained behaviour of the water.³

It is possible to interpret σ as a tension: consider a rectangular patch of surface with length l and width w at constant temperature (see Fig. 1.2). One may increase its

² The definition of these tensors can be found in App. B.1.

³ Note that this is a rather phenomenological explanation of the surface energy. A sounder derivation can be done by considering the statistical mechanics of the system (see for instance [RW02]).

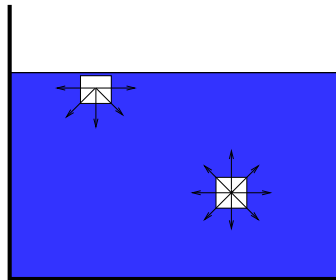


Figure 1.1: Energetics of interfaces: bond number of a molecule in the bulk compared to one at the interface (schematic)

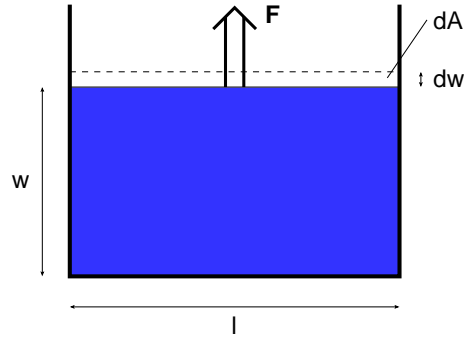


Figure 1.2: Interpretation of the interfacial energy as a surface tension

area by dA by applying a force F to one side of the patch. The free energy input into the system is equal to the force times displacement:⁴

$$dE = Fdw = \sigma dA = \sigma ldw . \quad (1.2)$$

The interface is thus under a tension $\sigma = \frac{F}{l}$, which is the so called *interfacial* or *surface tension*. It is tangential to the interface, even for interfaces that are not flat as we will see in the following chapters. The higher it is, the higher the force that is acting on a line per unit length. For water its value is about 73 mN m^{-1} at room temperature ($T = 293 \text{ K}$). The water-vapor system is not the only example where surface tension plays a dominant role. Other liquid-fluid⁵ interfaces also exhibit a nonvanishing surface tension (for some values see Table 1.1).⁶

To obtain the total energy of a liquid-fluid interface in general one has to integrate σ over the whole surface. The resulting Hamiltonian is therefore:

$$H = \int_{\Sigma} dA \sigma , \quad (1.3)$$

where Σ is the surface domain. If one wants to find out what a stable surface for given boundary conditions looks like, one has to search for local minima of the Hamiltonian (1.3) by setting the variation $\delta H = 0$. This leads to a minimization of surface area (see above). Interfaces that are dominated by surface tension only and are not subject to further constraints (see Sec. 1.1.2) are therefore called *minimum area surfaces* or simply *minimal surfaces*.

⁴ We only will consider interfaces in their ground states, which is why we do not worry about entropic contributions to the free energy (for a general discussion, see again Ref. [RW02]).

⁵ A fluid can either be a liquid or a vapor/gas.

⁶ Note that the symbol σ will be used for the surface tension of a liquid-fluid interface in general.

Table 1.1: Surface tension for selected substances at room temperature ($T = 293$ K)
a) against air [BM93, p. 8] b) against water [Isr92, p. 315]

| (a) | | (b) | |
|------------------|-----------------------------|------------------|-----------------------------|
| <i>substance</i> | $\sigma / \text{mN m}^{-1}$ | <i>substance</i> | $\sigma / \text{mN m}^{-1}$ |
| heptane | 20 | cyclohexanol | 4 |
| ethanol | 22 | chloroform | 28 |
| formamide | 57 | benzene | 35 |
| water | 73 | cyclohexan | 51 |
| Hg | 486 | octane | 51 |

1.1.2 Soap and soap-like molecules

Not only interfaces between pure phases (such as water and water vapor) but also solutions are subject to surface forces and surface tension. Prominent examples, especially for the demonstration of minimum area surfaces, are soap solutions and soap films (see Fig. 1.3).

A soap solution can be produced by dissolving a metal salt of a fatty acid with a long hydrocarbon tail in water [Ise92, p. 21]. In natural soaps the metal is either sodium or potassium; it is dispersed throughout the water. The fatty acid anion may be laurate, myristate, oleate, etc. (see upper part of Table 1.2 for more examples and chemical structures).

Fatty acid anions are *amphiphiles*. This means that they consist of two different parts: the negatively charged carboxyl group is *hydrophilic*, *i. e.* “water-loving”, whereas the neutral hydrocarbon chain is *hydrophobic*, *i. e.* “water-hating”. The hydrophobic part of the molecule disturbs the hydrogen bonds that exist between the water molecules close to it. These can only be maintained if the water sacrifices a part of its entropy. This phenomenon is called the *hydrophobic effect* (or Tanford effect) and is the main reason why the hydrocarbon chains try to avoid water [GKD⁺04, A3.13]. The hydrophilic carboxyl groups, however, can form hydrogen bonds with the water and therefore try to stay in it.

This leads to the formation of a monomolecular layer of the anions at the interface: the hydrocarbon chains are directed out of the interface, whereas the carboxyl groups are adsorbed into the interface surrounded by water molecules and positive metal ions. The bulk water also contains some additional amphiphiles depending on the concentration of the soap solution (see Fig. 1.4(a)).

The surface ions are also called *surfactants*. It is possible to synthesize artificial surfactants, which can be classified due to their charge as anionic, cationic, nonionic

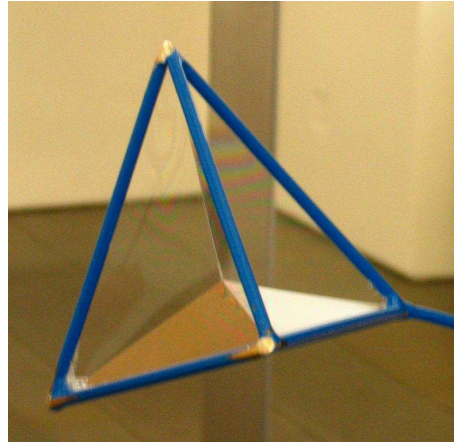


Figure 1.3: The soap film: a minimum area surface (photographed at “Mathematicum Gießen”)

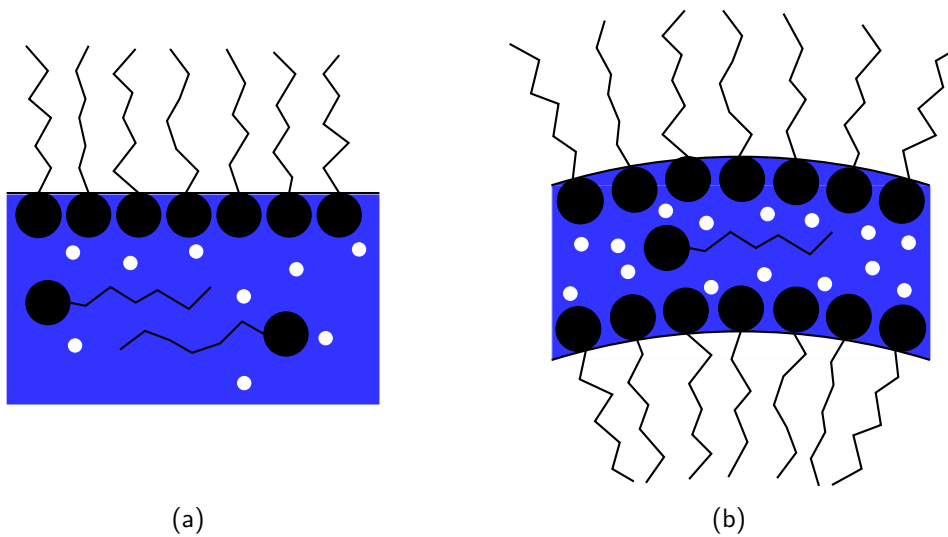


Figure 1.4: Structure of a) a soap solution b) a soap film
The black particles are the fatty acid anions and the white particles are the positive metal counterions.

| <i>substance</i> | <i>chemical structure</i> | <i>type</i> |
|---|--|---|
| laurate myristate palmitate stearate | $\text{CH}_3-(\text{CH}_2)_{10}-\text{COO}^-$ $\text{CH}_3-(\text{CH}_2)_{12}-\text{COO}^-$ $\text{CH}_3-(\text{CH}_2)_{14}-\text{COO}^-$ $\text{CH}_3-(\text{CH}_2)_{16}-\text{COO}^-$ | fatty acid anions (natural soap molecules) |
| oleate | $\text{CH}_3-(\text{CH}_2)_7-\text{CH}=\text{CH}-(\text{CH}_2)_7-\text{COO}^-$ | |
| cetyl (hexadecyl) sulfate | $\text{CH}_3-(\text{CH}_2)_{15}-\text{O}-\text{SO}_3^-$ | anionic surfactant |
| cetyl trimethyl ammonium | $\text{CH}_3-(\text{CH}_2)_{14}-\text{CH}_2-\overset{\text{CH}_3}{\underset{\text{CH}_3}{\text{N}^+}}-\text{CH}_3$ | cationic |
| pentaoxyethylene dodecyl ether | $\text{CH}_3-(\text{CH}_2)_{10}-\text{CH}_2-\text{O}-(\text{CH}_2-\text{CH}_2-\text{O})_5-\text{H}$ | neutral |
| cetyl dimethyl glycine | $\text{CH}_3-(\text{CH}_2)_{14}-\text{CH}_2-\overset{\text{CH}_3}{\underset{\text{CH}_3}{\text{N}^+}}-\text{CH}_2-\text{COO}^-$ | zwitterionic |

Table 1.2: Examples of surfactants ([GKD⁺04, A3.8]), [Isr92, p. 342 et seq.]. The fatty acid anions can be further divided into saturated (laurate, etc.) and unsaturated (oleate) ions.

and zwitterionic. The last category has both positively and negatively charged groups. Some examples can be found in Table 1.2.

The length of one surfactant molecule is on the order of a few nanometers. It occupies an area of roughly 0.5 nm^2 at the interface [Ise92, p. 18]. Increasing the concentration of surfactant molecules at the interface lowers the resulting surface tension until saturation is reached (about $25 - 35 \text{ mN m}^{-1}$ for a soap solution [GKD⁺04, A3.13]). If the concentration of surfactants is further increased, new physical phenomena occur, that will be discussed in the next section.

Solutions of surfactants may be utilized to form films: a soap film, for example, consists of a thin layer of water in-between two monolayers composed of soap ions (see Fig. 1.4(b)). It is 5 nm to $20 \text{ }\mu\text{m}$ thick [Ise92, p. 7] and has a surface tension which is twice the value of a soap solution, since it has *two* sides.



Figure 1.5: The soap bubble: a constant mean curvature surface

A soap film is stable against rupture because of a stabilizing effect which is also called *Marangoni effect*: as soon as one patch of the film stretches, the concentration of soap ions decreases at that part, which leads to an increase in surface tension. In contrast, an increasing concentration of soap ions leads to a decrease in surface tension. This negative feedback is the reason why the film is relatively stable. In addition, the surfactant ions hinder the diffusion of water molecules into the surroundings, which stabilizes the film further.⁷

A closed soap film is also called soap bubble (see Fig. 1.5). Its surface is curved, which causes a pressure difference between the interior and the exterior: evidently the surface tension tries to decrease the bubble's size, which leads to a compression of the inner compartment. A stable soap bubble must therefore have a higher pressure p_i inside compared to the pressure p_e outside. This results in a further contribution to the energy, which can be included into the Hamiltonian (1.3) via the term $-PV$:

$$H = \int_{\partial V} dA \sigma - PV, \quad (1.4)$$

where $P = p_i - p_e$ is the excess pressure and ∂V the area of the interface enclosing the volume V .

For a spherical bubble with radius a and constant surface tension Hamiltonian (1.4) turns into:

$$H_{\text{sphere}} = 4\pi a^2 \sigma - P_{\text{sphere}} \frac{4\pi}{3} a^3. \quad (1.5)$$

A local minimum can be found by setting the derivative of H_{sphere} with respect to a to zero:

$$\frac{dH_{\text{sphere}}}{da} = 8\pi\sigma a - 4\pi P_{\text{sphere}} a^2 \stackrel{!}{=} 0, \quad (1.6)$$

⁷ This dynamical effect will not be studied further here. It is only mentioned in order to explain why one can deal with stable soap films.

which yields the well-known expression for the *Laplace pressure* of a spherical bubble

$$P_{\text{sphere}} = \frac{2\sigma}{a} . \quad (1.7)$$

To find the equilibrium state for all surfaces whose energetics are described by Hamiltonian (1.4), one has to set the first variation of (1.4) to zero. This leads to the general *formula of Laplace* (see App. C, Eqn. (C.23))

$$P = \sigma K , \quad (1.8)$$

where K is the total curvature (see App. B.1). Surfaces that can be defined via $K = \text{const}$ as in Eqn. (1.8) are also called *constant mean curvature surfaces*. Apart from the sphere many other examples of such a surface can be found (for instance the nodoid, see [LFL01]).

A volume term similar to the one in Eqn. (1.4) may also be used to *fix the volume* of a closed surface to a constant value V_0 :

$$H = \int_{\partial V} dA \sigma - P(V - V_0) , \quad (1.9)$$

where P acts as a Lagrange multiplier.

This section gave a short overview of different interfaces that have one thing in common: their energetics can be described by a Hamiltonian which is a surface integral over the surface tension σ —including or excluding further constraints such as constant volume. This type of interface will be called “soap film type” in the following.

In the next two sections other possible contributions to the energy will be discussed.

1.2 Bending

1.2.1 Curvature energy

Other contributions to the total energy of an interface apart from surface tension are bending deformations in the direction normal to the interface. In a harmonic expansion the energy due to any deformation of the interface is proportional to the square of the deformation (cf. Hooke’s law). In the particular case of *bending* one has to consider quadratic expressions of the *curvature*: a surface has two principal curvatures k_1 and k_2 at every point, which are the eigenvalues of the local curvature tensor K_{ab} . The corresponding eigenvectors define two orthogonal principal directions (see App. B.1). It is therefore necessary to include *two independent terms* in the expression for the energy that depend on a quadratic combination of the two curvatures and are furthermore invariant scalars: one possible choice is a linear combination of the squares of the principal curvatures, k_1^2 and k_2^2 [Can70]. If we,

however, consider an *isotropic* interface, the two constants of that linear combination have to be identical. Thus, the two terms are not independent any more.

A better choice is therefore a combination of $I_1 = (k_1 + k_2)^2$ and $I_2 = (k_1^2 + k_2^2)$ [LL86]. The first invariant is equal to the square of the total curvature, $I_1 = K^2$ (see App. B.1). Instead of I_2 it is, however, technically smarter to choose $\frac{1}{2}(I_1 - I_2)$ as the second invariant because this combination is equal to the Gaussian curvature $K_G = k_1 k_2$, for which many mathematical relations are known. Including surface tension the complete Hamiltonian is then according to Helfrich [Hel73]:

$$H = \int_{\Sigma} dA \left[\sigma + \frac{\kappa}{2}(K - K_0)^2 + \bar{\kappa} K_G \right], \quad (1.10)$$

where the proportionality coefficients κ and $\bar{\kappa}$ are called the *bending rigidity* and the Gaussian bending rigidity or *saddle-splay modulus*, respectively. The additional constant K_0 is the spontaneous curvature. If its value is not equal to zero, the surface prefers to be bent to a certain extent in its minimal energy state. Note that the Gaussian curvature part is a topological constant due to the Gauss-Bonnet theorem (see App. B.2) and can therefore be neglected in most variational problems.

One of the most important examples where the Hamiltonian (1.10) becomes relevant is the case of a lipid bilayer (see Fig. 1.6), which will be introduced in the following.

1.2.2 Self-assembly of amphiphiles

In Sec. 1.1.2 we discussed surfactants in water and noticed that the surface tension at the interface decreases for an increasing concentration of surfactants until a certain point is reached. If one exceeds this point, which is also called the *critical micelle concentration* (cmc), the surface tension stays constant. Other physical properties, such as osmotic pressure or electrical conductivity of the solution also exhibit a discontinuity. What happens? At the cmc it becomes energetically more favorable for the surfactants to self-assemble within the bulk of the fluid and shield their hydrophobic parts against the water instead of trying to squeeze themselves into the already densely packed monolayer at the interface. The cmc depends on properties of the surfactant (for instance the surface area of the hydrophobic part) and the conditions the solution is in (*e. g.* salt concentration).

Typical structures that result from self-assembly are spherical, cylindrical or inverted micelles⁸, bilayers and vesicles (see Table 1.3). What kind of aggregate evolves depends on the geometry of the surfactant: it can be quite well determined by the value of the *packing parameter* $v/(a_0 l_c)$, where l_c and v are the length and the volume of the hydrophobic part of one surfactant molecule and a_0 is its effective head group area [Isr92].

⁸ Inverted micelles can of course only form if the surfactant is in a hydrophobic solvent such as oil.

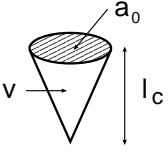
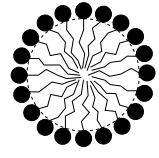
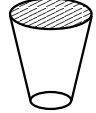
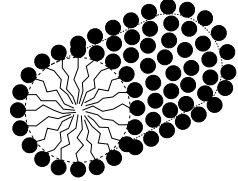
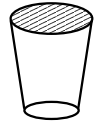
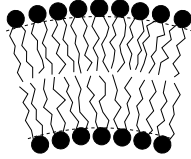
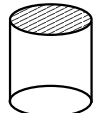
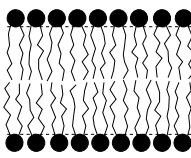
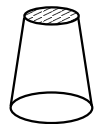
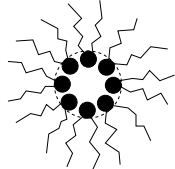
| <i>surfactant</i> | <i>packing parameter</i> | <i>packing shape</i> | <i>structure</i> |
|--|-----------------------------|---|---|
| single-chained surfactants with large head-group areas (<i>e.g.</i> sodium dodecyl sulfate in low salt) | $< \frac{1}{3}$ |  cone |  spherical micelle |
| single-chained surfactants with small head-group areas (<i>e.g.</i> sodium dodecyl sulfate in high salt; nonionic lipids) | $\frac{1}{3} - \frac{1}{2}$ |  truncated cone |  cylindrical micelle |
| double-chained surfactants with large head-group areas and fluid chains (<i>e.g.</i> PC, DGDG) | $\frac{1}{2} - 1$ |  truncated cone |  flexible bilayer, vesicle |
| double-chained surfactants with small head-group areas, anionic lipids in high salt, saturated frozen chains (<i>e.g.</i> PE) | ~ 1 |  cylinder |  planar bilayer |
| double-chained surfactants with small head-group areas, nonionic lipids, poly (cis) unsaturated chains, high T (<i>e.g.</i> unsat. PE) | > 1 |  inverted truncated cone or wedge |  inverted micelles |

Table 1.3: Self-assembly: structures and appropriate packing parameters $v/(a_0 l_c)$. The packing shape sketches the shape of one amphiphilic molecule. The black circles in the structures are the hydrophilic, the chains the hydrophobic parts of the surfactants. [Isr92, p. 381]

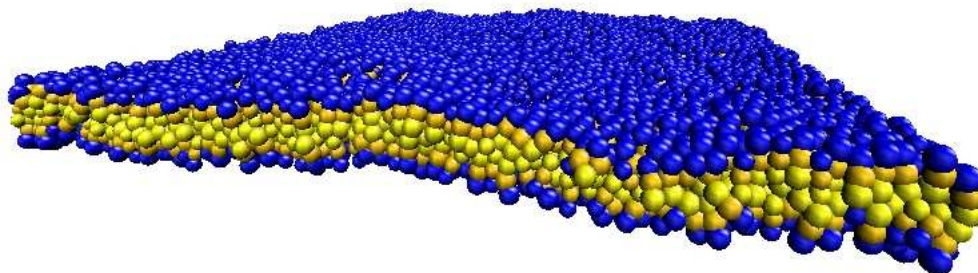


Figure 1.6: Computer simulation of a coarse grained lipid bilayer. The blue spheres are the hydrophilic headgroups of the surfactants, the yellow and orange ones symbolize the hydrophobic tails.

From Table 1.3 we obtain a typical value of the packing parameter for flexible bilayer membranes: it lies between $\frac{1}{2}$ and 1. Surfactants with such a parameter usually possess two hydrocarbon chains.

It is also possible that two or more different surfactants self-assemble into one structure as long as they do not phase-separate. For example, micelle-forming lysolecithin (packing parameter $< \frac{1}{2}$; see Table 1.4) and normally not self-assembling cholesterol (packing parameter > 1) may form bilayer vesicles [Isr92, p. 382]. In nature, a mixture of surfactants can often be found in biological membranes, which will be considered a bit closer in the next section.

1.2.3 Membranes in cell biology

Membranes in cell biology mostly consist of double-chained phospho- or glycolipids (see Table 1.4). The chains contain an even number of carbon atoms (14 – 24 typically) and one of them is often unsaturated (which means there exists a double bond between two of the carbon atoms) or branched. Such surfactants exhibit the following properties that are essential for biological function [Isr92, pp. 375/387]:

- The lipids self-assemble into thin bilayer membranes (see Figs. 1.6 and 1.7) whose function it is to form cell walls and also to separate functional compartments in the cell (organelles).
- The cmc is very low ($10^{-6} - 10^{-10}$ M for bilayer-forming lipids as opposed to $10^{-2} - 10^{-5}$ M for micelle-forming surfactants). The membrane therefore stays the same even for a very low concentration of lipids in the surroundings.
- The membrane behaves as a two-dimensional fluid at physiological temperatures, which is important for processes such as budding and subsequent vesicle formation.

| <i>substance</i> | <i>chemical structure</i> | <i>type</i> |
|---|---------------------------|----------------------|
| lysophosphatidylcholine (lysolecithin) | | lyso-phospholipid |
| phosphatidylethanolamine (PE) | | glycero-phospholipid |
| phosphatidylcholine (PC) | | |
| digalactosyl-diglyceride (DGDG) | | glycero-glycolipid |
| sphingomyelin | | sphingo-phospholipid |

Table 1.4: Examples of membrane lipids. R1 and R2 correspond to hydrocarbon chains of fatty acids (see for instance Table 1.2). [GKD⁺04, A3.8f]

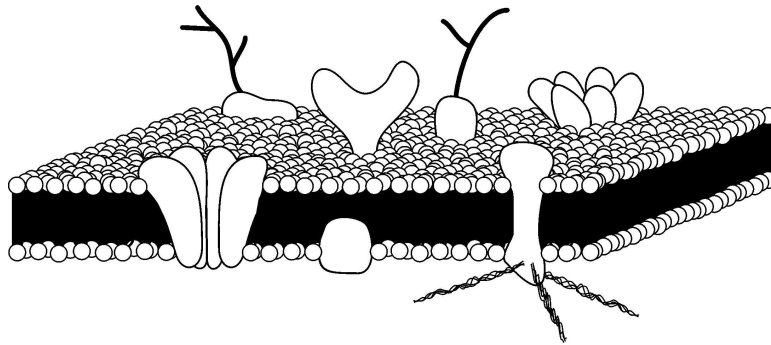


Figure 1.7: The cell membrane consists of a lipid bilayer to which different kinds of macromolecules (e. g. proteins) are bound. [BGK03, p. 258]

Other surfactants that are common in biological membranes are the already mentioned lysolecithin and cholesterol. These may influence the fluidity of the membrane according to their geometry (see previous section).

In addition to the basic lipid bilayer, other types of molecules may be present in the membrane (see Fig. 1.7): proteins perform most of the specific functions of membranes such as enzymatic reactions or ion pumping. One can distinguish between *integral* and *peripheral* membrane proteins. The latter are only connected indirectly to the membrane via the hydrophilic head groups of the lipids. Integral proteins have one or more parts embedded in the bilayer. Most of them span the entire membrane and are therefore called *transmembrane* proteins.

Interactions between proteins are an important field of study because their aggregation in the membrane is quite often important for biological function. In the following, forces between membrane inclusions such as proteins will therefore be considered (see Sec. 6.2.2) as one example of interface mediated interactions.

The thickness of a lipid membrane is of the order of 5 nm whereas its lateral extension may reach micrometers (size of a cell). This is why a continuum description as explained in the introductory remarks of this chapter is often applicable. It turns out that membrane energetics are mainly dominated by bending [Hel73]. Therefore, the Hamiltonian (1.10) is suitable to describe a fluid membrane. For typical phospholipid membranes, κ is of the order of a few tens of $k_B T$, where $k_B T$ is the thermal energy. Values for σ are found to be in a broad range from 0 up to about 10 mN/m [MH01]. The Gaussian bending rigidity $\bar{\kappa}$ is rather difficult to measure because the topology needs to be changed during the measurement. Its value is usually negative and also smaller than that of κ in the same system [GKD⁺04, A3.24].

It should be mentioned that the Hamiltonian (1.10) is also valid for other interfaces such as those containing block copolymers. Focusing on lipid bilayer membrane here, however, we will call the type of interface where bending plays the main role the “fluid membrane type”.

1.3 Other interfaces

Based on the Hamiltonian (1.1) one can systematically consider possible contributions to the energy, order by order in the dimension of the integrand which is length L [CGS03]: the easiest Hamiltonian density one can think of is $\mathcal{H} = 1$, which was already considered in connection with surface tension.

The next order, $1/L$, involves the extrinsic geometry of the interface:

$$\int_{\Sigma} dA K . \quad (1.11)$$

In Hamiltonian (1.10) the spontaneous curvature K_0 is included in this linear term as a constant prefactor.

In second order, $1/(L^2)$, one gets⁹

$$\int_{\Sigma} dA K^2 \quad \text{and} \quad \int_{\Sigma} dA K^{ab} K_{ab} . \quad (1.12)$$

A third term in second order stems from the intrinsic scalar curvature \mathcal{R} , which is, however, not independent due to (see App. B.1, Eqns. (B.40) and (B.42))

$$\mathcal{R} = K^2 - K^{ab} K_{ab} = 2K_G . \quad (1.13)$$

In the Hamiltonian (1.10), where all contributions up to this order are included, the $K^{ab} K_{ab}$ term is therefore dropped. In addition to that, the Gauss-Bonnet theorem (see App. B.2) states that the surface integral over \mathcal{R} is just a topological constant for two-dimensional surfaces without boundaries. In that case only one term in second order is independent.

In third and fourth order one has according to [CGS03]:

$$\int_{\Sigma} dA K^3 \quad \text{and} \quad \int_{\Sigma} dA \mathcal{R} K . \quad (1.14)$$

and¹⁰

$$\int_{\Sigma} dA \mathcal{R}^2 \quad \int_{\Sigma} dA \mathcal{R} K^2 \quad \int_{\Sigma} dA K^4 \quad \text{and} \quad \int_{\Sigma} dA (\nabla_a K)(\nabla^a K) . \quad (1.15)$$

Even the terms in (1.15) may describe certain properties of an interface such as in geometric models for “egg-carton” membranes [GH96] and tubular structures [FG97].

In the following, however, we will restrict ourselves to terms up to second order, while only sometimes referring to higher order terms.

⁹ Note that the sum convention will be used in this work, *i. e.* whenever a pair of identical indices appears with one being superscript and the other subscript, it will be summed over them (see also App. A). For example: $K^{ab} K_{ab} \equiv \sum_{a,b=1}^2 K^{ab} K_{ab}$.

¹⁰ Note that all following terms are of fourth order in $1/L$. The last term, however, contains only 6 derivatives of the embedding function \mathbf{X} , whereas the others contain 8.

2 Stresses in interfaces

2.1 The stress tensor in three-dimensional elasticity theory and its analog for surfaces

Elasticity theory describes the deformations of solid bodies, regarded as continuous media (see for instance [LL86, pp. 3–5] for the following).

Let us consider a small cubic part ΔV of an arbitrarily shaped body in Euclidean space \mathbb{R}^3 : in thermal equilibrium the sum of all forces exerted on the cube is zero. However, if the whole body experiences an external deforming mechanical force, internal forces arise, ultimately caused by molecular interactions. These are called *internal stresses*. Due to their molecular origin, they act over a very short range. Therefore, any forces felt inside the cube are determined by the ones acting on its *surfaces*.

To cope with the directionality of these forces it is quite convenient to introduce the *stress tensor* $\boldsymbol{\sigma}$: In the orthonormal basis $\{\mathbf{x}, \mathbf{y}, \mathbf{z}\}$, the component σ_{ij} is the i th component of the total *internal* force on the unit area perpendicular to the \mathbf{j} axis (see Fig. 2.1(a)) with $i, j \in \{x, y, z\}$. For example, σ_{xx} is the force in x -direction on the unit area perpendicular to the \mathbf{x} axis, whereas σ_{yx} and σ_{zx} act on the same area but in y - and z -direction, respectively.

Then, the total internal force can be written as the integral of the stress tensor over the surface $\partial\Delta V$ of the cube.¹ One gets for the components:

$$(\mathbf{F}_{\text{body}})_i = \sum_{j=x}^z \oint_{\partial\Delta V} dA_j \sigma_{ij} = \sum_{j=x}^z \int_{\Delta V} dV \partial_j \sigma_{ij} \quad (i \in \{x, y, z\}), \quad (2.1)$$

where Stokes' theorem was used in the second step and ∂_j is the partial derivative with respect to j . The symbol dA_j denotes the j th component of the vectorial area element which is perpendicular to $\partial\Delta V$.

If one considers two-dimensional flat interfaces instead of three-dimensional bodies, the same argument as above can be made: the (surface) stress tensor \mathbf{f} is now a force per length acting on a unit line element. Since the force can still act in

¹ Note that the stress tensor is defined with an additional minus sign here compared to [LL86]: Eqn. (2.1) yields the *internal* force that balances the force from the exterior due to Newton's third law. In [LL86] the stress tensor is defined in such a way that Eqn. (2.1) yields the total *external* force exerted on the body.

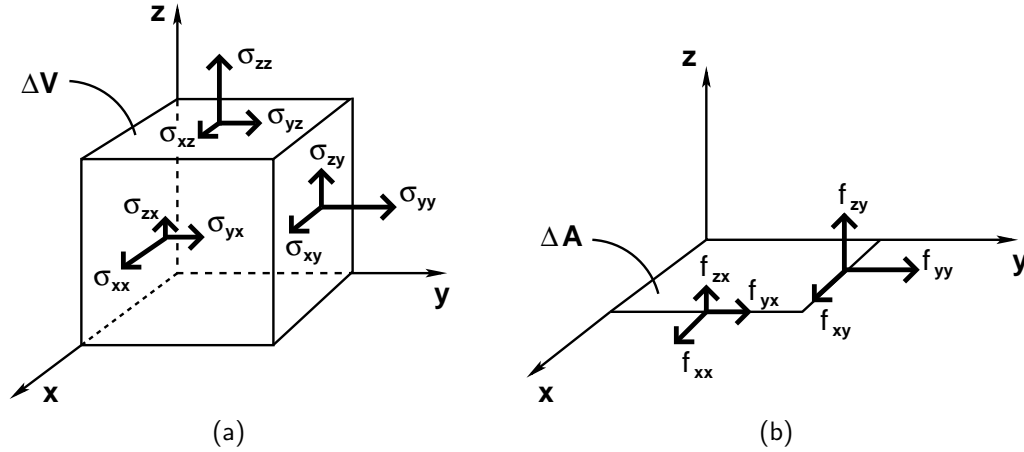


Figure 2.1: Components of the stress tensor a) in 3D b) in 2D

three directions, the tensor has six components. Take, for instance, f_{xy} : it is the x component of the internal force acting on the unit line element perpendicular to the y axis (see Fig. 2.1(b)) with respect to the surface basis $\{\mathbf{x}, \mathbf{y}\}$.

The total internal force on a surface patch ΔA is equal to

$$(\mathbf{F}_{\text{surface}})_i = \sum_{j=x}^y \oint_{\partial\Delta A} dl_j f_{ij} = \sum_{j=x}^y \int_{\Delta A} dA \partial_j f_{ij} \quad (i \in \{x, y, z\}), \quad (2.2)$$

where again Stokes' theorem is exploited and dl_j denotes the j th component of the line element ds times the unit normal which at every point is perpendicular to the boundary curve $\partial\Delta A$ of ΔA .

Generally, we do not want to restrict ourselves to flat interfaces. The stress tensor must thus be generalized in order to calculate forces in curved manifolds. Let us consider a two-dimensional simply connected surface domain Σ_0 with local frame $\{\mathbf{e}_a, \mathbf{n}\}$, $a \in \{1, 2\}$ (see also App. B.1). The stress tensor \mathbf{f} can then be written as a pair of vectors $\mathbf{f}_a \in \mathbb{R}^3$, where \mathbf{f}_a is the force acting on the unit line element perpendicular to the \mathbf{e}_a axis in every point of the surface patch.² With this definition Eqn. (2.2) turns into³

$$\boxed{\mathbf{F}_{\Sigma_0} = \oint_{\partial\Sigma_0} ds \, l_a \mathbf{f}^a = \int_{\Sigma_0} dA \, \nabla_a \mathbf{f}^a}, \quad (2.3)$$

where the vector $\mathbf{l} = l^a \mathbf{e}_a$ is the outward pointing unit normal to the boundary curve $\partial\Sigma_0$, which by construction is also tangential to Σ (see Fig. 2.2). The variable s measures the arc length on $\partial\Sigma_0$. The symbol ∇_a denotes the metric-compatible covariant derivative on the surface (see App. B.1).

² In the case of a flat interface such as in Fig. 2.1(b), $\mathbf{e}_1 = \mathbf{x}$ and $\mathbf{e}_2 = \mathbf{y}$. Thus: $\mathbf{f}_1 \equiv \mathbf{f}_x =$

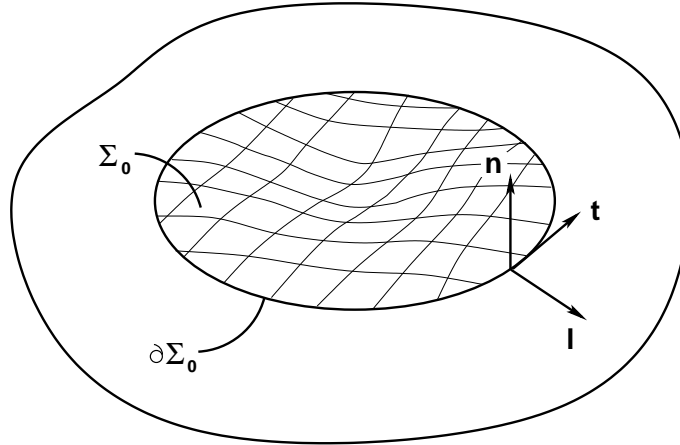


Figure 2.2: Curved surface domain Σ_0 : at the boundary $\partial\Sigma_0$ a local orthonormal frame $\{\mathbf{l}, \mathbf{t}, \mathbf{n}\}$ can be introduced with \mathbf{l} being the outward pointing unit normal to the boundary curve and \mathbf{t} the unit tangent vector. The unit vector \mathbf{n} is normal to the surface *and* the boundary curve.

Equation (2.3) will be exploited in Chap. 5 to calculate two-body interactions between colloids that are bound to an interface. In this chapter we will first begin with deriving the stress tensor for interfaces in general and for special cases.

2.2 Derivation of the surface stress tensor

2.2.1 Approach 1: Variation in the embedding functions

Implementation of the variation

Let us go back to the general reparametrization invariant surface Hamiltonian (1.1) as introduced in the last chapter on p. 4:

$$H_\Sigma[\mathbf{X}] = \int_\Sigma dA \mathcal{H}(g_{ab}, K_{ab}, \nabla_a K_{bc}, \dots), \quad (2.4)$$

where $dA = \sqrt{g} d^2\xi$ with $g = |g_{ab}|$ (see App. B.1).

To find the equilibrium shape of the surface, *i. e.* the one which minimizes this Hamiltonian, we need to calculate its response to an infinitesimal deformation of the embedding functions $\mathbf{X} \rightarrow \mathbf{X} + \delta\mathbf{X}$ (see [CG02b] for the following). In order to do so, one first has to know how the geometry, *i. e.* g_{ab} , \sqrt{g} , K_{ab} , etc. changes (see App. C for the necessary expressions).

$(f_{xx}, f_{yx}, f_{zx})^T$ and $\mathbf{f}_2 \equiv \mathbf{f}_y = (f_{xy}, f_{yy}, f_{zy})^T$.

³ Indices may be raised and lowered with help of the metric g_{ab} and its inverse g^{ab} (see App. B.1).

The deformation may be decomposed into a part tangential and one normal to the surface:

$$\begin{aligned}\delta\mathbf{X} &= (\mathbf{e}_a \cdot \delta\mathbf{X})\mathbf{e}_a + (\mathbf{n} \cdot \delta\mathbf{X})\mathbf{n} \\ &= \Phi^a \mathbf{e}_a + \Psi \mathbf{n} .\end{aligned}\tag{2.5}$$

In the same manner, the first variation of the functional (2.4) can be partitioned into contributions originating from purely tangential and purely normal variations:

$$\delta H = \delta_{\parallel} H + \delta_{\perp} H .\tag{2.6}$$

Note that the Hamiltonian shall be restricted to a simply connected surface domain Σ_0 for the following. For ease of notations its boundary $\partial\Sigma_0$ is chosen to be simply connected, too [CG02b].

For an arbitrary deformation one gets for the variation of the Hamiltonian

$$\delta H_{\Sigma_0} = \int_{\Sigma_0} d^2\xi \left[(\delta\sqrt{g})\mathcal{H} + \sqrt{g}(\delta\mathcal{H}) \right] .\tag{2.7}$$

The decomposition yields for the tangential deformation

$$\begin{aligned}\delta_{\parallel} H_{\Sigma_0} &= \int_{\Sigma_0} d^2\xi \left[(\delta_{\parallel}\sqrt{g})\mathcal{H} + \sqrt{g}(\delta_{\parallel}\mathcal{H}) \right] \\ &\stackrel{\text{(C.9),(C.20)}}{=} \int_{\Sigma_0} dA \left[(\nabla_a \Phi^a)\mathcal{H} + (\Phi^a \nabla_a \mathcal{H}) \right] \\ &= \int_{\Sigma_0} dA \nabla_a (\mathcal{H} \Phi^a) ,\end{aligned}\tag{2.8}$$

where we made use of the fact that the Hamiltonian density \mathcal{H} is a surface scalar. Note therefore that the tangential variation (2.8) is a pure boundary term:

$$\int_{\Sigma_0} dA \nabla_a (\mathcal{H} \Phi^a) = \oint_{\partial\Sigma_0} ds \mathcal{H} l_a \Phi^a ,\tag{2.9}$$

where $\mathbf{l} = l^a \mathbf{e}_a$ is the outward pointing unit normal to the boundary curve $\partial\Sigma_0$ as introduced in the previous section (see Fig. 2.2).

The normal variation can be cast as a bulk part plus a pure divergence

$$\begin{aligned}\delta_{\perp} H_{\Sigma_0} &= \int_{\Sigma_0} d^2\xi \left[(\delta_{\perp}\sqrt{g})\mathcal{H} + \sqrt{g}(\delta_{\perp}\mathcal{H}) \right] \\ &= \int_{\Sigma_0} dA \left[\mathcal{E}(\mathcal{H})\Psi + \nabla_a S^a[\Psi] \right] .\end{aligned}\tag{2.10}$$

The term $\mathcal{E}(\mathcal{H})$ is the bulk Euler-Lagrange derivative of \mathcal{H} with respect to surface deformations. It is purely normal. Note that its vanishing, as usual, determines the shape of the interface. Hence, $\mathcal{E} = 0$ is also called the ‘‘shape equation’’.

All surface gradients and higher derivatives of Ψ are collected via integration by parts in the linear differential operator S^a

$$S^a[\Psi] = S_{(0)}^a \Psi + S_{(1)}^{ab} \nabla_b \Psi + \dots \quad (2.11)$$

One example of how $\mathcal{E}(\mathcal{H})$ and $S^a[\Psi]$ can be extracted from the normal variation (2.10) will be shown at the end of this section.

Combining the two independent variations, (2.8) and (2.10), according to (2.6) we get as the first variation of the functional (2.4) [CG02b]:⁴

$$\boxed{\delta H_{\Sigma_0} = \int_{\Sigma_0} dA \mathcal{E}(\mathcal{H}) \mathbf{n} \cdot \delta \mathbf{X} + \int_{\Sigma_0} dA \nabla_a Q^a}, \quad (2.12)$$

where the divergence in (2.12) originates from the tangential variations as well as the derivatives of normal variations:

$$Q^a = S^a[\Psi] + \mathcal{H} \Phi^a. \quad (2.13)$$

The stress tensor—a conserved Noether current

Now, suppose $\delta \mathbf{X} = \mathbf{a} \in \mathbb{R}^3$ is simply an arbitrary *constant translation*, that of course leaves the Hamiltonian invariant. In this case, the differential operator Q^a is simply proportional to \mathbf{a} as one can see by inserting $\Psi = \mathbf{n} \cdot \mathbf{a}$ and $\Phi^a = \mathbf{e}^a \cdot \mathbf{a}$ into Eqn. (2.13) and exploiting the linearity of S^a . Eqn. (2.12) then turns into

$$\begin{aligned} \delta H_{\Sigma_0} &= \int_{\Sigma_0} dA \mathcal{E}(\mathcal{H}) \mathbf{n} \cdot \mathbf{a} - \int_{\Sigma_0} dA \nabla_a (\mathbf{f}^a \cdot \mathbf{a}) \\ &= \mathbf{a} \cdot \int_{\Sigma_0} dA \left[\mathcal{E}(\mathcal{H}) \mathbf{n} - \nabla_a \mathbf{f}^a \right] \stackrel{!}{=} 0. \end{aligned} \quad (2.14)$$

Here, the vector \mathbf{f}^a is introduced according to

$$Q^a = -\mathbf{f}^a \cdot \mathbf{a}. \quad (2.15)$$

The integral in Eqn. (2.14) must be equal to zero because \mathbf{a} can be arbitrarily chosen. Moreover, the integrand in Eqn. (2.14) vanishes pointwise because Σ_0 may be arbitrarily chosen as well. Thus,

$$\nabla_a \mathbf{f}^a = \mathcal{E}(\mathcal{H}) \mathbf{n}. \quad (2.16)$$

Examples of \mathbf{f}^a and $\mathcal{E}(\mathcal{H})$ for a few Hamiltonians will be calculated in Sec. 2.3 and can be found in Table 2.1 on p. 29.

⁴ Note that $\Psi = \mathbf{n} \cdot \delta \mathbf{X}$ according to Eqn. (2.5).

One may decompose \mathbf{f}^a into its tangential and normal parts

$$\mathbf{f}^a = f^{ab}\mathbf{e}_b + f^a\mathbf{n} , \quad (2.17)$$

which by exploiting the Weingarten and Gauss equations (B.30) and (B.32) yields

$$\nabla_a\mathbf{f}^a = (\nabla_a f^{ab} + K_a^b f^a)\mathbf{e}_b + (\nabla_a f^a - K_{ab}f^{ab})\mathbf{n} . \quad (2.18)$$

The projections of Eqn. (2.16) onto the surface and the surface normal, respectively, can then be written as

$$\nabla_a f^a - K_{ab}f^{ab} = \mathcal{E}(\mathcal{H}) , \quad (2.19)$$

$$\nabla_a f^{ab} + K_a^b f^a = 0 . \quad (2.20)$$

The normal projection (2.19) is equal to the Euler-Lagrange derivative $\mathcal{E}(\mathcal{H})$. The two tangential projections (2.20) are consistency conditions on f^a and f^{ab} that reflect the reparametrization invariance of the Hamiltonian; indeed, they are independent of the Euler-Lagrange derivative.

If we now focus on *true equilibrium surfaces*, which are stationary with respect to *arbitrary* variations⁵, the Euler-Lagrange (“shape”) equation $\mathcal{E}(\mathcal{H}) = 0$ also holds, and Eqn. (2.16) becomes

$$\boxed{\nabla_a \mathbf{f}^a = 0} . \quad (2.21)$$

This is a conservation law for the vector \mathbf{f}^a . Its existence is simply a consequence of Noether’s theorem: a continuous symmetry implies an associated conserved current (\mathbf{f}^a in this case).

It is not by chance that the symbol \mathbf{f}^a is chosen for the Noether current: it is exactly the *surface stress tensor* as it was discussed in Sec. 2.1. One can see that by having a closer look at Eqn. (2.14) for $\mathcal{E}(\mathcal{H}) = 0$:

$$\delta H_{\Sigma_0} = -\mathbf{a} \cdot \int_{\Sigma_0} dA \nabla_a \mathbf{f}^a . \quad (2.22)$$

This equation states that an infinitesimal change in energy is equal to the negative product of an infinitesimal translation times an integral. Thus, this integral must be a force. If we compare it with Eqn. (2.3), it becomes clear that \mathbf{f}^a must be the surface stress tensor.

If there are *global constraints* imposed on the surface geometry, the Hamiltonian contains further terms that have to be varied as well. Take, for instance, the case

⁵ Such an arbitrary variation could for instance be one, where the boundary is fixed and only the interior of the surface is changed.

of a constant volume (see Sec. 1.1.2, p. 10): an additional term $-PV$ enters the Hamiltonian. Its variation yields

$$\delta(-PV) \stackrel{(C.19)}{=} -P \int_{\Sigma_0} dA \Psi , \quad (2.23)$$

which leaves us with the modified shape equation $\mathcal{E}(\mathcal{H}) = P$. Eqn. (2.21) is replaced by

$$\nabla_a \mathbf{f}^a = P \mathbf{n} . \quad (2.24)$$

If one wants to have the stress tensor divergence free as originally, which will become important later (see Sec. 5.1), one may redefine it by writing the unit normal vector as a pure divergence [Guv04b]:⁶

$$\mathbf{n} = \frac{1}{2} \nabla_a \left[(\mathbf{X} \cdot \mathbf{e}^a) \mathbf{n} - (\mathbf{X} \cdot \mathbf{n}) \mathbf{e}^a \right] , \quad (2.25)$$

$$\Rightarrow \check{\mathbf{f}}^a := \mathbf{f}^a - \frac{1}{2} P \left[(\mathbf{X} \cdot \mathbf{e}^a) \mathbf{n} - (\mathbf{X} \cdot \mathbf{n}) \mathbf{e}^a \right] , \quad (2.26)$$

and thus

$$\nabla_a \check{\mathbf{f}}^a = 0 . \quad (2.27)$$

Example: The Hamiltonian density K^n

In order to bring the abstract notions introduced in this section to life, let us focus on the Hamiltonian density $\mathcal{H} = K^n$. The tangential variation of the corresponding Hamiltonian is simply:

$$\delta_{\parallel} H_{\Sigma_0} \stackrel{(2.8)}{=} \int_{\Sigma_0} dA \nabla_a (K^n \Phi^a) . \quad (2.28)$$

For the normal variation we get

$$\begin{aligned} \delta_{\perp} H_{\Sigma_0} &\stackrel{(2.10)}{=} \int_{\Sigma_0} d^2 \xi \left[(\delta_{\perp} \sqrt{g}) K^n + \sqrt{g} (\delta_{\perp} K^n) \right] \\ &\stackrel{(C.9)}{=} \int_{\Sigma_0} dA \left[K^{n+1} \Psi + n K^{n-1} (\delta_{\perp} K) \right] \\ &\stackrel{(C.16)}{=} \int_{\Sigma_0} dA \left[K^{n+1} \Psi + n K^{n-1} (-\Delta \Psi - K_{ab} K^{ab} \Psi) \right] \\ &= \int_{\Sigma_0} dA \left[-n \Delta K^{n-1} + K^{n-1} (K^2 - n K_{ab} K^{ab}) \right] \Psi \\ &\quad - n \int_{\Sigma_0} dA \nabla_a \left[K^{n-1} (\nabla^a \Psi) - (\nabla^a K^{n-1}) \Psi \right] , \end{aligned} \quad (2.29)$$

⁶ This relation can be checked by straightforward calculation.

where we exploited the product rule of differentiation in the last step. The symbol $\Delta = \nabla_a \nabla^a$ denotes the metric-compatible Laplacian.

Following Eqn. (2.10) and (2.12) the Euler-Lagrange derivative $\mathcal{E}(\mathcal{H})$ and the differential operators $S^a[\Psi]$ and Q^a are:

$$\mathcal{E}(\mathcal{H}) = -n\Delta K^{n-1} + K^{n-1}(K^2 - nK_{ab}K^{ab}) \quad (2.30)$$

$$S^a[\Psi] = -n \left[K^{n-1}(\nabla^a \Psi) - (\nabla^a K^{n-1})\Psi \right] \quad (2.31)$$

$$Q^a = -n \left[K^{n-1}(\nabla^a \Psi) - (\nabla^a K^{n-1})\Psi \right] + K^n \Phi^a . \quad (2.32)$$

For a translation $\delta \mathbf{X} = \mathbf{a}$ one therefore gets:

$$\begin{aligned} Q^a &= -n \left[K^{n-1} \nabla^a (\mathbf{n} \cdot \mathbf{a}) - (\nabla^a K^{n-1}) \mathbf{n} \cdot \mathbf{a} \right] + K^n \mathbf{e}^a \cdot \mathbf{a} \\ &\stackrel{(B.30)}{=} - \left[(nK^{n-1}K^{ab} - K^n g^{ab}) \mathbf{e}_b - n(\nabla^a K^{n-1}) \mathbf{n} \right] \cdot \mathbf{a} . \end{aligned} \quad (2.33)$$

Comparing with Eqn. (2.15) yields the following result for the surface stress tensor:

$$\mathbf{f}^a = (nK^{n-1}K^{ab} - K^n g^{ab}) \mathbf{e}_b - n(\nabla^a K^{n-1}) \mathbf{n} . \quad (2.34)$$

If we include the constraint of constant volume, the shape equation reads

$$-n\Delta K^{n-1} + K^{n-1}(K^2 - nK_{ab}K^{ab}) \stackrel{(2.24)}{=} P . \quad (2.35)$$

2.2.2 Approach 2: Using auxiliary variables

Implementation of constraints

In the previous section we have seen how the surface stress tensor can be obtained via a variation $\mathbf{X} \rightarrow \mathbf{X} + \delta \mathbf{X}$ of the embedding functions. This, however, turned out to be a rather involved calculation as it became apparent in the example worked out at the end of the previous section. The reason for this difficulty is that the tensors g_{ab} , K_{ab} , \dots indirectly depend on \mathbf{X} via the structural relationships⁷

$$g_{ab} = \mathbf{e}_a \cdot \mathbf{e}_b \quad \text{and} \quad K_{ab} = \mathbf{e}_a \cdot \partial_b \mathbf{n} , \quad (2.36)$$

and

$$\mathbf{e}_a = \partial \mathbf{X} / \partial \xi^a = \partial_a \mathbf{X} , \quad \mathbf{e}_a \cdot \mathbf{n} = 0 , \quad \text{and} \quad \mathbf{n}^2 = 1 , \quad (2.37)$$

and therefore have to be varied as well (see App. C).

Here, an alternative way will be presented: the quantities g_{ab} , K_{ab} , \mathbf{e}_a , and \mathbf{n} are treated as *independent* auxiliary variables [Guv04a]. Consequently, Eqns. (2.36) and

⁷ Cf. Eqns. (B.2), (B.4), (B.5), and (B.20), in App. B.1. A discussion why just these structural relationships are chosen for the following can be found in [Guv04a].

(2.37) have to be enforced via Lagrange multiplier functions. The new functional $H_C[g_{ab}, K_{ab}, \nabla_a K_{bc}, \dots, \mathbf{X}, \mathbf{e}_a, \mathbf{n}, \lambda^{ab}, \Lambda^{ab}, \mathbf{f}^a, \lambda_\perp^a, \lambda_n]$ is then:

$$\begin{aligned} H_C &= H[g_{ab}, K_{ab}, \nabla_a K_{bc}, \dots] + \int dA \mathbf{f}^a \cdot (\mathbf{e}_a - \partial_a \mathbf{X}) \\ &+ \int dA [\lambda^{ab}(g_{ab} - \mathbf{e}_a \cdot \mathbf{e}_b) + \Lambda^{ab}(K_{ab} - \mathbf{e}_a \cdot \partial_b \mathbf{n})] \\ &+ \int dA [\lambda_\perp^a (\mathbf{e}_a \cdot \mathbf{n}) + \lambda_n (\mathbf{n}^2 - 1)] . \end{aligned} \quad (2.38)$$

The original Hamiltonian H is now considered to be a function of the *independent* variables g_{ab} , K_{ab} , and its covariant derivatives, whereas λ^{ab} , Λ^{ab} , \mathbf{f}^a , λ_\perp^a , and λ_n are the Lagrange multipliers fixing the constraints (2.36) and (2.37). This greatly simplifies the variational problem because now we do not have to determine how the deformation $\delta \mathbf{X}$ propagates through to g_{ab} , \sqrt{g} , K_{ab} , etc.

Let us study the Euler-Lagrange equations for \mathbf{X} , \mathbf{e}_a , \mathbf{n} , g_{ab} and K_{ab} , respectively,

$$\nabla_a \mathbf{f}^a = 0 , \quad (2.39a)$$

$$\mathbf{f}^a = (\Lambda^{ac} K_c^b + 2\lambda^{ab}) \mathbf{e}_b - \lambda_\perp^a \mathbf{n} , \quad (2.39b)$$

$$0 = (\nabla_b \Lambda^{ab} + \lambda_\perp^a) \mathbf{e}_a + (2\lambda_n - \Lambda^{ab} K_{ab}) \mathbf{n} , \quad (2.39c)$$

$$\lambda^{ab} = T^{ab}/2 , \quad (2.39d)$$

$$\Lambda^{ab} = -\mathcal{H}^{ab} . \quad (2.39e)$$

In Eqn. (2.39b) the Weingarten equations $\partial_a \mathbf{n} = K_a^b \mathbf{e}_b$ (B.30) have been used, in Eqn. (2.39c) the Gauss equations $\nabla_a \mathbf{e}_b = -K_{ab} \mathbf{n}$ (B.32). We also define

$$\mathcal{H}^{ab} := \frac{\delta \mathcal{H}}{\delta K_{ab}} \quad \text{and} \quad T^{ab} := -2(\sqrt{g})^{-1} \frac{\delta(\sqrt{g} \mathcal{H})}{\delta g_{ab}} , \quad (2.40)$$

where we call T^{ab} the intrinsic stress tensor associated with the metric g_{ab} .

It is not by accident that the symbol \mathbf{f}^a denotes the Lagrange multiplier that anchors \mathbf{e}_a to the embedding \mathbf{X} . Indeed, it is identical to the surface stress tensor as it has been introduced in the two previous sections. This can be seen if one considers a variation of the Hamiltonian H_C : for a constant translation $\delta \mathbf{X} = \mathbf{a}$ one gets [Guv04a]

$$\delta H_C = -\mathbf{a} \cdot \int dA \nabla_a \mathbf{f}^a , \quad (2.41)$$

which is the analog to Eqn. (2.22).

Combining Eqns. (2.39), we find an expression for \mathbf{f}^a where all other Lagrange multipliers are eliminated. From Eqn. (2.39c) we get $\lambda_\perp^a = -\nabla_b \Lambda^{ab}$ because \mathbf{e}_a and \mathbf{n} are linearly independent. Inserting this and Eqns. (2.39d, 2.39e) into Eqn. (2.39b) yields:

$$\boxed{\mathbf{f}^a = (T^{ab} - \mathcal{H}^{ac} K_c^b) \mathbf{e}_b - (\nabla_b \mathcal{H}^{ab}) \mathbf{n}} . \quad (2.42)$$

This general expression can be used to calculate the stress tensor once the Hamiltonian density is specified, as we show in Sec. 2.3 for a few examples.

The stress tensor including pressure

Eqns. (2.39) and (2.42) change if one imposes further *physical* constraints. These can be enforced as usual by further Lagrange multipliers.

If the surface, for instance, encloses a fixed volume, a term $-PV$ has to be included in the functional (cf. Secs. 1.1.2 and 2.2.1):

$$H_{C,V \text{ fixed}} = \tilde{H}_C - PV \stackrel{\text{(C.17)}}{=} \tilde{H}_C - \frac{1}{3}P \int dA \mathbf{n} \cdot \mathbf{X} . \quad (2.43)$$

Notice that the original Lagrange multiplier functions \mathbf{f}^a, \dots of H_C have to be replaced by $\tilde{\mathbf{f}}^a, \dots$ in \tilde{H}_C because the additional term in the functional also induces changes in the other multipliers: Looking at the Euler-Lagrange equations (2.39), we notice that Eqns. (2.39b) for \mathbf{e}_a and (2.39e) for K_{ab} are as before; the others change slightly:

$$\nabla_a \tilde{\mathbf{f}}^a = \frac{1}{3}P \mathbf{n} , \quad (2.44a)$$

$$\tilde{\mathbf{f}}^a = (\tilde{\Lambda}^{ac} K_c^b + 2\tilde{\lambda}^{ab}) \mathbf{e}_b - \tilde{\lambda}_\perp^a \mathbf{n} , \quad (2.44b)$$

$$0 = (\nabla_b \tilde{\Lambda}^{ab} + \tilde{\lambda}_\perp^a - \frac{1}{3}P \mathbf{X} \cdot \mathbf{e}^a) \mathbf{e}_a \\ + (2\tilde{\lambda}_n - \tilde{\Lambda}^{ab} K_{ab} - \frac{1}{3}P \mathbf{X} \cdot \mathbf{n}) \mathbf{n} , \quad (2.44c)$$

$$\tilde{\lambda}^{ab} = \frac{1}{2}T^{ab} + \frac{1}{6}P(\mathbf{X} \cdot \mathbf{n})g^{ab} , \quad (2.44d)$$

$$\tilde{\Lambda}^{ab} = \Lambda^{ab} = -\mathcal{H}^{ab} , \quad (2.44e)$$

where T^{ab} and \mathcal{H}^{ab} are defined as in Eqn. (2.40). The Lagrange multiplier function $\tilde{\Lambda}^{ab}$ is the only one that is equal to its counterpart Λ^{ab} . In Eqn. (2.44c) we made use of completeness $\mathbf{X} = (\mathbf{X} \cdot \mathbf{e}^a) \mathbf{e}_a + (\mathbf{X} \cdot \mathbf{n}) \mathbf{n}$. To get Eqn. (2.44d) it is necessary to know that

$$\frac{\delta(\sqrt{g})}{\delta g_{ab}} = \frac{1}{2} \sqrt{g} g^{ab} , \quad (2.45)$$

which can be derived by exploiting Eqn. (C.7).

Combining Eqns. (2.44) in the same way as Eqns. (2.39) above results in the following expression for the surface stress tensor:

$$\tilde{\mathbf{f}}^a = \left[T^{ac} - \mathcal{H}^{ac} K_c^b + \frac{1}{3}P(\mathbf{X} \cdot \mathbf{n})g^{ab} \right] \mathbf{e}_b - \left[\nabla_b \mathcal{H}^{ab} + \frac{1}{3}P(\mathbf{X} \cdot \mathbf{e}^a) \right] \mathbf{n} \quad (2.46)$$

$$= \mathbf{f}^a - \frac{1}{3}P \left[(\mathbf{X} \cdot \mathbf{e}^a) \mathbf{n} - (\mathbf{X} \cdot \mathbf{n}) \mathbf{e}^a \right] , \quad (2.47)$$

where \mathbf{f}^a is the original stress tensor (2.42). Applying identity (2.25) for the normal vector again, allows Eqn. (2.44a) to be rewritten as

$$\nabla_a \mathbf{f}^a = P \mathbf{n} , \quad (2.48)$$

which is identical to Eqn. (2.24).

2.3 The surface stress tensor of special interfaces

In Sec. 2.2.2 the general expression

$$\mathbf{f}^a = (T^{ab} - \mathcal{H}^{ac} K_c^b) \mathbf{e}_b - \nabla_b \mathcal{H}^{ab} \mathbf{n} \quad (2.49)$$

for the surface stress tensor has been derived. Here, Eqn. (2.49) will be specialized to a few important standard cases (see Chap. 1). In addition, the Euler-Lagrange derivative \mathcal{E} will be calculated via Eqn. (2.19).

The simplest Hamiltonian density is $\mathcal{H} = 1$ which is (up to a constant prefactor) the Hamiltonian density of a soap film (see Sec. 1.1.2). According to Eqn. (2.40) we get: $\mathcal{H}^{ab} = \delta \mathcal{H} / \delta K_{ab} = 0$ and $T^{ab} = -2(\sqrt{g})^{-1} \delta(\sqrt{g} \mathcal{H}) / \delta g_{ab} \stackrel{(2.45)}{=} -g^{ab}$. Thus,

$$\mathbf{f}^a \stackrel{(2.49)}{=} -g^{ab} \mathbf{e}_b , \quad \text{and} \quad (2.50)$$

$$\mathcal{E} \stackrel{(2.19)}{=} \nabla_a f^a - K_{ab} f^{ab} = -K_{ab} (-g^{ab}) \stackrel{(B.26)}{=} K . \quad (2.51)$$

Note that the functional derivatives δ in this first case are equal to the partial derivatives ∂ because \mathcal{H} does not depend on higher derivatives of g_{ab} or K_{ab} .

This is also true for the Hamiltonian density $\mathcal{H} = K^n = (g^{ab} K_{ab})^n$ (with $n \in \mathbb{N}$, where the case $n = 2$ is relevant for fluid membranes, see Sec. 1.2). One derives:⁸ $\mathcal{H}^{ab} = n K^{n-1} g^{ab}$ and $T^{ab} = 2n K^{n-1} K^{ab} - K^n g^{ab}$ which gives

$$\mathbf{f}^a = (n K^{n-1} K^{ab} - K^n g^{ab}) \mathbf{e}_b - n (\nabla^a K^{n-1}) \mathbf{n} , \quad \text{and} \quad (2.52)$$

$$\mathcal{E} = \left[\mathcal{R} - \left(1 - \frac{1}{n}\right) K^2 - \Delta \right] n K^{n-1} . \quad (2.53)$$

Note that Eqns. (2.52) and (2.53) are identical to the results obtained earlier via the variational approach (see Eqns. (2.34) and apply Eqn. (B.40) to (2.30)).

Consider now $\mathcal{H} = K^{ab} K_{ab}$: applying Eqn. (2.49) in this case yields for the stress tensor

$$\mathbf{f}^a = (2K^{ac} K_c^b - K^{cd} K_{cd} g^{ab}) \mathbf{e}_b - 2(\nabla_b K^{ab}) \mathbf{n} . \quad (2.54)$$

⁸ One has to be careful, however, when differentiating with respect to g_{ab} : the tensor K_{ab} is the independent variable—which is why a derivative with respect to g_{ab} yields zero—whereas K^{ab} depends on the metric through its inverse and thus yields a nontrivial term when differentiated.

Before discussing the Euler-Lagrange derivative, let us rewrite this expression with the help of Eqns. (B.39, B.40) and (B.15, B.35), respectively:

$$\begin{aligned} \mathbf{f}^a &= \left[2(KK^{ab} - R^{ab}) - (K^2 - \mathcal{R})g^{ab} \right] \mathbf{e}_b - 2(\nabla_a K) \mathbf{n} \\ &= \left[(2KK^{ab} - K^2 g^{ab}) + (\mathcal{R}g^{ab} - 2R^{ab}) \right] \mathbf{e}_b - 2(\nabla_a K) \mathbf{n} , \end{aligned} \quad (2.55)$$

where R_{ab} is the Ricci tensor. In *two* dimensions (see Eqns. (B.41) and (B.42)):

$$\mathcal{R}g^{ab} - 2R^{ab} = 0 . \quad (2.56)$$

Thus, the stress tensor for $\mathcal{H} = K^{ab}K_{ab}$ is exactly the same as for $\mathcal{H} = K^2$ (cf. Eqn. (2.52) for $n = 2$). One can therefore also read off the Euler-Lagrange equation for $\mathcal{H} = K^{ab}K_{ab}$ from Eqn. (2.53):

$$\mathcal{E} = \left[\mathcal{R} - \frac{1}{2}K^2 - \Delta \right] 2K . \quad (2.57)$$

Exploiting the linearity of the stress tensor with respect to \mathcal{H} and respecting $\mathcal{R} \stackrel{(B.40)}{=} K^2 - K^{ab}K_{ab}$ one immediately gets⁹

$$\mathbf{f}^a = 0 \quad \Rightarrow \quad \mathcal{E} = 0 , \quad (2.58)$$

for $\mathcal{H} = \mathcal{R}$.

Finally, let us consider $\mathcal{H} = \frac{1}{2}(\nabla_c K)(\nabla^c K) \equiv \frac{1}{2}(\nabla K)^2$. Now one has to keep in mind that \mathcal{H}^{ab} and T^{ab} are functional derivatives

$$\mathcal{H}^{ab} = \frac{\delta \mathcal{H}}{\delta K_{ab}} = \frac{\partial \mathcal{H}}{\partial K_{ab}} - \nabla_c \left(\frac{\partial \mathcal{H}}{\partial \nabla_c K_{ab}} \right) , \quad (2.59)$$

because \mathcal{H} depends on derivatives of K_{ab} . We get

$$\mathcal{H}^{ab} = -\nabla_c (g^{ab} \nabla^c K) = -g^{ab} \Delta K . \quad (2.60)$$

It is a bit more difficult to determine T^{ab} . To avoid mistakes, let us consider the variation of the Hamiltonian $H = \frac{1}{2} \int dA (\nabla K)^2$ with respect to the metric g_{ab} and identify T^{ab} at the end of the calculation. The variation yields:

$$\delta_g H = \int d^2 \xi \delta_g \left[\frac{\sqrt{g}}{2} (\nabla K)^2 \right] = \int dA \frac{1}{2\sqrt{g}} \left\{ \delta_g [\sqrt{g}] (\nabla K)^2 + \sqrt{g} \delta_g [(\nabla K)^2] \right\} . \quad (2.61)$$

The first term can be obtained with the help of Eqn. (2.45):

$$\delta_g [\sqrt{g}] = \frac{1}{2} \sqrt{g} g^{ab} \delta g_{ab} . \quad (2.62)$$

⁹ The stress tensor for $\mathcal{H} = \mathcal{R}$ is only equal to zero in *two* dimensions due to Eqn. (2.56). In general it is: $\mathbf{f}^a = 2(R^{ab} - \frac{1}{2}\mathcal{R}g^{ab})\mathbf{e}_b = 2G^{ab}\mathbf{e}_b$, where G^{ab} is the *Einstein tensor*.

| \mathcal{H} | \mathcal{E} | f^a | f^{ab} |
|---|--|-----------------------|---|
| 1 | K | 0 | $-g^{ab}$ |
| K^n | $[\mathcal{R} - (1 - \frac{1}{n})K^2 - \Delta]nK^{n-1}$ | $-n \nabla^a K^{n-1}$ | $(nK^{ab} - Kg^{ab})K^{n-1}$ |
| $K^{ab}K_{ab}$ | $[\mathcal{R} - \frac{1}{2}K^2 - \Delta]2K$ | $-2 \nabla^a K$ | $(2K^{ab} - Kg^{ab})K$ |
| \mathcal{R} | 0 | 0 | 0 |
| $\frac{1}{2}(\nabla K)^2 \equiv \frac{1}{2} \cdot (\nabla_c K)(\nabla^c K)$ | $(\Delta + K^2 - \mathcal{R})\Delta K - K^{ab} \cdot [(\nabla_a K)(\nabla_b K) - \frac{1}{2}g_{ab}(\nabla K)^2]$ | $\nabla^a \Delta K$ | $(\nabla^a K)(\nabla^b K) - \frac{1}{2}g^{ab} \cdot (\nabla K)^2 - K^{ab} \Delta K$ |

Table 2.1: Euler-Lagrange derivative $\mathcal{E}(\mathcal{H})$ and the components of the stress tensor $\mathbf{f}^a = f^{ab}\mathbf{e}_b + f^a\mathbf{n}$ for several simple scalar surface Hamiltonian densities \mathcal{H} . Notice that K^2 and $K^{ab}K_{ab}$ yield identical \mathcal{E} and \mathbf{f}^a (see text in this section).

For the second we need to calculate¹⁰

$$\begin{aligned}
 \delta_g [(\nabla K)^2] &= \delta_g [g^{ab}(\nabla_a K)(\nabla_b K) + 2g^{ab}(\nabla_a K)\delta_g[\nabla_b K]] \\
 &= -(\nabla^a K)(\nabla^b K)\delta g_{ab} + 2g^{ab}(\nabla_a K)\nabla_b(K_{cd}\delta g^{cd}) \\
 &= -(\nabla^a K)(\nabla^b K)\delta g_{ab} - 2g^{ab}(\nabla_a K)\nabla_b(K^{cd}\delta g_{cd}), \quad (2.63)
 \end{aligned}$$

where $\delta_g g^{ab} = -g^{ac}g^{bd}\delta g_{cd}$ was exploited twice (cf. Eqn. (C.5)).

Inserting Eqns. (2.62) and (2.63) in (2.61) we get

$$\delta_g H = \int dA \frac{1}{2} \left[\frac{1}{2}g^{ab}(\nabla K)^2 - (\nabla^a K)(\nabla^b K) \right] \delta g_{ab} - \int dA g^{ab}(\nabla^a K)\nabla_b(K^{cd}\delta g_{cd}). \quad (2.64)$$

The last term can be rewritten as

$$\begin{aligned}
 \int dA g^{ab}(\nabla^a K)\nabla_b(K^{cd}\delta g_{cd}) &= - \int dA K^{ab}\Delta K \delta g_{ab} \\
 &\quad + \int dA \nabla_b \left[g^{ab}(\nabla^a K)K^{cd}\delta g_{cd} \right], \quad (2.65)
 \end{aligned}$$

where the second term of the right hand side is a total divergence and can be cast as a boundary term. Therefore, it does not contribute to T^{ab} :

$$\delta_g H \stackrel{(2.40)}{=} -\frac{1}{2} \int dA T^{ab} \delta g_{ab} + \text{boundary terms}, \quad (2.66)$$

¹⁰ Note that one again has to be careful (cf. footnote 8, p. 27): not only K^{ab} but also ∇^a now depends on the metric through its inverse. However, ∇_a is independent of g_{ab} because it acts on the scalar K and can thus be written as $\partial/\partial\xi^a$ (see App. B.1).

with

$$T^{ab} = (\nabla^a K) (\nabla^b K) - \frac{1}{2} g^{ab} (\nabla K)^2 - 2K^{ab} \Delta K . \quad (2.67)$$

Thus, we get with the help of Eqns. (2.49) and (2.19)

$$\mathbf{f}^a = \left[(\nabla^a K) (\nabla^b K) - \frac{1}{2} g^{ab} (\nabla K)^2 - K^{ab} \Delta K \right] \mathbf{e}_b + \nabla^a \Delta K \mathbf{n} , \quad \text{and} \quad (2.68)$$

$$\mathcal{E} = (\Delta + K^2 - \mathcal{R}) \Delta K - K^{ab} \left[(\nabla_a K) (\nabla_b K) - \frac{1}{2} g_{ab} (\nabla K)^2 \right] , \quad (2.69)$$

for $\mathcal{H} = \frac{1}{2} (\nabla K)^2$.

All results of this section are summarized in Table 2.1. In Chaps. 5 and 6 they will be exploited to calculate interface mediated forces between colloidal particles.

3 One colloidal particle at an interface

In the previous two chapters we have discussed free interfaces and stresses in them. Let us now consider what happens when a second component comes into play: a solid particle that is bound to the interface, either because of adhesion or because it is embedded in it.¹

In this thesis, the focus is on interfaces whose energetics can be described by the Hamiltonian (1.1). In Sec. 3.1.2 we will see that gravity cannot be described with such a functional. One may neglect gravity, however, if one restricts the size of the particle to length scales smaller than $1\ \mu\text{m}$ (see Sec. 3.1.2). Furthermore, the mesoscopic view on the system as introduced in Chap. 1 on p. 3 should still be appropriate, which is why the particle should also be bigger than 1 nm.

Particles of that size are called *colloidal particles* [BM93, p. 105]. This name was coined by the Scottish scientist Thomas Graham when investigating solutions, in which the dissolved species was not able to diffuse through a semi-permeable membrane (“κόλλα” means “glue” in Greek) [DGR02, I1.16]. Typical examples of colloidal particles are polymers, in particular biopolymers such as proteins, but also smoke or dust particles.

In this chapter, the focus will be on systems where *one* colloidal particle is bound to a liquid-gas interface (Sec. 3.1) and a fluid membrane (Sec. 3.2), respectively.

3.1 The three-phase boundary solid/liquid/gas

3.1.1 The Young-Dupré equation

The standard derivation

First, consider the case of a three-phase boundary solid/liquid/gas: Assume that a liquid drop adheres to an ideally flat solid substrate surrounded by a gas.² In equilibrium the drop will have a certain shape which is determined by the interplay

¹ The latter case is of particular interest in the case of fluid membranes because proteins can be modeled as solid membrane inclusions (see Secs. 1.2.3 and 3.2.2).

² Note that all results in this section also hold for solid-liquid-fluid interfaces in general. The gas as third phase is only chosen for notational simplicity.

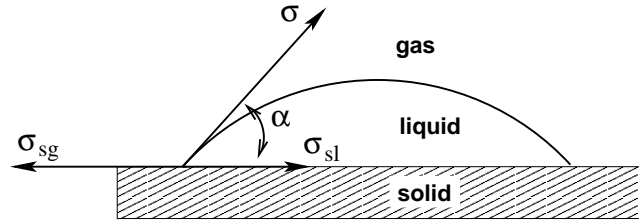


Figure 3.1: Balance of forces at the three-phase boundary solid/liquid/gas

of three different components: the surface tension σ of the liquid-gas interface, the surface tension σ_{sg} of the solid-gas, and the tension σ_{sl} of the solid-liquid interface.³ Because of that interplay, the angle between the solid and the liquid surface on the three-phase contact line will adjust to a special value. This angle α is called the contact angle and is depicted in Fig. 3.1 together with the three tensions.

In the horizontal direction forces caused by the tensions must balance in equilibrium. By simple vector addition we obtain the equation (see again Fig. 3.1):

$$\sigma_{sg} = \sigma \cos \alpha + \sigma_{sl} . \quad (3.1)$$

The energy per area that is *gained* by bringing a separate liquid drop and a separate solid together so that their surfaces are partially in contact with each other is called the adhesion energy u . It consists of two components: energy is gained because the two separate surfaces do not exist anymore. However, to form the new contact area energy must be expended. Thus, we can write:

$$u = (\sigma + \sigma_{sg}) - \sigma_{sl} . \quad (3.2)$$

Combining Eqns. (3.1) and (3.2) we get:

$$u = \sigma (1 + \cos \alpha) . \quad (3.3)$$

This equation is the well-known Young-Dupré equation (see for instance [BM93, p. 55 et seq.]). It is a local condition that holds at every point of the contact line.

Derivation via the stress tensor

In the previous section we have viewed σ , σ_{sg} , and σ_{sl} as tensions that are tangential to the surface in agreement with the introductory remarks of Sec. 1.1.1. Why could we do this? The reason is that we actually balanced the stress tensors, which are

³ Note that the concept of surface tension—until now only applied to liquid-fluid interfaces—may be generalized to include solid-fluid interfaces.

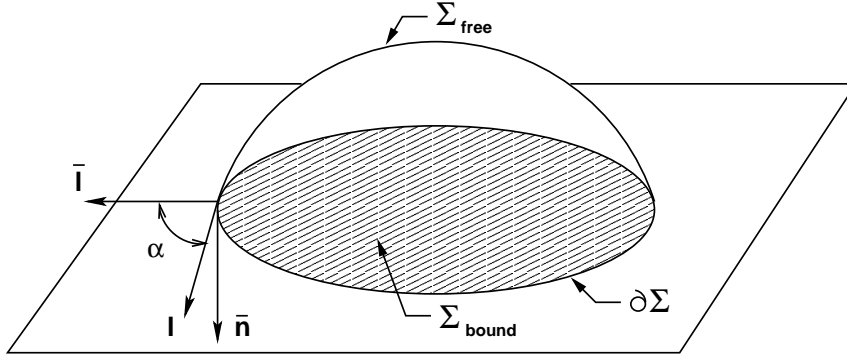


Figure 3.2: Geometry of a liquid drop on a flat solid substrate

purely tangential to the surface in the case of a liquid-fluid interface. Its absolute values are equal to the interfacial energies as we have seen in Chapter 2.

Let us therefore consider how one can formally derive the result (3.3) by using the surface stress tensors [CG02a]. For that purpose the free part and the bounded part of the surface of the liquid drop must be considered separately: for the free part of the surface Σ_{free} the stress tensor can be written as ($\mathcal{H} = \sigma$, see Table 2.1):

$$\mathbf{f}^a = -\sigma g^{ab} \mathbf{e}_b . \quad (3.4)$$

For the bounded part Σ_{bound} one has to take into account the adhesion energy. We get [CG02a]):

$$\bar{\mathbf{f}}^a = -(\sigma - u) \bar{g}^{ab} \bar{\mathbf{e}}_b . \quad (3.5)$$

In equilibrium the forces must balance at every point of the boundary curve $\partial\Sigma$. Consider the stress due to the free part (direction of $\mathbf{l} = l_a \mathbf{e}^a$ see Fig. 3.2):

$$l_a \mathbf{f}^a \stackrel{(3.4)}{=} -l_a \sigma g^{ab} \mathbf{e}_b = -\sigma \mathbf{l} . \quad (3.6)$$

For the bounded part one can do the same. The unit normal $\bar{\mathbf{l}}$ on the boundary pointing tangentially out of Σ_{bound} (see Fig. 3.2) can be written as:

$$\bar{\mathbf{l}} = \bar{l}_a \bar{\mathbf{e}}^a . \quad (3.7)$$

Thus, we get for the bounded part:

$$\bar{l}_a \bar{\mathbf{f}}^a \stackrel{(3.5)}{=} -\bar{l}_a (\sigma - u) \bar{g}^{ab} \bar{\mathbf{e}}_b \stackrel{(3.7)}{=} -(\sigma - u) \bar{\mathbf{l}} . \quad (3.8)$$

Balancing the forces at the boundary yields:

$$-\sigma \mathbf{l} - (\sigma - u) \bar{\mathbf{l}} + \mathbf{f}_c = 0 , \quad (3.9)$$

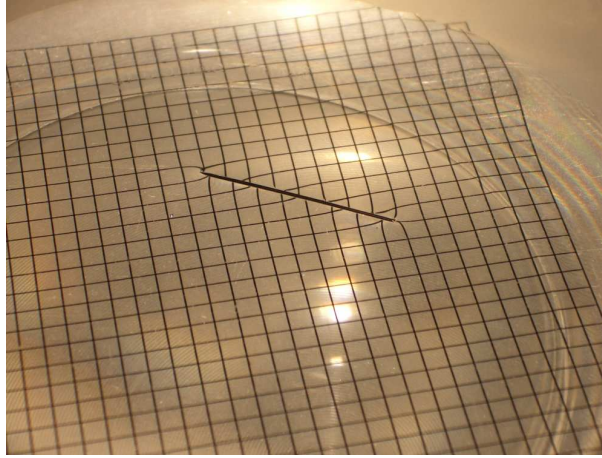


Figure 3.3: Sewing needle floating on water

where \mathbf{f}_c is introduced as a force of constraint (per length) that balances the force component *normal* to the solid caused by $l_a \mathbf{f}^a$: $\mathbf{f}_n = -\sigma \mathbf{l} \cdot \bar{\mathbf{n}} = -\mathbf{f}_c$. This force must be provided by the substrate.

The projection *horizontal* to the solid yields:

$$\begin{aligned} -\sigma \mathbf{l} \cdot \bar{\mathbf{l}} - (\sigma - u) \bar{\mathbf{l}} \cdot \bar{\mathbf{l}} &= 0 \\ -\sigma \mathbf{l} \cdot \bar{\mathbf{l}} - \sigma + u &= 0 \\ \sigma (\mathbf{l} \cdot \bar{\mathbf{l}} + 1) &= u. \end{aligned} \tag{3.10}$$

\mathbf{l} and $\bar{\mathbf{l}}$ are unit vectors, therefore $\mathbf{l} \cdot \bar{\mathbf{l}} = \cos(\angle(\mathbf{l}, \bar{\mathbf{l}})) = \cos \alpha$. The angle between the two vectors is equal to the contact angle α . Thus, (3.10) is exactly the Young-Dupré equation (3.3).

This type of calculation seems to be a very convenient strategy for identifying contact boundary conditions, particularly if one is interested in more general surface Hamiltonians (such as bending). Unfortunately, contrary to what one might believe after consulting Ref. [CG02a], it becomes incorrect in these cases. The correct generalization is currently under study [Guv04b].

3.1.2 Force balance for a colloidal particle floating on a liquid

For a solid particle adhering to a liquid-gas interface, all forces caused by the tensions σ , σ_{sg} and σ_{sl} have to be included into the force balance. Observe that this has implications beyond the Young-Dupré equation, since as we have just seen this equation does not bother with forces normal to the solid substrate. In addition to the tensions, gravity also has to be taken into account—at least for macroscopic particles like a sewing needle floating on water (see Fig. 3.3).

A heavy particle causes deformations of the originally flat interface due to its weight. For the *liquid*, surface tension and gravity are the only physical quantities contributing to the energy. The former is already included in the Hamiltonian (1.3), but for the latter we have to add a potential energy contribution:

$$H = \int_{\Sigma} dA \sigma + E_{\text{pot}} . \quad (3.11)$$

To get an expression for E_{pot} it is convenient to change into a surface parametrization that is called *Monge gauge*. In this parametrization the surface is described in terms of its height $h(x, y) = h(\mathbf{r})$ above an underlying reference plane as a function of the orthogonal coordinates x and y . This is clearly applicable as long as the surface has no overhangs (see App. B.3).

Imagine now to lift a small cylinder of the liquid with area A to a height h above its original position. It then gains a potential energy of $\int_0^h dh' (Ah' \Delta\rho)g = \frac{1}{2} \Delta\rho g h^2 A$, where $\Delta\rho := \rho_l - \rho_g$ is the density difference between the density of the liquid ρ_l and the density of the gas ρ_g , and g is the acceleration due to gravity.

This can be generalized to get the potential energy of the free liquid:

$$E_{\text{pot}} = \frac{1}{2} \int_{\Sigma} dx dy \Delta\rho g h^2 . \quad (3.12)$$

A characteristic length ℓ of the system can now be obtained by combining the corresponding quantities $\Delta\rho$, g and σ :

$$\ell := \sqrt{\frac{\sigma}{g\Delta\rho}} . \quad (3.13)$$

The length ℓ is called the *capillary length* ($[\ell] = \text{m}$). For a water-air interface its value is about $\sqrt{0.073/(10 \times 1000)} \text{ m} \approx 2.7 \text{ mm}$ at room temperature. An interpretation of ℓ can be found if one considers surfaces that deviate only weakly from a plane (see App. B.3). The infinitesimal area element dA can then be written approximately as $dA = 1 + \frac{1}{2}(\nabla h)^2$ (see Eqn. (B.53)), which yields for the Hamiltonian (3.11):

$$\begin{aligned} H &= \frac{1}{2} \int_{\Sigma} dx dy \left[\sigma (\nabla h)^2 + \Delta\rho g h^2 \right] \\ &\stackrel{(3.13)}{=} \frac{1}{2} \Delta\rho g \int_{\Sigma} dx dy \left[(\ell \nabla h)^2 + h^2 \right] , \end{aligned} \quad (3.14)$$

neglecting the constant due to the first term in the expansion of dA . The shape equation for this Hamiltonian can be written as:⁴

$$(\nabla^2 - \frac{1}{\ell^2}) h = 0 . \quad (3.15)$$

⁴ Note that the symbol ∇^2 denotes the Laplacian of the (x,y) plane in contrast to the metric-compatible Laplacian Δ of the curvilinear surface.

A mode analysis now provides an interpretation for the capillary length. Considering a surface patch of area $\Lambda \times \Lambda$ one may write⁵

$$h(x, y) = h(\mathbf{r}) = \sum_{\mathbf{q}} h_{\mathbf{q}} \exp(i\mathbf{q} \cdot \mathbf{r}) , \quad (3.16)$$

with

$$\mathbf{q} = \frac{2\pi}{\Lambda} \begin{pmatrix} \nu_x \\ \nu_y \end{pmatrix} \quad \text{with } \nu_x, \nu_y \in \mathbb{Z} . \quad (3.17)$$

Then, the Hamiltonian (3.14) is proportional to

$$H \propto \sum_{\mathbf{q}} |h_{\mathbf{q}}|^2 [(\ell \mathbf{q})^2 + 1] . \quad (3.18)$$

The inverse of the vector \mathbf{q} is a measure for the length on which perturbations arise. If it is much smaller than the capillary length ℓ , the term $(\ell \mathbf{q})^2$ becomes the dominant term in Eqn. (3.18) and gravity can be neglected.

One may therefore neglect deformations due to the weight of the particle and—as a consequence—the weight of the particle itself, if one considers the interface on length scales much smaller than the capillary length, which is the case in the colloidal domain (compare the size of a colloidal particle ($\lesssim 1 \mu\text{m}$) to the capillary length of a typical liquid-gas interface such as water-air (about 1 mm)).

Consider therefore a *weightless* colloidal particle floating on the liquid: the area of the surface is minimized if the surface is flat. At the boundary the tensions σ , σ_{sg} , and σ_{sl} can balance according to the Young-Dupré equation. Hence, one would naively expect that in equilibrium the colloid immerses just deep enough into the liquid such as to match the appropriate contact angle with a flat liquid surface. But there is a problem: what happens to the *normal* force at the contact line? For the naive scenario to hold, it would have to be balanced by another force (which was called force of constraint in Sec. 3.1.1).

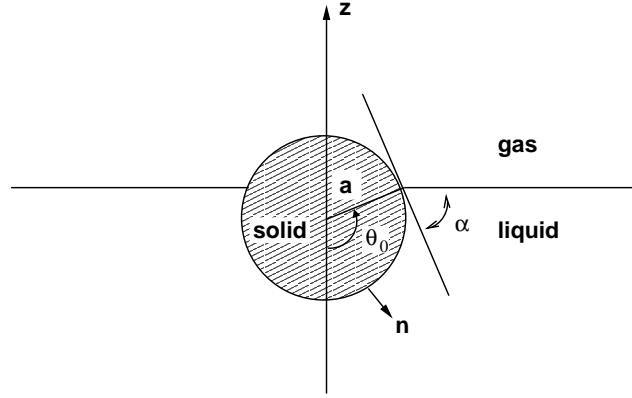
It turns out that such a force exists: it is the force \mathbf{F}_L caused by the Laplace pressure (see Sec. 1.1.2).⁶ Hence, at least for cylindrical and spherical particles, the objects we will mainly deal with, the suspicion that the liquid surface remains flat is indeed confirmed, even though the deeper reason for this is a bit more subtle.

Let us derive that for the case of a sphere⁷ with radius a and fixed angle θ_0 of immersion (see Fig. 3.4). We will show that all forces will balance if the interface is flat. If we require the Young-Dupré equation to hold, the tangential forces at the contact line already balance, and we will subsequently only have to worry about the normal ones. Our proposed counter-balance force \mathbf{F}_L consists of two parts:

⁵ One takes a Fourier sum instead of an integral because the area is not infinite.

⁶ Equation (1.7) can also be applied to a solid sphere here because both solid-fluid interfaces are treated as the liquid-gas one by assigning surface tensions to all of them.

⁷ The calculation can be done in the same manner for a cylinder.


Figure 3.4: Sphere floating on a liquid

$\mathbf{F}_L = \mathbf{F}_{\text{sg}} + \mathbf{F}_{\text{sl}}$. The force \mathbf{F}_{sg} is caused by the Laplace pressure P_{sg} which acts on the upper part Σ_{sg} of the sphere being in contact with the gas. \mathbf{F}_{sl} is caused by the Laplace pressure P_{sl} which acts on the lower part Σ_{sl} of the sphere being in contact with the liquid.

The relevant component of the forces is the vertical projection parallel to \mathbf{z} . The horizontal projections in fact cancel out because of the axial symmetry. For the vertical components we get, using spherical coordinates (r, θ, ϕ) :⁸

$$\begin{aligned} \mathbf{F}_{\text{sg}} \cdot \mathbf{z} &= - \int_{\Sigma_{\text{sg}}} dA P_{\text{sg}} \mathbf{n} \cdot \mathbf{z} = -P_{\text{sg}} a^2 \int_0^{2\pi} d\phi \int_0^{\pi-\theta_0} d\theta \sin \theta \cos \theta \\ &= -\frac{\pi}{2} a^2 P_{\text{sg}} [1 - \cos(2\theta_0)] \\ P_{\text{sg}} &\stackrel{=}{=} \frac{2\sigma_{\text{sg}}}{a} \quad -\pi a \sigma_{\text{sg}} [1 - \cos(2\theta_0)] , \end{aligned} \quad (3.19)$$

and

$$\begin{aligned} \mathbf{F}_{\text{sl}} \cdot \mathbf{z} &= - \int_{\Sigma_{\text{sl}}} dA P_{\text{sl}} \mathbf{n} \cdot \mathbf{z} = -P_{\text{sl}} a^2 \int_0^{2\pi} d\phi \int_{\pi-\theta_0}^{\pi} d\theta \sin \theta \cos \theta \\ &= \frac{\pi}{2} a^2 P_{\text{sl}} [1 - \cos(2\theta_0)] \\ P_{\text{sl}} &\stackrel{=}{=} \frac{2\sigma_{\text{sl}}}{a} \quad \pi a \sigma_{\text{sl}} [1 - \cos(2\theta_0)] . \end{aligned} \quad (3.20)$$

Combining the two forces yields

$$\begin{aligned} \mathbf{F}_L \cdot \mathbf{z} &= \pi a [1 - \cos(2\theta_0)] (\sigma_{\text{sl}} - \sigma_{\text{sg}}) \stackrel{(3.1)}{=} -\pi a [1 - \cos(2\theta_0)] \sigma \cos \alpha \\ &= -2\pi a \sin^2 \theta_0 \sigma \cos \alpha . \end{aligned} \quad (3.21)$$

⁸ Note that θ measures from the “north pole”.

The force normal to the solid \mathbf{F}_n at the three-phase boundary is equal to (cf. Sec. 3.1.1 and remember that the surface tension is a force per unit line and therefore has to be multiplied by the length of the contact line):

$$\mathbf{F}_n = (2\pi a \sin \theta_0) \sigma \sin \alpha . \quad (3.22)$$

Therefore, the component parallel to \mathbf{z} is:

$$\begin{aligned} \mathbf{F}_n \cdot \mathbf{z} &= (2\pi a \sin \theta_0) \sigma \sin \alpha \cos \alpha \stackrel{\alpha=(\pi-\theta_0)}{=} (2\pi a \sin \theta_0) \sigma \sin (\pi - \theta_0) \cos \alpha \\ &= 2\pi a \sin^2 \theta_0 \sigma \cos \alpha . \end{aligned} \quad (3.23)$$

This is indeed exactly canceled by the force due to the Laplace pressure, Eqn. (3.21), which proves that our assumption was correct and the interface is really flat—at least in the case of spherical or cylindrical colloids.

3.1.3 Pinning of the contact line

For *arbitrarily shaped* particles the situation is different: As before, the contact line at the three-phase boundary tries to adjust to the Young-Dupré equation in every point. This, however, would be generally impossible if the interface were to remain flat. In addition to that, *pinning* of the contact line may occur. This describes the situation where the contact line is pinned to impurities on the surface such that the Young-Dupré equation is generally not satisfied. One can observe that, for example, every morning when eating cornflakes for breakfast (see Fig. 3.5). Even in the case of spherical or cylindrical particles, pinning may lead to a nontrivial contact line and thus to interface deformations.

If one wants to know the actual shape of the interface in this case, one has to solve the shape equation $K = 0$ (see Table 2.1), which in small gradient expansion (see Eqn. (B.52)) turns into

$$\boxed{\nabla^2 h(\mathbf{r}) = 0} . \quad (3.24)$$

The boundary conditions fix the height h at the contact line \mathcal{C} . This problem evidently corresponds to the Dirichlet problem for a potential in electrostatics. In both cases, the solution can be obtained by using the Green function $G(\mathbf{r}, \mathbf{r}')$ of the two-dimensional Laplacian, which is $\frac{\ln|\mathbf{r}-\mathbf{r}'|}{2\pi}$. Applying Green's second identity, one gets for the height function (or potential in electrostatics) [Jac75]:

$$h(\mathbf{r}) = \oint_{\mathcal{C}} ds' \left[\frac{\partial h(\mathbf{r}')}{\partial n'} G(\mathbf{r}, \mathbf{r}') - h(\mathbf{r}') \frac{\partial G(\mathbf{r}, \mathbf{r}')}{\partial n'} \right] , \quad (3.25)$$

where s' is the arc length of the boundary curve \mathcal{C} and $\frac{\partial}{\partial n'}$ the derivative along the vector normal to the colloid. Solving this integral equation yields the shape of the surface.

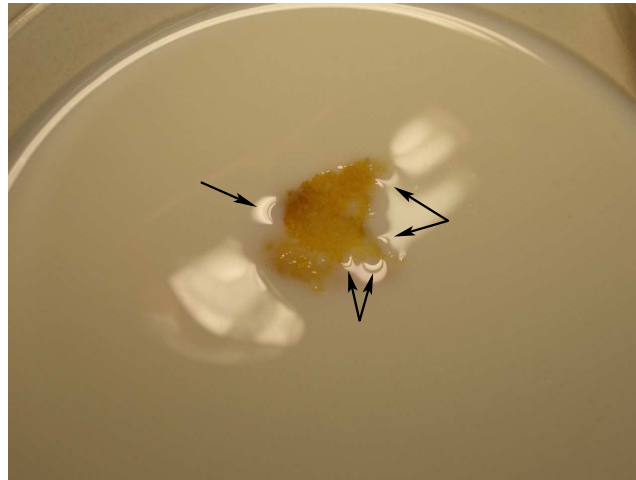


Figure 3.5: One cornflake on milk. Some spots where pinning of the contact line occurs are denoted by the black arrows.

3.2 Colloidal particle bound to a fluid membrane

Apart from liquid-gas interfaces (or more generally “soap film type” interfaces, see Sec. 1.1) the main focus in this work lies on fluid membranes (see Sec. 1.2). In the present section we will therefore study the binding of a colloidal particle to a fluid membrane.

One may distinguish two possible binding mechanisms: the colloid can either *adhere* to the membrane due to attractive interactions (see Sec. 3.2.1) or it may be *embedded* in it (see Sec. 3.2.2).

3.2.1 Adhesion

In the case of adhesion, boundary conditions analogous to the Young-Dupré equation can be found. The first one follows from the fact that a membrane cannot have any kinks, because this would lead to a singularity in the curvature energy (see Eqn. (1.10)). This implies

$$\alpha = \pi , \tag{3.26}$$

where α is the contact angle at the particle-membrane contact line. But since the Hamiltonian for a fluid membrane is of higher order in surface derivatives than the Hamiltonian for a liquid-fluid interface, there will be one more boundary condition which fixes the next order in surface derivatives, namely the contact *curvature*.

But what does this boundary condition actually look like? And how can the shape of the membrane be determined if a colloidal particle adheres to it?

Fluid membrane vesicle on a solid substrate

First, let us consider a fluid membrane vesicle adhering to a solid substrate: this situation is similar to the case where a liquid drop is bound to a solid substrate (see Fig. 3.2); in particular its geometry is essentially the same. However, the Hamiltonian is different [CG02a]:⁹

$$H = \int_{\Sigma} dA \left[\sigma + \frac{\kappa}{2}(K - K_0)^2 \right] - \int_{\Sigma_{\text{bound}}} dA u - PV, \quad (3.27)$$

where u is the adhesion energy per area. The topology of the vesicle shall be fixed, which permits us to neglect the Gaussian curvature term (cf. Hamiltonian (1.10)). However, an excess pressure P is included (cf. Hamiltonian (1.4)).

At the boundary, the curvature tensors K_{ab} and \bar{K}_{ab} of the membrane and the substrate, respectively, may be written with respect to the local coordinate frame $\{\mathbf{l}, \mathbf{t}\}$ as

$$K_b^a = \begin{pmatrix} K_{\perp} & K_{\perp\parallel} \\ K_{\perp\parallel} & K_{\parallel} \end{pmatrix}, \quad \text{and} \quad \bar{K}_b^a = \begin{pmatrix} \bar{K}_{\perp} & \bar{K}_{\perp\parallel} \\ \bar{K}_{\perp\parallel} & \bar{K}_{\parallel} \end{pmatrix}. \quad (3.28)$$

A variation of the Hamiltonian then yields the equilibrium boundary conditions [CG02a]:

$$K_{\perp} - \bar{K}_{\perp} = \sqrt{\frac{2u}{\kappa}}, \quad K_{\parallel} = \bar{K}_{\parallel}, \quad \text{and} \quad K_{\perp\parallel} = \bar{K}_{\perp\parallel}. \quad (3.29)$$

These also have to hold when a colloidal particle adheres to a fluid membrane.

Adhesion of a spherical colloid to a fluid membrane

Let us now restrict ourselves to the case of a colloid adhering to an elastic symmetric ($K_0 = 0$) fluid membrane with fixed topology and no excess pressure. The general Hamiltonian (1.10) then simplifies to:

$$H = \int_{\Sigma} dA \left(\sigma + \frac{\kappa}{2}K^2 \right) - \int_{\Sigma_{\text{bound}}} dA u. \quad (3.30)$$

Note that from the two elastic constants σ and κ one can define a characteristic length

$$\lambda := \sqrt{\frac{\kappa}{\sigma}}, \quad (3.31)$$

that separates length scales over which bending or tension are the dominant term.

⁹ Note that instead of the spontaneous curvature K_0 a term linear in the total curvature K is included in the original Hamiltonian in Ref. [CG02a]. By multiplying out $(K - K_0)^2$ one can see that these are two equivalent ways of formulating the problem.

The shape of the *bound* membrane is fixed by the shape of the colloid. For the shape of the *free* membrane, one has to set the Euler-Lagrange derivative \mathcal{E} of the free part of the Hamiltonian

$$H_{\text{free}} = \int_{\Sigma} dA \left(\sigma + \frac{\kappa}{2} K^2 \right), \quad (3.32)$$

to zero. From Table 2.1 one derives

$$-\kappa \Delta K + \frac{\kappa}{2} K(K^2 - 2K_{ab}K^{ab}) + \sigma K \stackrel{!}{=} 0. \quad (3.33)$$

Changing to Monge parametrization again and considering only the small gradient regime (where higher order terms are neglected and $K \stackrel{\text{(B.52)}}{=} -\nabla^2 h$), one gets $\kappa \nabla^2(\nabla^2 h) - \sigma \nabla^2 h = 0$, or with the help of Eqn. (3.31)

$$\boxed{\nabla^2(\nabla^2 - \frac{1}{\lambda^2})h = 0}. \quad (3.34)$$

This differential equation is solved by eigenfunctions of the Laplacian (corresponding to the eigenvalues 0 and λ^{-2}) while respecting the appropriate boundary conditions (3.26) and (3.29) [DB03].¹⁰

If one considers a *spherical* colloid adhering to a fluid membrane, the general solution of Eqn. (3.34) may be obtained by exploiting cylindrical symmetry and introducing a coordinate system with variables ρ and ϕ as depicted in Fig. 3.6:

$$h(\rho) = h_1 + h_2 \ln(\rho/\lambda) + h_3 I_0(\rho/\lambda) + h_4 K_0(\rho/\lambda), \quad (3.35)$$

where I_0 and K_0 are the modified Bessel functions of the first and the second kind, respectively.

The function $I_0(\rho/\lambda)$ diverges for $\rho \rightarrow \infty$. Thus, if one wants the profile to be flat at infinity, $h_3 = 0$. One also has to bear in mind that the energy density should still be integrable. This is not the case for the $\ln(\rho/\lambda)$ term. Therefore, h_2 also has to be zero.

The remaining coefficients can be determined by exploiting the continuity of the profile and the slope at the contact line.¹¹ One gets [DB03, Des04]

$$h(\rho) = -a \cos \theta_0 + \lambda \tan \theta_0 \frac{K_0(\rho/\lambda) - K_0(ka/\lambda)}{K_1(ka/\lambda)}, \quad \text{with } k := \sin \theta_0. \quad (3.36)$$

This is the solution in the small gradient regime for the *free* interface. The higher the angle θ_0 the worse this approximation becomes (see Fig. 4 in Ref. [DB03]).

¹⁰ Note that the Eqns. (3.29) are still relevant for the whole problem because the terms $\int_{\Sigma} dA \beta K$ and $-PV$, that were dropped out in (3.30), have no further influence on them.

¹¹ The conditions $K_{\parallel} = -1/a$ and $K_{\perp} = 0$ are then automatically fulfilled.

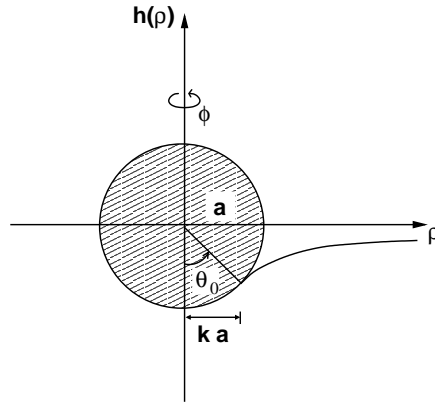


Figure 3.6: Sphere adhering to a fluid membrane

Note that the last remaining boundary condition

$$K_{\perp} = -\frac{1}{a} + \sqrt{\frac{2u}{\kappa}}, \quad (3.37)$$

derived from (3.29), has not been taken into account yet. It is recovered automatically if one searches for true equilibrium shapes of the whole complex by minimizing the *complete* Hamiltonian (3.30) via $\frac{\partial H}{\partial \theta_0} = 0$ [DB03, Des04].

If $\sigma = 0$, which means that the membrane is only characterized by bending, one can find an analytical solution even for the nonlinear Eqn. (3.33): for every possible angle of detachment θ_0 , the free part of the membrane forms a catenoid, which is an axially symmetric minimal surface with $K = 0$ at every point and therefore does not contribute to the energy [Kre91]. Since adhesion energy as well as bending energy are now simply proportional to the area of the sphere, the colloid is either completely wrapped by the membrane or not wrapped at all [Des04].

3.2.2 Membrane inclusions

Apart from *adhering* to an interface, colloidal particles may also be *embedded* in it. One typical example is a protein inclusion in a membrane (see Sec. 1.2.3).

Consider a cone-shaped protein: one may model such an inclusion as a circular disc with radius a that simply imposes a fixed contact angle α on its circular boundary (see for instance [GBP93]). At the spot where the inclusion sits the membrane has a “hole”. Because of that, there is no need to include an adhesion energy into the relevant Hamiltonian. For the same reason, the region of integration, Σ , is no longer simply connected. The Gaussian curvature term (cf. Hamiltonian (1.10)), however, can again be neglected due to the Gauss-Bonnet theorem: the geodesic curvature K_g is fixed at the contact line due to the fixed contact angle and the integral over

K_G is thus a topological invariant (see App. B.2). Therefore, Eqn. (3.30) turns into:

$$H = \int_{\Sigma} dA \left(\sigma + \frac{\kappa}{2} K^2 \right). \quad (3.38)$$

The shape of such a membrane can be obtained in a similar way as in the previous section. Now, however, the boundary condition is simpler: the derivative of the height function $h(\rho)$ is equal to the fixed contact angle α . One gets in small gradient expansion

$$h(\rho) = -\frac{\alpha\lambda}{K_1(a/\lambda)} K_0(a/\lambda) + \text{const}. \quad (3.39)$$

In addition, one may impose more complicated boundary conditions for inclusions that are anisotropic by locally fixing the extrinsic curvature tensor at the positions of the inclusions [BF03, MM02]. Here, we will, however, restrict ourselves to the case of *discoidal inclusions*.

Furthermore, a protein may cause a local change in thickness of the membrane bilayer if its hydrophobic part is smaller or larger than that of the bilayer (*hydrophobic mismatch*) [DPS93]. This effect, however, will also *not* be studied in this work.

4 Forces between interface-bound particles

4.1 Interface mediated interactions

In the previous chapter we have examined the manner in which a single particle deforms an interface to which it is bound. Conversely, a deformation in the interface can interact with a bound particle. A deformation field created by one particle at the interface may therefore interact with a second particle which is also bound to the same interface and spatially separated from the first one. The thereby induced forces are called *interface mediated interactions*.

In general, physical interactions between particles are mediated by fields: matter, for instance, curves spacetime itself; if it is charged, it will additionally interact through the electromagnetic field. Colloidal particles in suspension can also create an effective field by distorting the order of an embedding liquid crystal and thereby inducing an interaction of a more indirect nature [GFS03, PSLW97].

Interface mediated interactions are an important, purely geometrical example of such interactions. At first glance, it is not obvious whether two particles of a certain shape and bound to a certain interface will attract or repel each other: consider, for instance, two identical spherical particles adhering to the same side of an interface. In the case of a liquid-fluid interface including gravity the spheres attract each other [KN94]. If the interface were a tensionless fluid membrane and the particles were to adhere only partially,¹ they would feel a repulsion.²

One can find cases where the circumstances get even more confusing: consider two cylindrical particles adhering to the same side of an interface, such as the two sewing needles in Fig. 1 of the introduction. Let us neglect end effects and restrict ourselves to the case where the cylinders are parallel to each other. We then obtain an effectively one-dimensional problem, which exhibits a surprising feature: if one considers a liquid-fluid interface including gravity on the one hand, and a fluid membrane on the other, one will see that the shape of the interfaces is exactly the same as long

¹ Note that we have to arrange things “by hand” such as to avoid getting the equilibrium situation of complete or zero wrapping (see end of Sec. 3.2.1), which would not lead to interface deformations away from the sphere. This can be done, for instance, by making only one hemisphere attractive with respect to the membrane.

² The deformation of the free membrane due to *one* single sphere costs no energy (see Sec. 3.2.1). Bringing two spheres together can therefore only raise the energy. This leads to a repulsion.

| | <i>soap film</i> ($\mathcal{H} = \sigma$) no gravity + gravity | | <i>fluid membrane without tension</i> ($\mathcal{H} = \frac{\kappa}{2}K^2$) same opposite | | <i>fluid membrane under tension</i> ($\mathcal{H} = \sigma + \frac{\kappa}{2}K^2$) same opposite | |
|-----------|---|----------|--|-------------|---|------------------|
| cylinder | \emptyset | \oplus | \emptyset | \emptyset | \ominus | \oplus |
| sphere | \emptyset | \oplus | \emptyset | \emptyset | ? | ? |
| inclusion | — | — | \ominus | \ominus | \ominus | \oplus/\ominus |

Table 4.1: Sign of the interaction between *two identical colloids* depending on interface type and colloidal shape (\oplus = attraction, \ominus = repulsion, \oplus/\ominus = attraction or repulsion depending on the particles' distance, \emptyset = no interaction, — = not relevant). In the case of the membrane the particles may either adhere to the *same* or to *opposite* sides. Note that pinning is not included in this table because the sign of the force depends strongly on the shape and orientation of the pinned contact line (see Secs. 4.3 and 6.1).

as the contact angle is equal to π in both cases.^{3,4} But, although the shapes are identical, the forces are not! Even the sign is different: Two cylinders on a liquid-fluid interface attract each other (see Fig. 1), whereas two cylinders at the same membrane side feel a repulsion. This is understandable if one is clear on the fact that the energetics not only determines the *shape* of the interface but also the *stress tensor* (see Sec. 2), which can be different even though the shapes are the same. The stress tensor, however, determines the forces, as will be made clear in Chap. 5. These few introductory remarks serve to motivate our interest in the *sign* of interface mediated interactions. In Table 4.1 an overview of possible shape-interface combinations is provided. For inclusions, the interactions are only known in linear approximation, the question marks denote cases where the sign is not known at all. Most of the situations depicted in the table will be considered in the following: first by an energetical approach—which is the one used in the literature—and then by a stress tensor approach, which is the new idea this thesis is based upon.

³ In the membrane case this is a necessary boundary condition (see Eqn. (3.26)); in the liquid-fluid case one has to choose the materials to be completely non-wetting.

⁴ One can see that the shapes are identical for identical characteristic length scales, $\lambda = \ell$, by considering the two corresponding linearized shape Eqns. (3.15) and (3.34), which yield the same height function if one respects the appropriate boundary conditions for the two cylinders. By changing to an angle-arc length parametrization (see [SBL91] for instance), which is more convenient than Monge in this case, one can show that the shapes are identical even if one considers the complete *nonlinear* problem.

4.2 Forces via the energy

How can the interface mediated force be calculated for a given situation? To answer that question let us consider the energetics of a two particle system: *its complete energy is not equal to twice the energy of the one particle system.*⁵ *It rather depends on the relative positions of the two particles. Thus, a derivative of the energy with respect to the appropriate coordinates yields the interface mediated force.*

In order to get the energy for given particle positions, one has to find the energy minimizing shape of the two particle-interface system first. There is, however, a major obstacle: the relevant field equations are nonlinear differential equations. Even if the Hamiltonian density \mathcal{H} only depends on quadratic invariants such as in the case of the fluid membrane Hamiltonian (1.10), the interface is still curvilinear. This is the reason why it is usually impossible to obtain exact analytical solutions. One way to find at least approximate shapes is to restrict oneself to essentially flat interfaces, which allows one to parameterize the surface in Monge gauge, and expand the height function and all other surface quantities in a small gradient expansion (see App. B.3). One then gets linear differential equations which can be solved by Green functions. The boundary conditions at the contact lines, however, also have to hold (see Chap. 3). A superposition ansatz in the spirit of Nicolson [Nic49] that superimposes two single-particle solutions of the field equations normally violates these boundary conditions. But, even if one finds solutions where they are respected, it is not clear at all how the result can be generalized to the full nonlinear situation. Thus, the energy cannot be calculated in general. Consequently, there is also no chance to differentiate it to get the force. It is possible, however, to gain new insights by considering stresses: even if the exact shape is not known, certain symmetries may be exploited to obtain exact formulas for the force, the sign of which is sometimes evident.

Before demonstrating that, let us discuss the energetic approach a bit closer for the following situation, which we will restrict ourselves to in the rest of this work: Consider a system of two identical colloidal particles bound to an asymptotically flat interface, as is schematically sketched in Fig. 4.1. The surface is embedded in \mathbb{R}^3 . We call the basis vectors of this three-dimensional Euclidian space $\{\mathbf{x}, \mathbf{y}, \mathbf{z}\}$. For the following we choose the surface to be parallel to the (x, y) plane far away from the colloids and align their centers along the x -direction such that the origin of the coordinate system is exactly in the middle between the two particles.

Here, and also in all other examples in the following chapters, the focus will be on interfaces whose free parts can be described by the Hamiltonian density.⁶

$$\boxed{\mathcal{H} = \sigma + \frac{\kappa}{2} K^2} . \quad (4.1)$$

⁵ This is due to the fact that the energy is in general not a linear function of the profile.

⁶ Note in particular that gravity will be neglected by restricting the analysis to colloidal particles.

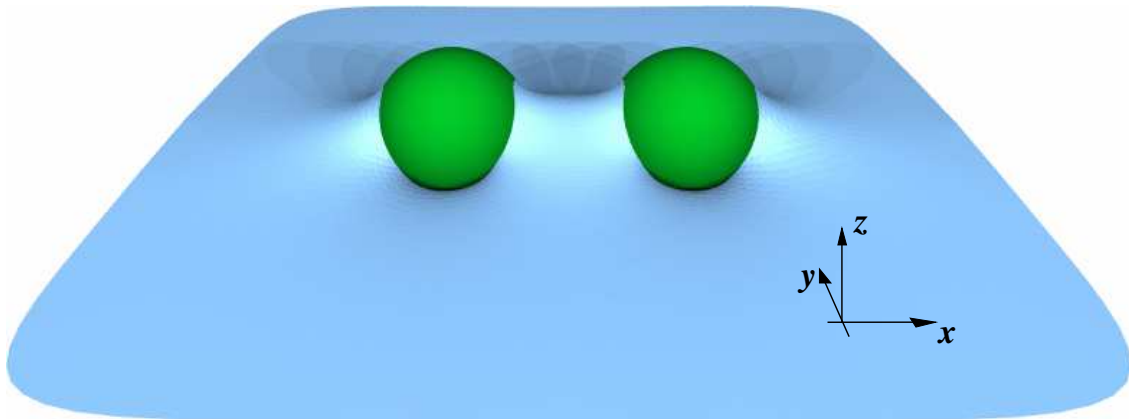


Figure 4.1: Two identical particles bound to an interface. Note that each particle deforms the interface; in-between the particles these deformations overlap.

For $\kappa \neq 0$ and $\sigma \neq 0$, \mathcal{H} describes an elastic symmetric fluid membrane under tension. However, Hamiltonian (4.1) is also applicable for soap films (setting $\kappa = 0$) and tensionless membranes (setting $\sigma = 0$). Remember that the characteristic length, marking the crossover between tension and bending dominance, was defined as $\lambda = \sqrt{\kappa/\sigma}$ (see Sec. 3.2.1).

Considering essentially flat interfaces, the Hamiltonian (4.1) can be rewritten in small gradient expansion (see App. B.3, Eqns. (B.52) and (B.53)) as:

$$H = \int dx dy \left[\frac{\sigma}{2} (\nabla h)^2 + \frac{\kappa}{2} (\nabla^2 h)^2 \right]. \quad (4.2)$$

Applying the general approach as described above one starts an analysis of this Hamiltonian by determining the energy minimizing shape of the surface for a given attachment of two particles, that is $h(x, y)$. This can be done by solving the shape equation with the appropriate boundary conditions. After reinserting the resulting height function back into Eqn. (4.2), the energy can be calculated, which will then parametrically depend on the distance d between the bound particles. A derivative of the energy with respect to d yields the forces between them. This program has been followed very frequently in the literature (see for instance [SDJ00, FG02, Wei03, WKH98]), which is why we will limit ourselves to a brief discussion of one example below. Explicit results for specific situations can be found in Chap. 6 where the quantitative comparison to the stress tensor approach (see Chap. 5) will be drawn.

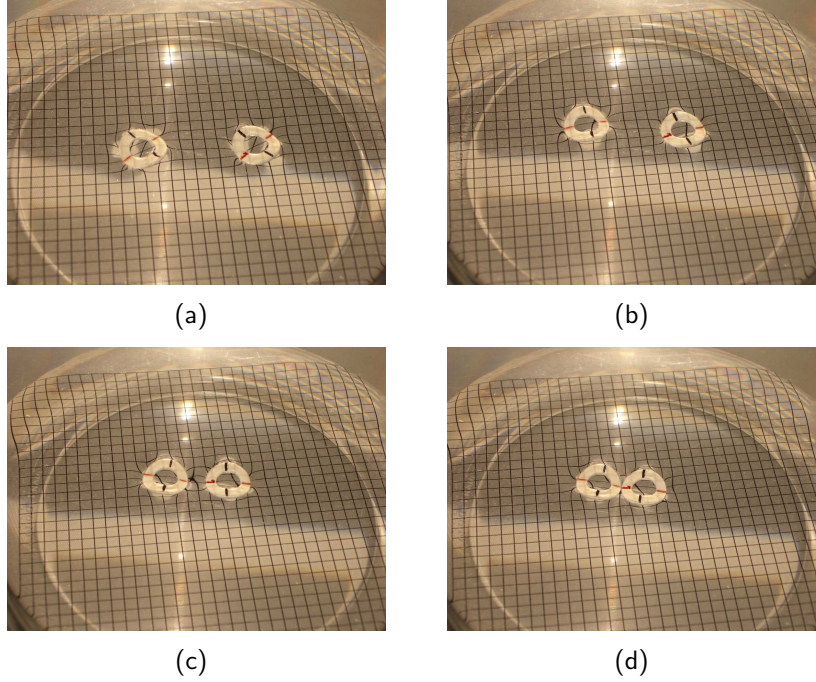


Figure 4.2: Interaction of two quadrupoles on water. The two polyamide rings are kinked in such a way that their contact line forms a quadrupole.

4.3 Example: Two quadrupoles on a soap film

Let us now consider one brief example here: a soap film where

$$H = \frac{\sigma}{2} \int dx dy (\nabla h)^2 . \quad (4.3)$$

The interface has to fulfill the shape equation, which in small gradient expansion becomes (see Eqn. (3.24))

$$\nabla^2 h(x, y) = 0 . \quad (4.4)$$

In Sec. 3.1.2 we noticed that a spherical or cylindrical colloidal particle does not deform the interface. Therefore, no deformation field exists and the force between two particles adhering to the interface must be equal to zero for all separating distances d (see Table 4.1).

This changes if one allows for pinning (see Sec. 3.1.3). The height function can then be calculated in a similar way to Eqn. (3.25): however, one now has to integrate over both contact lines. The force is then obtained as described above.

Consider two spherical particles with a contact line that departs only weakly from a circle and let us expand its shape in a multipole series. The lowest multipole order that causes a nontrivial term in lowest order of the energy is the *quadrupole* [FG02, SDJ00] (see Fig. 4.1 where the particles' contact lines are quadrupoles).

Fig. 4.2 gives an illustration of such a situation: two polyamide rings are carefully put on a water-air interface. They are deformed in such a way that their circumference is a quadrupole in the above-mentioned sense: the red marking denotes the axis at which the ring is bent down, the black at which it is bent up. Both particles deform the interface. As soon as their deformations overlap they start to interact. One observes that identical colors “attract” (as can be seen for the red markers in Fig. 4.2).

One might suspect that the weight of the particles is the driving force, just as in the case of the two floating sewing needles (see Fig. 1 of the introduction). This is, however, not true: by carefully pushing one of the markers of one quadrupole to a same-color marker of the other quadrupole, one can easily check that red and black markings actually *repel* each other. This shows that gravity is not the dominant effect because it should result in an attraction irrespective of the quadrupole orientation. Although macroscopic, the model system in Fig. 4.2 is therefore appropriate to demonstrate forces between colloidal particles. Note also that electrostatic or magnetic interactions can be excluded due to the material of the rings.

In Sec. 6.1 the interface mediated forces for that particular case will be calculated explicitly in order to understand the experimental observations mentioned here. In the same chapter, calculations for other examples will also be presented.

5 Forces via the stress tensor

5.1 General approach

Apart from differentiating energies, interface mediated forces can also be expressed via integrals over the surface stress tensor. Before discussing that approach, however, let us shortly summarize what has been achieved so far: in the first chapter, we have learned how free interfaces can be described and sorted according to their energetics. In Chap. 2, we have considered stresses in interfaces and have found an expression for the total internal force on a strained surface patch Σ_0 in terms of the surface stress tensor \mathbf{f}^a :

$$\mathbf{F}_{\Sigma_0} = \int_{\Sigma_0} dA \nabla_a \mathbf{f}^a = \oint_{\partial\Sigma_0} ds l_a \mathbf{f}^a, \quad (5.1)$$

where $\mathbf{l} = l^a \mathbf{e}_a$ is the outward pointing unit normal to the boundary curve (see Eqn. (2.3)). We then have derived expressions for the surface stress tensor of most of the interfaces discussed in Chap. 1.

In Chap. 3, it has been explained how the shape of the interface can be determined if one colloid is bound to it. This gave us the tools for studying the energetics of interface mediated interactions in Chap. 4.

With all of this being done, it is now quite easy to formulate the problem in terms of the stress tensor. Consider Eqn. (5.1) again: it is by definition clear that the total force must be zero in equilibrium if there are no external stresses acting on Σ_0 . The situation changes as soon as external stresses act: a source of stress, *e. g.* a colloidal particle adhering to a part of Σ_0 , can cause a non-zero total force on the patch. Note that this force can be calculated as the line integral of the surface stress tensor along *any* curve including the source as long as it is closed and encircles only this particular source, because the stress tensor is *divergence free* (see Chap. 2, Eqn. (2.21)).¹

These general considerations can be applied to special situations of interface mediated interactions between colloidal particles: let us look again at two identical

¹ Contrary to colloids, which act *locally*, a pressure difference P across the interface constitutes a *continuous* source of stress. However, we have seen that in this case it is possible to define a new stress tensor $\check{\mathbf{f}}^a$ which is again divergence free (see Eqn. (2.27)). This should allow a treatment of the interaction problem similar to the cases without excess pressure but in the present work we will not follow up on this program.

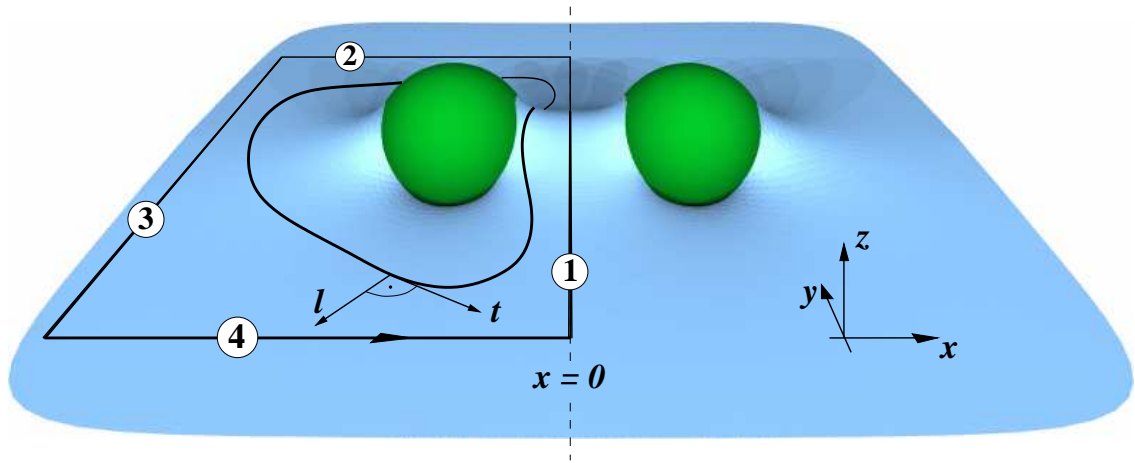


Figure 5.1: Illustration of how the force on one of a pair of particles bound to an interface is given as a closed line integral of the surface stress tensor. The contour can subsequently be deformed to exploit the symmetry of the situation.

colloidal particles bound to an asymptotically flat surface as in Chap. 4. The coordinate system is the same as before with the centers of the colloids being aligned along the x -direction such that the origin is exactly in the middle between the two particles (see Sec. 4.2 and Fig. 5.1).

A situation like that can only be stationary if external constraining forces fix the particles' positions (see Sec. 4.2). These forces are the sources of stress one actually picks up while integrating. However, we want to know the force acting on one of the particles if there were no constraining forces. An additional minus sign stems from this.

Note also that only the *separation* of the particles shall be fixed. Their height and orientation are free to change and therefore equilibrate. The same holds for the contact lines between surface and colloid.

The calculation of the forces between the two colloids can be simplified if the situation displays one of the two following symmetries: either a symmetry plane, which is equal to the (y, z) plane (*symmetric* situation) or a twofold symmetry axis, which coincides with the y axis (*antisymmetric* situation), exist. The *symmetric* case is, for example, present if the two particles adhere at the same side of the surface, the *antisymmetric* one if they are at opposite sides (see Fig. 5.2).

If we restrict ourselves to such configurations, we can exploit the fact that the contour of the line integral (5.1) can be deformed: as it is sketched in Fig. 5.1, the contour can be pulled open wide enough such that the surface is finally flat at branches 2, 3, and 4 and the stress tensor thus very simple. The contributions from branches 2 and 4 will in fact cancel each other; the only mathematically involved term stems from branch 1. An integration as in Eqn. (5.1) yields the force on the

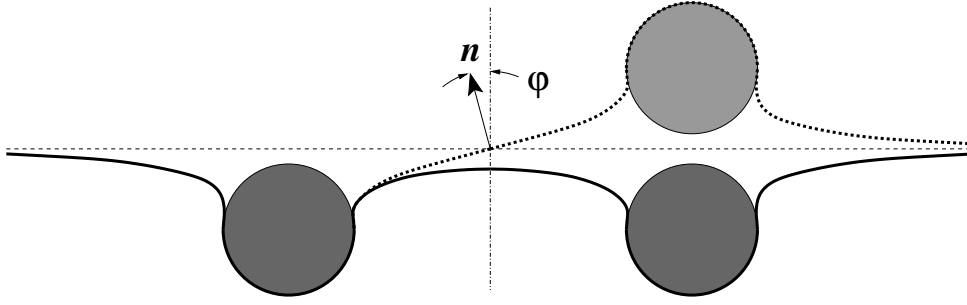


Figure 5.2: Illustration of the geometry of a symmetric (solid line) and an antisymmetric (dotted line) two-particle attachment. The symbol φ denotes the angle between the surface normal \mathbf{n} and the z axis.

colloid. In all of the following it will be the force on the left particle which is actually calculated, but due to Newton's third law this force is of course equal and opposite to the force on the right particle.

With this in mind, the general approach can now be turned into exact analytical expressions.

5.2 Explicit force formulas

Let us focus again on the case of an elastic symmetric fluid membrane, described by the Hamiltonian density

$$\mathcal{H} = \sigma + \frac{\kappa}{2} K^2 . \quad (5.2)$$

From Table 2.1, one reads off the associated surface stress tensor:

$$\mathbf{f}^a = \left[\kappa (K^{ab} - \frac{1}{2} K g^{ab}) K - \sigma g^{ab} \right] \mathbf{e}_b - \kappa (\nabla^a K) \mathbf{n} . \quad (5.3)$$

The force on the left particle will be calculated in a coordinate system with the (orthonormal) tangent vectors $\{\mathbf{t}, \mathbf{l}\}$ as basis vectors on the contour, where $\mathbf{t} = t^a \mathbf{e}_a$ points along the integration line and $\mathbf{l} = l^a \mathbf{e}_a$ points normally outward (see Fig. 5.1). This simplifies the relevant quantities: the extrinsic curvature tensor is diagonal along branch 1 because this branch is a line of curvature now due to the symmetry. Thus, the principal curvatures are equal to $K_{\perp} = l^a l^b K_{ab}$ and $K_{\parallel} = t^a t^b K_{ab}$.

For the force on the left particle stemming from branch 1 (see Fig. 5.1) one gets according to Eqns. (5.1) and (5.3):

$$\begin{aligned} \mathbf{F}_1 &= - \int_1 ds l_a \mathbf{f}^a \\ &= - \int_1 ds \left\{ \left[\kappa (l_a K^{ab} - \frac{1}{2} K l^b) K - \sigma l^b \right] \mathbf{e}_b - \kappa (l_a \nabla^a K) \mathbf{n} \right\} . \end{aligned} \quad (5.4)$$

Recall that the minus sign out front comes from the fact that the interface mediated force on the particle is opposite to the external force necessary to counterbalance it (cf. discussion in Sec. 5.1). The first term of the integrand can be rewritten by exploiting completeness, $g_b^c = l_b l^c + t_b t^c$:

$$\begin{aligned} l_a K^{ab} e_b &= l_a K^{ab} (l_b l^c + t_b t^c) e_c \\ &= l_a l_b K^{ab} \mathbf{l} + l_a t_b K^{ab} \mathbf{t} \\ &= K_{\perp} \mathbf{l}, \end{aligned} \tag{5.5}$$

where $l_a t_b K^{ab} = 0$ because the integration runs along a line of curvature. Furthermore, one defines $\nabla_{\perp} := l_a \nabla^a = \partial/\partial l$. With this, Eqn. (5.4) turns into

$$\mathbf{F}_1 = - \int_1 ds \left\{ \left[\kappa \left(K_{\perp} - \frac{1}{2} K \right) K - \sigma \right] \mathbf{l} - \kappa (\nabla_{\perp} K) \mathbf{n} \right\}. \tag{5.6}$$

Since the trace K of the extrinsic curvature tensor can be written as $K = K_{\perp} + K_{\parallel}$, this simplifies the force further to

$$\boxed{\mathbf{F}_1 = - \int_1 ds \left\{ \left[\frac{1}{2} \kappa (K_{\perp}^2 - K_{\parallel}^2) - \sigma \right] \mathbf{l} - \kappa (\nabla_{\perp} K) \mathbf{n} \right\}}. \tag{5.7}$$

This equation is one of the central results of this work. In order to understand its implications better, let us now look separately at the two different possible symmetries: either a symmetry plane (*symmetric* situation) or a symmetry axis (*antisymmetric* situation) exist (see Fig. 5.2 and discussion in Sec. 5.1).

The symmetric case

Let us first consider the *symmetric* case: tangent and normal vector on branch 1 lie in the (y, z) plane, hence $\mathbf{l} = \mathbf{x}$ (where \mathbf{x} is the unit vector pointing in the horizontal x -direction). The derivative of K in the direction of \mathbf{l} along branch 1, $\nabla_{\perp} K$, is zero due to mirror symmetry. On branch 3 the surface is flat and thus the stress tensor is equal to $\mathbf{f}_{a,3} = -\sigma \mathbf{e}_a$. With this information the total force $\mathbf{F}_1 + \mathbf{F}_3 = F_{\text{sym}} \mathbf{x}$ on the left particle can be written as:

$$\boxed{F_{\text{sym}} = \sigma \Delta L - \frac{1}{2} \kappa \int_1 ds (K_{\perp}^2 - K_{\parallel}^2)}, \tag{5.8}$$

where $\Delta L > 0$ is the excess length of branch 1 compared to branch 3.

The contribution due to tension is attractive: it is positive, points therefore into the positive x -direction and thus *towards* the other particle. Unfortunately, the curvature contribution has no evident sign in general. However, for two *parallel cylinders* adhering to the *same side* of the interface the overall sign becomes obvious,

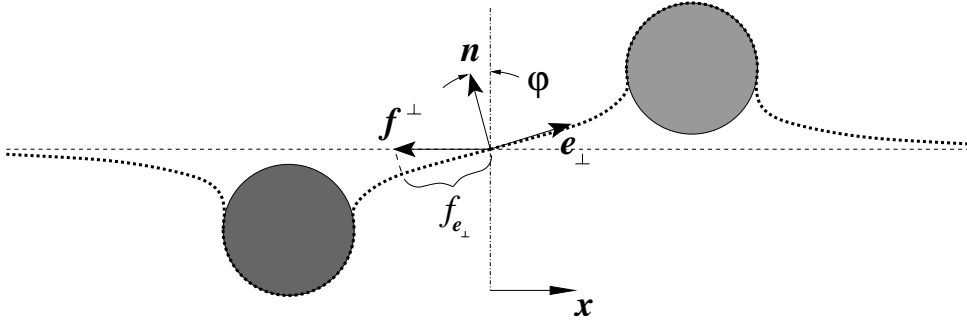


Figure 5.3: Two cylinders at opposite interface sides. The vector \mathbf{f}_\perp is the surface stress tensor at the midline, \mathbf{e}_\perp the outward pointing unit normal to the midline, which is also tangential to the surface, and f_{e_\perp} is the projection of \mathbf{f}_\perp onto \mathbf{e}_\perp .

as long as the particles are long enough such that end effects can be neglected: the contribution K_\parallel^2 then vanishes because the mid-curve becomes a line. For the same reason $\Delta L = 0$. This leads to the formula

$$F_{\text{sym,cyl}}/L = -\frac{1}{2}\kappa K_\perp^2, \quad (5.9)$$

where L is the length of one cylinder. Thus, the two cylinders repel each other.

The antisymmetric case

In the *antisymmetric* case branch 1 is a twofold symmetry axis and therefore a line; hence $K_\parallel = K_\perp = 0$. While the sign of $\nabla_\perp K_\parallel$ is not obvious, the derivative $\nabla_\perp K_\perp$ is smaller than zero because K_\perp changes sign from positive to negative. The profile on the midline is always tilted by the angle $\varphi(s)$ in the direction indicated in Fig. 5.2, because situations with more than one nodal point in the height function between the particles are expected to have higher energies. The horizontal separation of the particles is fixed; other degrees of freedom, such as the height or the tilt, are allowed to equilibrate (see Sec. 5.1). The force on the left particle is therefore again parallel to \mathbf{x} , $\mathbf{F}_{\text{antisym}} = F_{\text{antisym}}\mathbf{x}$, and given by

$$F_{\text{antisym}} = \int_1 ds \left[\sigma(\cos \varphi(s) - 1) - \kappa \sin \varphi(s) \nabla_\perp (K_\perp + K_\parallel) \right], \quad (5.10)$$

where it was exploited that $\mathbf{x} \cdot \mathbf{l} = \cos \varphi$ and $\mathbf{x} \cdot \mathbf{n} = -\sin \varphi$ at the midpoint. Note that the tension contribution is repulsive this time but the sign of the curvature term is again not obvious.

If we restrict ourselves to the case of two *parallel cylinders* at *opposite sides* of the interface, however, then $\nabla_\perp K_\parallel$ is equal to zero. Furthermore, $|\mathbf{f}_a|$ is constant on

each of the three membrane segments. The stress tensor at branch 1, $\mathbf{f}^\perp := \mathbf{f}_{a,1}$, must be horizontal to the \mathbf{x} axis because vertical components equilibrate to zero as mentioned above (see Fig. 5.3). Defining $\mathbf{e}_\perp := \mathbf{l}$ at branch 1, one can write:

$$f_{\mathbf{e}_\perp} := \mathbf{f}^\perp \cdot \mathbf{e}_\perp = (\mathbf{f}^\perp \cdot \mathbf{x})(\mathbf{x} \cdot \mathbf{e}_\perp) . \quad (5.11)$$

From this it follows that $\mathbf{f}^\perp \cdot \mathbf{x} = \text{sign}(f_{\mathbf{e}_\perp}/\mathbf{x} \cdot \mathbf{e}_\perp) |\mathbf{f}^\perp|$. We know that $\mathbf{x} \cdot \mathbf{e}_\perp = \cos \varphi > 0$ and $f_{\mathbf{e}_\perp} = -\sigma < 0$. Therefore, we find $\mathbf{f}^\perp = -|\mathbf{f}^\perp| \mathbf{x}$ at the midpoint. This reduces Eqn. (5.10) to

$$F_{\text{antisym,cyl}}/L = |\mathbf{f}^\perp| - \sigma = \sqrt{\sigma^2 + (\kappa \nabla_\perp K_\perp)^2} - \sigma \geq 0 , \quad (5.12)$$

which now implies particle attraction. The length L is again the length of one cylinder.

Eqns. (5.8)–(5.10) and (5.12) are the promised analytical force formulas which link the *force* of interaction between two attached particles to the *geometry* of the surface at the midplane between them. It is worth to reemphasize that they are *exact*, even in the nonlinear regime. To check their validity in full generality is thus difficult, because basically no analytical results are known in the nonlinear case. In the next chapter, in which such a check shall be performed, we will therefore content ourselves to a comparison with analytically known results in the linear small gradient regime.

6 Comparison between the approaches

The idea of this chapter is to illustrate the validity of the general stress tensor approach by focusing on a few important examples of two particles being attached to either a soap film (see Sec. 6.1) or a membrane (see Sec. 6.2).

The following problems have already been considered in Refs. [SDJ00, FG02, Wei03, WKH98] where their energetics have been studied. Note, however, that this was only done in the small gradient regime, using the Hamiltonian

$$H = \int dx dy \left[\frac{\sigma}{2} (\nabla h)^2 + \frac{\kappa}{2} (\nabla^2 h)^2 \right], \quad (6.1)$$

and appropriate values for σ and κ (see Eqn. (4.2)).

To draw a quantitative comparison between the results of the literature and the ones of the stress tensor approach, the force can be calculated in two ways: first, by differentiating the energy found in the literature with respect to the particle separation following the energy approach as it is explained in Sec. 4.2. Second, by inserting the given height profile $h(x, y)$ into the force formulas derived in the previous chapter. In all cases the outcome turns out to give coinciding results, which validates our new formulas, at least in the linear regime.

6.1 Soap film type

For soap films, $\kappa = 0$ and we have

$$H = \frac{\sigma}{2} \int dx dy (\nabla h)^2. \quad (6.2)$$

In Sec. 4.3 we found out that two spherical or cylindrical particles on a soap film do not interact with each other if their attachment to the film is governed by a simple stress-adhesion balance (Young-Dupré equation). For symmetric and antisymmetric configurations this can be confirmed via the stress tensor approach: consider two parallel cylindrical colloids adhering to the same side of the soap film (*symmetric situation*). Equation (5.8) states that the force is then proportional to the excess length if one neglects end effects. The excess length, however, is equal to zero as long as the contact lines are straight. Therefore, the force is also zero. Likewise, in

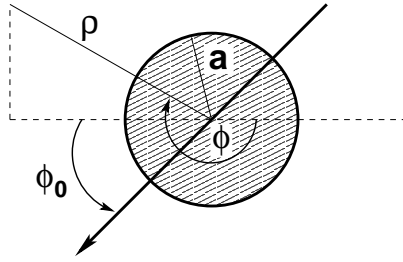


Figure 6.1: Coordinates chosen for one quadrupole (seen from above)

the *antisymmetric* situation the soap film between both cylinders is flat as long as the verticle particle positions can equilibrate. Therefore, $\varphi(s) = 0$ (see Fig. 5.2) and Eqn. (5.10) yields zero for the force, just as in the symmetric case. In an analogous way one obtains the same result for the case of spheres.

Let us now consider *pinning* again and restrict ourselves to two spherical particles with radius a and a contact line that only weakly departs from a circle (cf. Sec. 4.3). Stamou *et al.* [SDJ00] have studied this case by using a superposition ansatz in the spirit of Nicolson [Nic49]: first, the height function of one isolated particle is calculated with the correct boundary conditions. Then, the complete height function is assumed to be the sum of the two single-particle fields of each of the two colloids. Strictly speaking, this approach destroys the boundary conditions at the particles' contact lines but it gives the correct result in leading order in the limit of large separation.¹ Using polar coordinates ρ and ϕ , the solution of the shape Eqn. (4.4) for a single sphere can be written as [SDJ00]

$$h_{\text{sphere}}(\rho, \phi) = A_0 \log \left(\frac{a}{\rho} \right) + \sum_{m=1}^{\infty} A_m \cos [m(\phi - \phi_{m,0})] \left(\frac{a}{\rho} \right)^m, \quad (6.3)$$

with multipole coefficients A_m and phase angles $\phi_{m,0}$. The former can be determined as follows: The monopole A_0 vanishes because there is no external force such as gravity dragging on the particle. The dipole coefficient A_1 parameterizes the *tilt* of the contact line relative to the z axis; it also vanishes if there is no external torque acting on the sphere. All higher multipole coefficients can be read off from the Fourier expansion of the contact line at $\rho = a$, in particular the quadrupole coefficient $Q := A_2$. It is intuitively obvious and indeed confirmed by a more careful calculation [FG02, SDJ00] that the quadrupole is the lowest multipole order that causes a nontrivial term in lowest order of the energy.

¹ Note that it is also possible to solve the shape equation exactly in small gradient expansion [FG02]. However, both calculations yield the same energy in lowest order. Therefore, the easier approach is presented here.

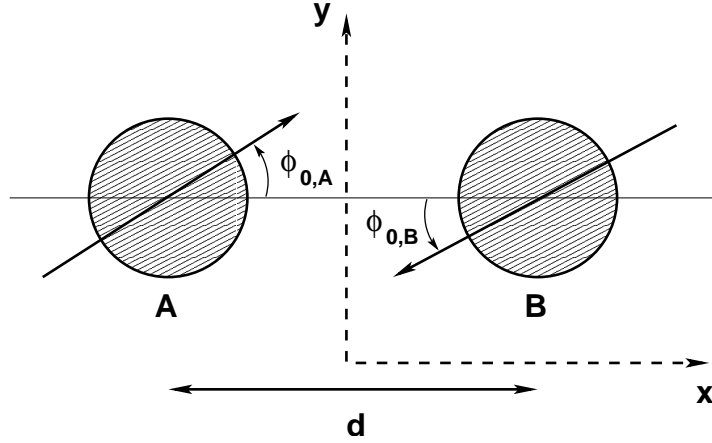


Figure 6.2: Two quadrupoles on a soap film (seen from above)

One can therefore restrict the calculation to the single-particle height function [SDJ00]

$$h_{\text{sphere}}(\rho, \phi) = Q \cos[2(\phi - \phi_0)] \left(\frac{a}{\rho}\right)^2, \quad (6.4)$$

where $\phi_0 := \phi_{2,0}$ is the angle that represents the rotation of the particle about z (see Fig. 6.1).

If the complete height function is then just a superposition as mentioned above, the force on the left particle in lowest order is given by [FG02, SDJ00]

$$\mathbf{F}_{\text{sym,soap}} = -\mathbf{F}_{\text{antisym,soap}} = 48\pi\sigma Q^2 \frac{a^4}{d^5} \mathbf{x} \quad (6.5)$$

for a symmetric ($\phi_{0,A} = -\phi_{0,B}$) and an antisymmetric ($\phi_{0,A} = 0, \phi_{0,B} = \pi/2$) situation, respectively (see Fig. 6.2). Note that this outcome coincides with the experimental findings in Sec. 4.3.

We now want to derive this result using the alternative stress tensor approach.

Symmetric situation

Let us consider the symmetric case first. According to Eqn. (5.8) the excess length of branch 1 compared to branch 3 must be determined. This can be written as

$$\begin{aligned} \Delta L &= \lim_{L \rightarrow \infty} \left\{ \int_{-L/2}^{L/2} dy \left[\sqrt{1 + h_y^2(0, y)} - 1 \right] \right\} \\ &= \lim_{L \rightarrow \infty} \left(\int_{-L/2}^{L/2} dy \left\{ \frac{1}{2} h_y^2(0, y) + \mathcal{O}[(\nabla h)^4] \right\} \right). \end{aligned} \quad (6.6)$$

In Cartesian coordinates one gets for the height function at the symmetry line between both particles:

$$h(0, y) = 2Q \cos[2(\arctan \frac{2y}{d} + \phi_{0,A})] \frac{a^2}{y^2 + \frac{d^2}{4}}. \quad (6.7)$$

By differentiating with respect to y and inserting the result into the small gradient term of Eqn. (6.6) one obtains

$$\begin{aligned} \Delta L &= \lim_{L \rightarrow \infty} \left[96Q^2 \frac{a^4}{d^5} \arctan \frac{L}{d} + \mathcal{O}(L^{-1}) \right] \\ &= 48\pi Q^2 \frac{a^4}{d^5}, \end{aligned} \quad (6.8)$$

which yields the same attractive force as Eqn. (6.5) once Eqn. (5.8) is applied.

Antisymmetric situation

In the antisymmetric case the force can be calculated according to Eqn. (5.10):

$$\begin{aligned} F_{\text{antisym,soap}} &= \sigma \lim_{L \rightarrow \infty} \left[\int_{-L/2}^{L/2} dy \left(\mathbf{n} \cdot \mathbf{z} - 1 \right) \right] \\ &= \sigma \lim_{L \rightarrow \infty} \left[\int_{-L/2}^{L/2} dy \left(\frac{1}{\sqrt{1 + h_x^2(0, y)}} - 1 \right) \right] \\ &= \sigma \lim_{L \rightarrow \infty} \left[\int_{-L/2}^{L/2} dy \left(-\frac{1}{2} h_x^2(0, y) + \mathcal{O}[(\nabla h)^4] \right) \right]. \end{aligned} \quad (6.9)$$

For the part of the height function between both particles one gets:

$$h(x, y) = Qa^2 \left\{ \frac{\cos [2(\arctan \frac{y}{\frac{d}{2} + x})]}{y^2 + (\frac{d}{2} + x)^2} - \frac{\cos [2(\arctan \frac{y}{\frac{d}{2} - x})]}{y^2 + (\frac{d}{2} - x)^2} \right\}, \quad (6.10)$$

which implies for the derivative with respect to x at $x = 0$:

$$h_x(0, y) = -\frac{32Qa^2 d(d^2 - 12y^2)}{(d^2 + 4y^2)^3}. \quad (6.11)$$

Inserting this into the small gradient expansion of Eqn. (6.9) yields a repulsive force which again is the same as in Eqn. (6.5).

6.2 Fluid Membrane type

For a fluid membrane the complete Hamiltonian (6.1) is relevant. Let us study two different situations, previously looked at in the literature [Wei03, WKH98]: two parallel adhering cylinders and two discoidal inclusions.

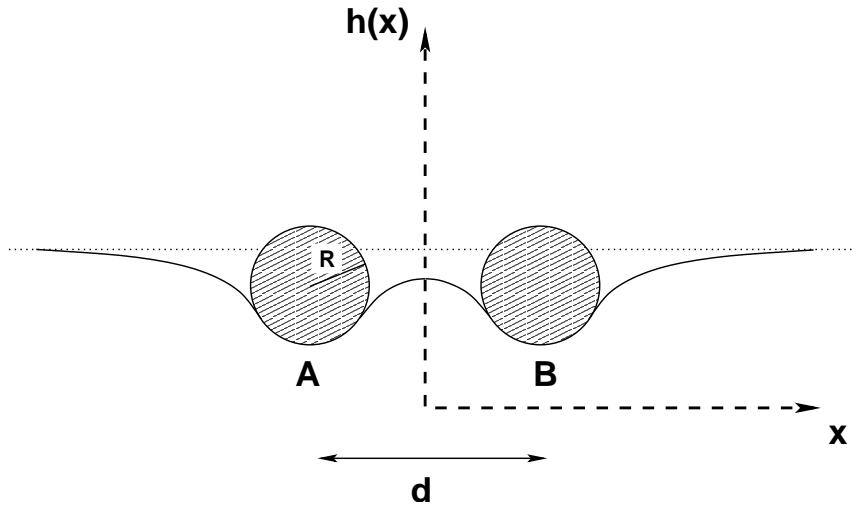


Figure 6.3: Two cylindrical colloids adhering to a membrane

6.2.1 Adhering cylinders

Two parallel cylinders may adhere to a membrane either in a *symmetric* situation (cylinders at the same membrane side) or an *antisymmetric* situation (cylinders at opposite membrane sides).

If they are long enough such as to neglect end effects, the height function of the surface only depends on one variable, x . The shape Eqn. (3.34) then turns into

$$\frac{\partial^2}{\partial x^2} \left(\frac{\partial^2}{\partial x^2} - \frac{1}{\lambda^2} \right) h(x) = 0, \quad (6.12)$$

for which a general solution is

$$h(x) = B_1 + B_2 x + B_3 \exp\left(-\frac{x}{\lambda}\right) + B_4 \exp\left(\frac{x}{\lambda}\right). \quad (6.13)$$

Respecting the boundary condition of continuous slope (contact angle equal to π , cf. Eqn. (3.26)) yields a height function for the inner region between the two colloids and the outer regions right and left of the two colloids, respectively. The total energy can then be obtained by adding the energies due to the different regions and additionally including the adhesion energy [Wei03].

Same membrane side

In the symmetric case, the author of Ref. [Wei03] shows that (again in small gradient expansion)

$$E_{\text{sym,cyl}}(d) = -\frac{(\kappa + 2R^2u)^2(1 + \tanh \frac{d}{2\lambda})}{4\sqrt{\sigma\kappa}R^2}, \quad (6.14)$$

as the result for the energy per unit length of the cylinder. In this expression R is the radius of one cylinder, u is the adhesion energy per area, $\lambda = \sqrt{\kappa/\sigma}$ the characteristic length first introduced in Eqn. (3.31), and d the distance between the two centers of the cylinders (see Fig. 6.3). To get the force per length L of the left cylinder, Eqn. (6.14) must be differentiated with respect to d :²

$$F_{\text{sym,cyl}}/L = -\frac{(\kappa + 2R^2u)^2}{8\kappa R^2 \cosh^2 \frac{d}{2\lambda}} . \quad (6.15)$$

We can now turn our focus once more to Chap. 5 in order to calculate the force via the stress tensor approach. Rewriting the relevant Eqn. (5.9) in small gradient expansion yields (see Eqn. (B.54a)):

$$F_{\text{sym,cyl}}/L = -\frac{1}{2}\kappa h_{xx}^2(0) . \quad (6.16)$$

We need to determine the height function in order to calculate the force. From Ref. [Wei03] one derives

$$h(x) = \frac{(\kappa + 2R^2u) \cosh \frac{x}{\lambda}}{2\sigma R \cosh \frac{d}{2\lambda}} + \text{const} . \quad (6.17)$$

According to Eqn. (6.16), the second derivative with respect to x at $x = 0$ must be determined, which is

$$h_{xx}(0) = \frac{(\kappa + 2R^2u)}{2\kappa R \cosh \frac{d}{2\lambda}} . \quad (6.18)$$

Inserting this into Eqn. (6.16) immediately yields the same force as the one that has been calculated in Eqn. (6.15).

Opposite membrane sides

For two cylinders at opposite sides of the membrane, the energy is given by [Wei03]

$$E_{\text{antisym,cyl}}(d) = -\frac{(\kappa + 2R^2u)^2(1 + \coth \frac{d}{2\lambda})}{4\sqrt{\sigma}\kappa R^2} , \quad (6.19)$$

which leads to the force²

$$F_{\text{antisym,cyl}}/L = \frac{(\kappa + 2R^2u)^2}{8\kappa R^2 \sinh^2 \frac{d}{2\lambda}} . \quad (6.20)$$

² The *direction* of the force is always opposite for the two particles. Hence, if one wants to encode this information in the *sign*, an additional minus sign is needed for the left particle, since it moves to the *negative* x -direction upon repulsion and to the positive upon attraction, respectively.

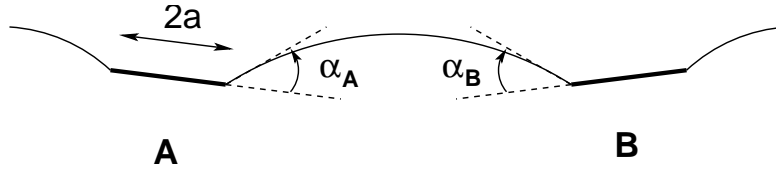


Figure 6.4: Contact angles α_A and α_B

The small gradient expansion of Eqn. (5.12) is

$$F_{\text{antisym,cyl}}/L = \frac{1}{2}\kappa (\lambda \nabla_{\perp} K_{\perp})^2 \stackrel{\text{(B.54a)}}{=} \frac{1}{2}\kappa [\lambda h_{xxx}(0)]^2 . \quad (6.21)$$

Taking again the height function from Ref. [Wei03] one arrives at

$$h(x) = \frac{(\kappa + 2R^2u) \sinh \frac{x}{\lambda}}{2\sigma R \sinh \frac{d}{2\lambda}} , \quad (6.22)$$

which yields

$$h_{xxx}(0) = \frac{(\kappa + 2R^2u)}{2\sigma \lambda^3 R \sinh \frac{d}{2\lambda}} . \quad (6.23)$$

Inserting this result into Eqn. (6.21) reproduces result (6.20).

6.2.2 Discoidal inclusions

The last situation we want to consider is that of two discoidal inclusions in a membrane, which can be understood as a simple model for protein transmembrane inclusions. This problem has been studied extensively in the literature, with and without tension (see *e. g.* [GBP93, WKH98]), because of its relevance for the aggregational behaviour of proteins (see Sec. 1.2.3).

The discs are assumed to have radius a and are connected to the membrane along a horizontal circle with fixed contact angles α_A and α_B (see Fig. 6.4). The distance d will measure the separation of the centers of these circles.

Without tension

The Hamiltonian in this case is again a special case of Eqn. (6.1). Now, $\sigma = 0$:

$$H = \frac{\kappa}{2} \int dx dy (\nabla^2 h)^2 . \quad (6.24)$$

The case of two discs in a membrane at vanishing tension was first investigated in Ref. [GBP93]. We will use the results of Refs. [WKH98], where the height functions are stated explicitly.

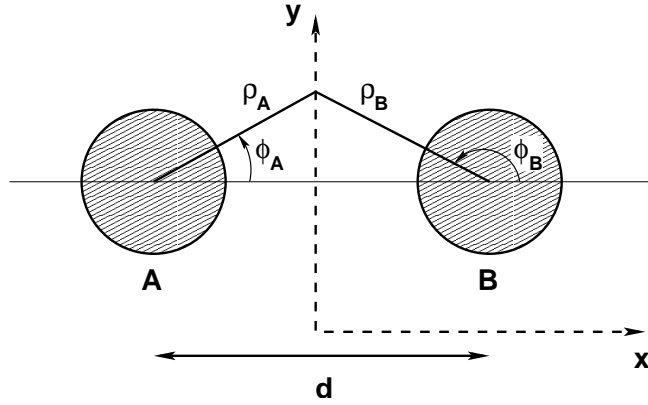


Figure 6.5: Two discolidal inclusions separated by a distance d (seen from above). Note that particle A is on the left and particle B is on the right hand side whereas in Ref. [WKH98] particle 1 is on the right. Note also that the angles ϕ_A and ϕ_B are chosen in accordance to ϕ_2 and ϕ_1 of Ref. [WKH98].

Let us focus again on a symmetric ($\alpha_A = \alpha_B = \alpha$) and an antisymmetric situation ($\alpha_A = -\alpha_B = \alpha$). In *both cases* the interaction energy is given by [WKH98, Eqn. (16)] (in lowest order a/d):

$$E_{\text{no ten,inc}}(d) = 8\pi\kappa\alpha^2 \frac{a^4}{d^4}, \quad (6.25)$$

which leads to the horizontal force (see footnote 2, p. 62)

$$F_{\text{no ten,inc}} = -32\pi\kappa\alpha^2 \frac{a^4}{d^5}. \quad (6.26)$$

The height function in Cartesian coordinates can be deduced from [WKH98] to be

$$\begin{aligned} h_{\pm}(x, y) = & C_1 \left(\ln \rho_A \pm \ln \rho_B \right) + C_2 \left(\pm \cos 2\phi_A + \cos 2\phi_B \right) \\ & + C_3 \left(\pm \frac{\cos 2\phi_A}{\rho_A^2} + \frac{\cos 2\phi_B}{\rho_B^2} \right) + \text{const}, \end{aligned} \quad (6.27)$$

where the coefficients are (omitting third and higher orders in a/d): $C_1 = \alpha a$, $C_2 = (\alpha a^3)/d^2$ and $C_3 = -(\alpha a^5)/2d^2$. The symmetric solution is denoted by h_+ , the antisymmetric by h_- .

The polar coordinates related to the center of projection of the respective inclusion on the (x, y) plane can be expressed in terms of the Cartesian coordinates x and y (see Fig. 6.5):

$$\rho_A = \sqrt{y^2 + \left(\frac{d}{2} + x\right)^2}, \quad \rho_B = \sqrt{y^2 + \left(\frac{d}{2} - x\right)^2} \quad (6.28)$$

$$\phi_A = \arctan \frac{y}{\frac{d}{2} + x}, \quad \phi_B = \pi - \arctan \frac{y}{\frac{d}{2} - x}. \quad (6.29)$$

For the symmetric situation Eqn. (5.8) must be applied. In small gradient expansion one gets (see Eqns. (B.54a) and (B.54b)):

$$\begin{aligned} F_{\text{no ten,inc,+}} &= -\frac{1}{2}\kappa \int_{-\infty}^{+\infty} dy \left[h_{xx}^2(0, y) - h_{yy}^2(0, y) \right] \\ &= -32\pi\kappa\alpha^2 \frac{a^4}{d^5}. \end{aligned} \quad (6.30)$$

In the antisymmetric case the force must be the same as we can prove by rewriting Eqn. (5.10) in small gradient expansion (see Eqns. (B.54a) and (B.54b)):

$$\begin{aligned} F_{\text{no ten,inc,-}} &= \kappa \int_{-\infty}^{+\infty} dy h_x(0, y) \left[h_{xxx}(0, y) + h_{yyx}(0, y) \right] \\ &= -32\pi\kappa\alpha^2 \frac{a^4}{d^5}. \end{aligned} \quad (6.31)$$

These results again show the equality of the two different methods.

Including tension

We now consider the complete Hamiltonian (6.1). The energy for small a/d and $a/\lambda < 1$ is given by [WKH98]

$$E_{\text{ten,inc,\pm}}(d) = 2\pi\kappa\alpha^2 \frac{a^2}{\lambda^2} \left[\pm K_0\left(\frac{d}{\lambda}\right) + \frac{a^2}{\lambda^2} K_2^2\left(\frac{d}{\lambda}\right) \right], \quad (6.32)$$

which corresponds to the force (see footnote 2, p. 62)

$$F_{\text{ten,inc,\pm}} = 2\pi\kappa\alpha^2 \frac{a^2}{\lambda^3} \left\{ \mp K_1\left(\frac{d}{\lambda}\right) - \frac{a^2}{\lambda^2} K_2\left(\frac{d}{\lambda}\right) \left[K_1\left(\frac{d}{\lambda}\right) + K_3\left(\frac{d}{\lambda}\right) \right] \right\}, \quad (6.33)$$

where \pm stands for the symmetric and the antisymmetric situation, respectively.³ The functions K_n are the modified Bessel functions of the second kind. It can be readily checked that Eqns. (6.32) and (6.33) turn into Eqns. (6.25) and (6.26) in the limit of zero tension, as they should.

The height function for this last case is according to [WKH98]

$$\begin{aligned} h_{\pm}(x, y) &= D_1 \left[K_0\left(\frac{\rho_A}{\lambda}\right) \pm K_0\left(\frac{\rho_B}{\lambda}\right) \right] \\ &+ D_2 \left[\mp K_1\left(\frac{\rho_A}{\lambda}\right) \cos \phi_A + K_1\left(\frac{\rho_B}{\lambda}\right) \cos \phi_B \right] \\ &+ D_3 \left[\mp \frac{\cos \phi_A}{\rho_A} + \frac{\cos \phi_B}{\rho_B} \right] \\ &+ D_4 \left[\pm K_2\left(\frac{\rho_A}{\lambda}\right) \cos 2\phi_A + K_2\left(\frac{\rho_B}{\lambda}\right) \cos 2\phi_B \right] \\ &+ D_5 \left[\pm \frac{\cos 2\phi_A}{\rho_A^2} + \frac{\cos 2\phi_B}{\rho_B^2} \right] + \text{const}, \end{aligned} \quad (6.34)$$

³ Note that the force in the symmetric case is *repulsive at all distances* whereas inclusions in the antisymmetric case *repel* each other at *small* separations, but *attract* each other at *larger* ones.

with the coefficients: $D_1 = -\alpha a$, $D_2 = -\frac{1}{2}\alpha\frac{a^3}{\lambda^2}K_1(\frac{d}{\lambda})$, $D_3 = -\frac{1}{2}D_2\frac{a^2}{\lambda}K_2(\frac{a}{\lambda})$, $D_4 = -\alpha\frac{a^3}{\lambda^2}K_2(\frac{d}{\lambda})$ and $D_5 = -\frac{1}{4}D_4\frac{a^3}{\lambda}K_3(\frac{a}{\lambda})$ in lowest order a/d and for $a/\lambda < 1$. The polar coordinates ρ_A , ρ_B , ϕ_A and ϕ_B are defined as in Eqns. (6.28,6.29) (see Fig. 6.5).

We finally apply our ansatz to this last situation. In the symmetric case ($\alpha_A = \alpha_B = \alpha$) the force in small gradient expansion is:

$$F_{\text{ten,inc,+}} = \int_{-\infty}^{+\infty} dy \left\{ \frac{\sigma}{2} h_y^2(0, y) - \frac{\kappa}{2} \left[h_{xx}^2(0, y) - h_{yy}^2(0, y) \right] \right\}. \quad (6.35)$$

The calculation to obtain this force is unfortunately rather involved. We can, however, get a result for small a/d and big d/λ by performing a Taylor expansion of the Bessel functions: we thereby obtain the first term of Eqn. (6.33). Regrettably, the second term is then overshadowed by the next orders neglected in our expansion.

In the antisymmetric case ($\alpha_A = -\alpha_B = \alpha$) the force is given by

$$F_{\text{ten,inc,-}} = \int_{-\infty}^{+\infty} dy \left\{ -\frac{\sigma}{2} h_x^2(0, y) + \kappa h_x(0, y) \left[h_{xxx}(0, y) + h_{yyx}(0, y) \right] \right\}. \quad (6.36)$$

If we go ahead and perform the same Taylor expansion as in the symmetric situation, we again arrive at the first term of Eqn. (6.33) but not at the second one, for the same reason as above.

7 Conclusions

The principal aim of this thesis has been the introduction of a new approach for obtaining exact results for interface mediated interactions. The key ideas and expressions of this approach can be found in Chap. 5. Although it is specialized to fluid membranes in this context, it is actually far more versatile: one can apply the central strategy to any interface whose energetics is determined by a Hamiltonian such as the one in Eqn. (1.1). Furthermore, it is fully covariant and therefore not restricted to a particular surface parametrization like Monge. Its results are also valid for large deformations as they are indeed found in experiments [KRS99], whereas the approach via the energetics (see Chap. 4) has only produced linear approximations for the forces in almost all calculations found in the literature. Within this linear regime both programs are consistent.

It should be stressed again that the new method is not a substitute for solving the nonlinear field equations. Instead, it shows that it is possible to gain information without the need to solve the shape equations explicitly by linking the *geometry* of the interface to the *forces* mediated by it. This can be an advantage because it is sometimes easy to guess certain properties of the overall *geometry*, while corresponding guesses about the surface *energy* may not be equally straightforward to make. In some cases this approach even yields the sign of the interactions, for instance, if two parallel cylinders adhere to a fluid membrane. At the very least, it provides non-trivial consistency conditions for analytical calculations.

One can now proceed and combine the stress tensor approach with any other analytical or numerical method which determines the surface shape. This is, for instance, possible with the program “Surface Evolver” [Bra04], which can find surfaces that minimize a prescribed surface energy functional. The surface shapes of Fig. 4.1, 5.1, and 7.1 were actually calculated with this program.

This thesis has just considered pair forces. If one wants to calculate interactions between more than two particles, it is important to remember that these are not simply expressible as a sum of the pair interactions. The superposition principle does not hold due to the nonlinearity of the theory.

This, however, poses no difficulty for the stress tensor approach because the underlying relation between surface geometry and force does not depend on whether or not a pair-decomposition is possible (see Fig. 7.1). For certain symmetric situations a clever choice of the contour of integration may again yield force expressions analogous to those obtained in Sec. 5.2.

Multi-body effects become particularly important, if one considers 2D bulk phases

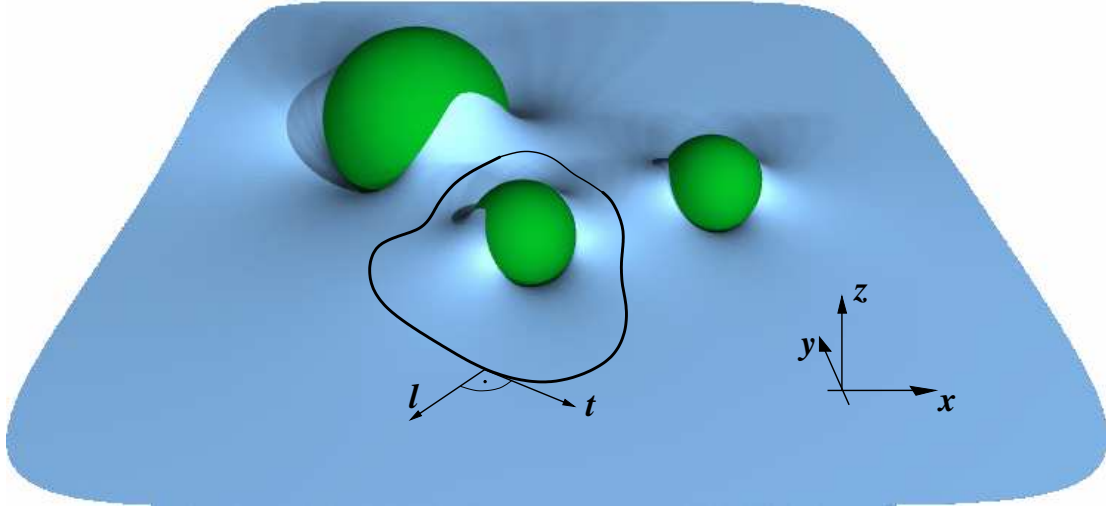


Figure 7.1: Three-body interactions. The force on one particle can be obtained as usual by integrating the surface stress tensor along the line of integration (cf. Eqn. (2.3)).

like a system consisting of many particles that adhere to the same side of an interface and repel each other. To determine state variables like the lateral pressure one may think about using a cell model like it is used, for instance, in nonlinear Poisson-Boltzmann theory [DH01]. The reason for that is that the situations are quite similar: Consider an overall neutral 3D system of likely charged colloids together with the appropriate number of oppositely charged counterions. In Poisson-Boltzmann theory these counterions are replaced by a charge density, which is treated in a mean field way. The colloids will typically organize such as to keep themselves mutually apart. One can then partition the volume into cells, each containing one colloid. Every cell has essentially the same volume and is neutral by construction, which means that different cells do not significantly interact with each other. The cell model then considers just one cell and calculates its free energy in dependence of the cell volume by solving the Poisson-Boltzmann equation. If one wants to know the pressure in this system, one has to differentiate this free energy with respect to the cell's volume. Remarkably, this turns out to lead to the simple “recipe” that the pressure is just given by the ion density at the cell boundary times the thermal energy $k_B T$.

In analogy to that, one might also partition the interface of the 2D bulk system into two-dimensional cells. Instead of solving the Poisson-Boltzmann equation, one now has to find a solution for the appropriate shape equation. Due to the nonlinearity, one cannot get analytical results in general as we have seen in this work. It should be possible, however, to consider the stress tensor at the cell boundary and relate geometrical properties at the boundary to the lateral pressure of the system.

A Conventions and used symbols

Conventions

The indices $\{a, b, c, d, e\}$ run from 1 to 2, whereas $\{i, j\} \in \{x, y, z\}$. Note that the sum convention is used in this thesis: if an index occurs twice in a product, once as a superscript and once as a subscript, one has to sum over that index from 1 to 2 even though no explicit summation sign is present. The equation $K = \sum_{a,b=1}^2 g^{ab} K_{ab}$, for instance, turns into $K = g^{ab} K_{ab}$.

Used symbols

The symbols in the following list are ordered alphabetically with roman letters first, followed by miscellaneous symbols and Greek letters. Reference is made to their first appearance in the text and, in some cases, to further information.

In Chap. 3 the bar ($\bar{}$) denotes substrate properties. The symbol \bar{K}_{ab} , for instance, is the curvature tensor of the substrate.

Note also that a few symbols are not listed due to the fact that they can be derived from the symbol that one gets when leaving out the sub- or superscript. The symbol \mathbf{F}_L , for instance, is a force because \mathbf{F} is a force (see list).

| | |
|------------------------------|---|
| a | radius of a spherical particle/bubble (Sec. 1.1.2, p. 9) <i>or</i> discoidal inclusion (Sec. 3.2.2, p. 42) <i>or</i> circle (App. B.2, p. 83) |
| a_0 | effective head group area of an amphiphile (Sec. 1.2.2, p. 11) |
| \mathbf{a} | spatial translation vector (Sec. 2.2.1, p. 21) |
| A, B | particle identifiers (Fig. 6.2, p. 59) |
| A_0, \dots, A_m | coefficients in the height function in the case of two particles on a soap film with a pinned contact line (Sec. 6.1, p. 58) |
| dA | area element (Sec. 1, p. 4; see also App. B.1, p. 77) |
| dA_j | j th component of the vectorial area element (Sec. 2.1, p. 17) |
| $\Delta A, \partial\Delta A$ | small surface patch and boundary of this patch, respectively (Sec. 2.1, p. 18) |
| \mathbf{b} | unit binormal vector of a curve (App. B.1, p. 79) |
| B_1, \dots, B_4 | coefficients in the height function in the case of two cylinders adhering to a membrane under tension (Sec. 6.2.1, p. 61) |

| | |
|--|---|
| \mathcal{C} | boundary curve (Sec. 3.1.3, p. 38) |
| C_1, \dots, C_3 | coefficients in the height function in the case of two discoidal inclusions in a membrane without tension (Sec. 6.2.2, p. 64) |
| d | distance between the centers of two colloids (Sec. 4.2, p. 48) |
| D_1, \dots, D_5 | coefficients in the height function in the case of two discoidal inclusions in a membrane under tension (Sec. 6.2.2, p. 66) |
| \mathbf{e}_a | set of tangent vectors on the surface (Sec. 2.1, p. 18; see also App. B.1, p. 75) |
| \mathbf{e}_\perp | outward pointing vector tangential to the surface and normal to the midline between the two colloids (Sec. 5.2, p. 56) |
| E_{pot} | potential energy (see Sec. 3.1.2 p. 35) |
| dE | infinitesimal energy (Sec. 1.1.1, p. 5) |
| \mathcal{E} | Euler-Lagrange derivative (Sec. 2.2.1, p. 20) |
| $f_{\mathbf{e}_\perp}$ | projection of \mathbf{f}^\perp onto \mathbf{e}_\perp (Sec. 5.2, p. 56) |
| f^{ab}, f^a | components of \mathbf{f}^a in the local frame $\{\mathbf{e}_a, \mathbf{n}\}$ (Sec. 2.2.1, p. 22) |
| \mathbf{f} | surface stress tensor (Sec. 2.1, p. 17) |
| \mathbf{f}_c | force of constraint (per length) (Sec. 3.1.1, p. 33) |
| \mathbf{f}_n | normal force (per length) (Sec. 3.1.1, p. 34) |
| \mathbf{f}^\perp | surface stress tensor at the midplane between the two colloids (Sec. 5.2, p. 56) |
| \mathbf{f}^a | surface stress tensor written as a pair of vectors (Sec. 2.1, p. 18) |
| $\tilde{\mathbf{f}}^a, \tilde{\tilde{\mathbf{f}}}^a$ | redefined surface stress tensor (Sec. 2.2.1, p. 23 and Sec. 2.2.2, p. 26, respectively) |
| F | absolute value of a force (Sec. 1.1.1, p. 5) |
| \mathbf{F} | force (Sec. 2.1, p. 17) |
| \mathcal{F} | scalar function defined on the surface (App. C, p. 89) |
| g | metric determinant (Sec. 2.2.1, p. 19; see also App. B.1, p. 77) <i>or</i> acceleration due to gravity (Sec. 3.1.2, p. 35) |
| g_{ab} | metric tensor (Sec. 1, p. 4 ; see also App. B.1, p. 77) |
| \mathbf{g} | matrix consisting of the components of g_{ab} (App. B.1, p. 77) |
| $G(\mathbf{r}, \mathbf{r}')$ | Green function (Sec. 3.1.3, p. 38) |
| G_{ab} | Einstein tensor (Sec. 2.3, p. 28) |
| h_1, \dots, h_4 | coefficients in the height function in the case of one sphere adhering to a membrane under tension (Sec. 3.2.1, p. 41) |
| $h(x, y)$ | height function in Monge parametrization (Sec. 3.1.2, p. 35; see also App. B.3, p. 84) |

| | |
|---|--|
| h_x, h_y | first derivatives of the height function in Monge parametrization with respect to x and y , respectively (Sec. 6.1, p. 59) |
| $h_{xx}, h_{yy}, h_{xy}, h_{yx}$ | second derivatives of the height function in Monge parametrization with respect to x and x, y and y , etc. (Sec. 6.2.1, p. 62) |
| h_q | Fourier coefficient of the height function h (Sec. 3.1.2, p. 36) |
| H | Hamiltonian (Sec. 1, p. 4) |
| H_C, \tilde{H}_C | original and redefined Hamiltonian of the auxiliary variables approach (Sec. 2.2.2, p. 25 and Sec. 2.2.2, p. 26, respectively) |
| \mathcal{H} | Hamiltonian density (Sec. 1, p. 3) |
| $\mathcal{H}^{ab} = \frac{\delta \mathcal{H}}{\delta K_{ab}}$ | functional derivative of the Hamiltonian density with respect to K_{ab} (Sec. 2.2.2, p. 25) |
| I_1, I_2 | invariant scalars (Sec. 1.2.1, p. 11) |
| k | geometrical factor (Sec. 3.2.1, p. 41) <i>or</i> curvature of a curve (App. B.1, p. 78) |
| k_1, k_2 | principal curvatures of a two-dimensional surface (Sec. 1.2.1, p. 10; see also App. B.1, p. 80) |
| k_B | Boltzmann constant (Sec. 1.2.3, p. 15) |
| K_{ab} | extrinsic curvature tensor (Sec. 1, p. 4; see also App. B.1, p. 79) |
| $K = g^{ab} K_{ab}$ | trace of the extrinsic curvature tensor (Sec. 1.1.2, p. 10; see also App. B.1, p. 81) |
| K_0 | spontaneous curvature (Sec. 1.2.1, p. 11) |
| K_g | geodesic curvature (Sec. 3.2.2, p. 42; see also App. B.1, p. 79) |
| K_G | Gaussian curvature (Sec. 1.2.1, p. 11; see also App. B.1, p. 81) |
| K_n | normal curvature (App. B.1, p. 79) |
| K_{\perp}, K_{\parallel} | normal curvatures perpendicular and parallel to a curve, respectively (Sec. 3.2.1, p. 40; see also App. B.1, p. 80) |
| $K_{\perp\parallel}$ | off-diagonal element of K_a^b (Sec. 3.2.1, p. 40) |
| $\ell = \sqrt{\frac{\sigma}{g\Delta\rho}}$ | capillary length (Sec. 3.1.2, p. 35) |
| l | length of a surface (Sec. 1.1.1, p. 4) |
| l_c | length of the hydrophobic part of an amphiphile (Sec. 1.2.2, p. 11) |
| dl_j | j th component of the line element ds times the unit vector which is perpendicular to the boundary curve (Sec. 2.1, p. 17) |
| l^a | components of \mathbf{l} in the local coordinate frame (Sec. 2.1, p. 18) |
| $\mathbf{l} = l^a \mathbf{e}_a$ | unit normal pointing outward of a surface patch along a boundary curve (tangential to the surface) (Sec. 2.1, p. 18) |

| | |
|---|--|
| L | length (Sec. 1.3, p. 16), <i>especially</i> length of a cylindrical colloid (Sec. 5.2, p. 55) |
| ΔL | excess length (Sec. 5.2, p. 54) |
| m, n | natural numbers (Sec. 6.1, p. 58 and Sec. 2.3, p. 27, respectively) |
| M_1, \dots, M_n | eigenvalues of \mathbf{M} (App. C, p. 88) |
| \mathbf{M}, \mathbf{M}_D | symmetric matrix and corresponding diagonal matrix, respectively (App. C, p. 88) |
| \mathbf{n} | unit vector normal to the surface (Sec. 2.1, p. 18) |
| p | genus of a closed surface (App. B.2, p. 83) |
| p_e, p_i | exterior and interior pressure, respectively (Sec. 1.1.2, p. 9) |
| P | pressure (Sec. 1.1.2, p. 9) |
| \mathbf{p} | unit principal vector of a curve (App. B.1, p. 79) |
| \mathbf{q} | wave vector (Sec. 3.1.2, p. 36) |
| Q | quadrupolar coefficient (Sec. 6.1, p. 58) |
| Q^a | linear differential operator (Sec. 2.2.1, p. 21) |
| r | class of a function (App. B.1, p. 75) |
| \mathbf{r} | position vector (Sec. 3.1.2, p. 35) |
| R | radius of a cylindrical colloid (Sec. 6.2.1, p. 62) |
| R_{ab} | Ricci tensor (Sec. 2.3, p. 28; see also App. B.1, p. 82) |
| $R^a{}_{bcd}$ | Riemann tensor (App. B.1, p. 82) |
| \mathcal{R} | Ricci scalar (Sec. 1.3, p. 16; see also App. B.1, p. 82) |
| s | arc length (Sec. 2.1, p. 18) |
| ds | line element (Sec. 2.1, p. 18) |
| S | point on a surface (App. B.1, p. 78) |
| S^a | linear differential operator (Sec. 2.2.1, p. 21) |
| t | parameter of a curve (App. B.1, p. 80) |
| t^a | components of \mathbf{t} in the local coordinate frame (Sec. 5.2, p. 53) |
| $t^{ab}, t_{b_1 b_2 \dots b_m}^{a_1 a_2 \dots a_n}$ | arbitrary tensors (see App. B.1, p. 77 et seq.) |
| $\mathbf{t} = t^a \mathbf{e}_a$ | tangent vector of a curve (Fig. 2.2, p. 19) |
| T | temperature (Sec. 1.1.1, p. 5) |
| T^{ab} | intrinsic surface stress tensor (Sec. 2.2.2, p. 25) |
| \mathbf{T} | transformation matrix (App. C, p. 88) |
| u | adhesion energy per area (Sec. 3.1.1, p. 32) |
| U | surface patch (App. B.1, p. 75) |
| v | volume of the hydrophobic part of an amphiphile |

| | |
|--|---|
| | (Sec. 1.2.2, p. 11) |
| V | volume (Sec. 1.1.2, p. 9) |
| V_0 | constant enclosed volume (Sec. 1.1.2, p. 10) |
| ∂V | surface enclosing a volume V (Sec. 1.1.2, p. 9) |
| dV, dV' | volume element (Sec. 2.1, p. 17 and App. C, p. 89, respectively) |
| $\Delta V, \partial\Delta V$ | small cubic volume and surface of this volume, respectively (Sec. 2.1, p. 17) |
| w | width of a surface (Sec. 1.1.1, p. 4) |
| dw | length element (Sec. 1.1.1, p. 5) |
| (x, y) | Cartesian coordinates of the reference plane (Sec. 3.1.2, p. 35) |
| dx, dy | infinitesimal change in x and y , respectively (Sec. 3.1.2, p. 35) |
| (x, y, z) | Cartesian coordinates in \mathbb{R}^3 (Sec. 2.1, p. 17) |
| $\{\mathbf{x}, \mathbf{y}, \mathbf{z}\}$ | set of orthonormal basis vectors in \mathbb{R}^3 (Sec. 2.1, p. 17) |
| $\mathbf{X}(\xi^1, \xi^2)$ | embedding functions of the surface (Sec. 1, p. 3) |
| X_x, X_y, X_z | component functions of \mathbf{X} in \mathbb{R}^3 (App. B.1, p. 75) |
| $\partial_a = \partial/\partial\xi^a$ | partial derivative on the surface (Sec. 2.2.2, p. 24) |
| ∂_i | partial derivative with respect to $i \in \{x, y, z\}$ (Sec. 2.1, p. 17) |
| $\frac{\partial}{\partial n}$ | partial derivative along the normal vector of a boundary curve (Sec. 3.1.3, p. 38) |
| $\frac{\partial(X_x, X_y, X_z)}{\partial(\xi^1, \xi^2)}$ | Jacobian matrix (App. B.1, p. 75) |
| $\nabla = (\partial_x, \partial_y)^T$ | nabla operator of the reference plane (Sec. 3.1.2, p. 35; see also App. B.3, p. 84) |
| ∇^2 | Laplacian on the reference plane (Sec. 3.1.2, p. 35; see also App. B.3, p. 85) |
| ∇_a | covariant derivative on the surface (Sec. 1, p. 4; see also App. B.1, p. 78) |
| $\nabla_{\perp} = l^a \nabla_a$ | derivative along \mathbf{l} (Sec. 5.2, p. 54) |
| α | contact angle (Sec. 3.1.1, p. 32) |
| γ | angle between \mathbf{e}_1 and \mathbf{e}_2 (App. B.1, p. 77) |
| Γ_{ab}^c | Christoffel symbol (App. B.1, p. 78) |
| $\delta = \delta_{\parallel} + \delta_{\perp}$ | variation with respect to the embedding functions \mathbf{X} (Sec. 2.2.1, p. 20; see also App. C, p. 87) |
| $\delta/\delta K_{ab}$ | functional derivative (in this case with respect to K_{ab}) (Sec. 2.2.2, p. 25) |
| δ_g | variation with respect to the metric g_{ab} (Sec. 2.3, p. 28) |
| δ_a^b | Kronecker symbol (App. B.1, p. 77) |

| | |
|--|--|
| $\Delta = \nabla_a \nabla^a$ | Laplacian on the surface (Sec. 2.2.1, p. 24; see also App. B.1, p. 78) |
| η | angle between \mathbf{n} and \mathbf{p} (App. B.1, p. 79) |
| θ_0 | angle of immersion/detachment (Sec. 3.1.2, p. 36) |
| κ | bending rigidity (Sec. 1.2.1, p. 11) |
| $\bar{\kappa}$ | Gaussian bending rigidity, also saddle-splay modulus (Sec. 1.2.1, p. 11) |
| $\lambda = \sqrt{\frac{\kappa}{\sigma}}$ | characteristic length (Sec. 3.2.1, p. 40) |
| $\lambda^{ab}, \Lambda^{ab}, \lambda_{\perp}^a, \lambda_n$ | Lagrange multiplier functions (Sec. 2.2.2, p. 25) |
| $\tilde{\lambda}^{ab}, \tilde{\Lambda}^{ab}, \tilde{\lambda}_{\perp}^a, \tilde{\lambda}_n$ | redefined Lagrange multiplier functions (Sec. 2.2.2, p. 26) |
| Λ | width of a surface patch (Sec. 3.1.2, p. 36) |
| ν_x, ν_y | integers (Sec. 3.1.2, p. 36) |
| ξ^a | set of local coordinates on the surface (Sec. 1, p. 3) |
| $d^2\xi = d\xi^1 d\xi^2$ | product of infinitesimal changes in ξ^1 and ξ^2 , respectively (Sec. 2.2.1, p. 19) |
| Ξ | subset of \mathbb{R}^2 (App. B.1, p. 75) |
| ρ_l, ρ_g | density of a liquid and a gas, respectively (Sec. 3.1.2, p. 35) |
| $\Delta\rho = \rho_l - \rho_g$ | density difference between a liquid and a gas (Sec. 3.1.2, p. 35) |
| σ | surface tension (Sec. 1, p. 3) |
| σ_{ij} | components of the stress tensor in 3D (Sec. 2.1, p. 17) |
| $\boldsymbol{\sigma}$ | stress tensor in 3D (Sec. 2.1, p. 17) |
| Σ | surface domain (Sec. 1, p. 4) |
| Σ_0 | simply connected surface domain (Sec. 2.1, p. 18) |
| $\partial\Sigma, \partial\Sigma_0$ | boundary curve of the surface domain Σ (Sec. 3.1.1, p. 33) and Σ_0 (Sec. 2.1, p. 18), respectively |
| φ | tilt angle between \mathbf{n} and \mathbf{z} at the midplane between the two colloids (Sec. 5.2, p. 53) |
| (ρ, ϕ) | polar coordinates of the reference plane (Sec. 3.2.1, p. 41) |
| (ρ, ϕ, θ) | spherical coordinates in \mathbb{R}^3 (Sec. 3.1.2, p. 37) |
| $d\phi, d\theta$ | angle elements (Sec. 3.1.2, p. 37) |
| $\phi_{1,0}, \dots, \phi_{m,0}$ | phase angles in the height function in the case of two particles on a soap film with a pinned contact line (Sec. 6.1, p. 58) |
| ϕ_0 | angle at which one quadrupole is rotated around \mathbf{z} (Sec. 6.1, p. 59) |
| Φ^a | local tangential variation of \mathbf{X} (Sec. 2.2.1, p. 20) |
| Ψ | local normal variation of \mathbf{X} (Sec. 2.2.1, p. 20) |

B Classical differential geometry of two-dimensional surfaces

B.1 Basic definitions

This section gives an overview of the basic notions of differential geometry for two-dimensional surfaces. It follows mainly Kreyszig [Kre91] in its discussion.

Definition of a surface

Let us consider the vector function $\mathbf{X}(\xi^1, \xi^2) \in \mathbb{R}^3$ with

$$\mathbf{X} : \mathbb{R}^2 \supset \Xi \ni (\xi^1, \xi^2) \mapsto \mathbf{X}(\xi^1, \xi^2) \in U \subset \mathbb{R}^3, \quad (\text{B.1})$$

where Ξ is an open subset of \mathbb{R}^2 . Let $\mathbf{X}(\xi^1, \xi^2)$ be of class $r \geq 1$ in Ξ , which means that one of its component functions X_i ($i \in \{x, y, z\}$) is of class r and the other ones are at least of this class.¹ Let furthermore the Jacobian matrix $\frac{\partial(X_x, X_y, X_z)}{\partial(\xi^1, \xi^2)}$ be of rank 2 in Ξ which implies that the vectors

$$\mathbf{e}_a := \frac{\partial \mathbf{X}}{\partial \xi^a} = \partial_a \mathbf{X}, \quad a \in \{1, 2\}, \quad (\text{B.2})$$

are linearly independent. The mapping (B.1) then defines a smooth two-dimensional surface patch U embedded in three-dimensional Euclidean space \mathbb{R}^3 with coordinates ξ^1 and ξ^2 (see Fig. B.1). A union Σ of surface patches is called a surface if two arbitrary patches U and U' of Σ can be joined by finitely many patches $U = U_1, U_2, \dots, U_{n-1}, U_n = U'$ in such a way that the intersection of two subsequent patches is again a surface patch [Kre91, p. 76]. To simplify the following let us restrict ourselves to a surface that can be covered by one patch U only.

The vectors \mathbf{e}_a , defined in Eqn. (B.2), are the tangent vectors of the surface. They are not normalized in general. Together with the unit normal

$$\mathbf{n} := \frac{\mathbf{e}_1 \times \mathbf{e}_2}{|\mathbf{e}_1 \times \mathbf{e}_2|}, \quad (\text{B.3})$$

they form a local basis (*local frame*) in \mathbb{R}^3 (see Fig. B.2):

$$\mathbf{e}_a \cdot \mathbf{n} = 0, \quad \text{and} \quad \mathbf{n} \cdot \mathbf{n} = 1. \quad (\text{B.4})$$

¹ A function of one or several variables is called a *function of class r* if it possesses continuous partial derivatives up to order r .

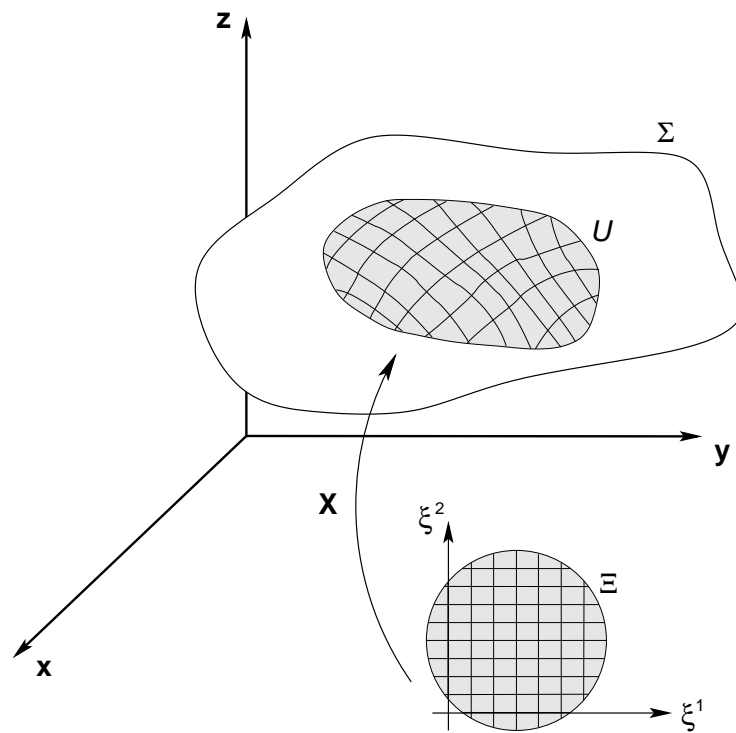


Figure B.1: Parametrization of a surface

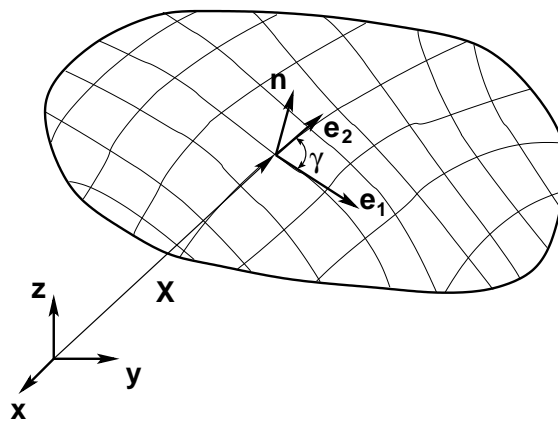


Figure B.2: Local frame on the surface

The metric tensor (first fundamental form)

With the tangent vectors \mathbf{e}_a , one can define the *metric tensor* (also called the *first fundamental form*)

$$g_{ab} := \mathbf{e}_a \cdot \mathbf{e}_b . \quad (\text{B.5})$$

This covariant second rank tensor is symmetric ($g_{ab} = g_{ba}$) and positive definite [Kre91, p. 86]. It helps to determine the infinitesimal Euclidean distance in terms of the coordinate differentials [Kre91, p. 82]

$$\begin{aligned} ds^2 &= [\mathbf{X}(\xi^1 + d\xi^1, \xi^2 + d\xi^2) - \mathbf{X}(\xi^1, \xi^2)]^2 = (\mathbf{e}_1 d\xi^1 + \mathbf{e}_2 d\xi^2)^2 \\ &= (\mathbf{e}_a d\xi^a)^2 = (\mathbf{e}_a \cdot \mathbf{e}_b) d\xi^a d\xi^b \\ &= g_{ab} d\xi^a d\xi^b , \end{aligned} \quad (\text{B.6})$$

where the sum convention is used in the last two lines (see App. A). The contravariant dual tensor of the metric may be defined via

$$g_{ac} g^{cb} := \delta_a^b := \begin{cases} 1, & \text{if } a = b \\ 0, & \text{if } a \neq b \end{cases} , \quad (\text{B.7})$$

where δ_a^b is the Kronecker symbol. The metric and its inverse can be used to raise and lower indices in tensor equations. Consider for instance the second rank tensor t_{ab} :

$$\text{Raising: } t_{ac} g^{cb} = t_a^b , \quad \text{and lowering: } t_a^c g_{cb} = t_{ab} . \quad (\text{B.8})$$

The determinant of the metric²

$$g := \det \mathbf{g} = |g_{ab}| = g_{11}g_{22} - g_{12}g_{21} \quad (\text{B.9})$$

can be exploited to calculate the infinitesimal area element dA : let γ be the angle between \mathbf{e}_1 and \mathbf{e}_2 (see Fig. B.2). Then

$$\begin{aligned} |\mathbf{e}_1 \times \mathbf{e}_2|^2 &= |\mathbf{e}_1|^2 |\mathbf{e}_2|^2 \sin^2 \gamma = g_{11}g_{22}(1 - \cos^2 \gamma) = g_{11}g_{22} - (\mathbf{e}_1 \cdot \mathbf{e}_2)^2 \\ &= g_{11}g_{22} - g_{12}g_{12} = g , \end{aligned} \quad (\text{B.10})$$

and thus

$$dA = |\mathbf{e}_1 \times \mathbf{e}_2| d\xi^1 d\xi^2 = \sqrt{g} d^2\xi . \quad (\text{B.11})$$

² Note that \mathbf{g} is the matrix consisting of the metric tensor components g_{ab} .

The covariant derivative

The partial derivative ∂_a is itself not a tensor. One therefore defines the covariant derivative ∇_a on a tensor $t_{b_1 b_2 \dots b_m}^{a_1 a_2 \dots a_n}$

$$\begin{aligned} \nabla_c t_{b_1 b_2 \dots b_m}^{a_1 a_2 \dots a_n} &= \partial_c t_{b_1 b_2 \dots b_m}^{a_1 a_2 \dots a_n} \\ &+ t_{b_1 b_2 \dots b_m}^{d a_2 \dots a_n} \Gamma_{dc}^{a_1} + t_{b_1 b_2 \dots b_m}^{a_1 d \dots a_n} \Gamma_{dc}^{a_2} + \dots + t_{b_1 b_2 \dots b_m}^{a_1 a_2 \dots d} \Gamma_{dc}^{a_n} \\ &- t_{d b_2 \dots b_m}^{a_1 a_2 \dots a_n} \Gamma_{b_1 c}^d - t_{b_1 d \dots b_m}^{a_1 a_2 \dots a_n} \Gamma_{b_2 c}^d - \dots - t_{b_1 b_2 \dots d}^{a_1 a_2 \dots a_n} \Gamma_{b_m c}^d, \end{aligned} \quad (\text{B.12})$$

where the Γ_{ab}^c are the *Christoffel symbols of the second kind* with

$$\Gamma_{ab}^c = (\partial_a \mathbf{e}_b) \cdot \mathbf{e}^c, \quad (\text{B.13})$$

and ∇_a is now a tensor. For the covariant differentiation of sums and products of tensors the usual rules of differential calculus hold. The metric-compatible Laplacian Δ can be defined as $\Delta := \nabla_a \nabla^a$.

Note in particular that

$$\nabla_a \mathbf{e}_b = \partial_a \mathbf{e}_b - \Gamma_{ab}^c \mathbf{e}_c, \quad \text{and} \quad (\text{B.14})$$

$$\nabla_a g_{bc} = \nabla_a g^{bc} = \nabla_a g = 0. \quad (\text{B.15})$$

Equation (B.15) is also called the *Lemma of Ricci*. It implies that raising and lowering of indices commutes with the process of covariant differentiation.

Orientable surfaces

The orientation of the normal vector \mathbf{n} in one point S of the surface depends on the choice of the coordinate system [Kre91, p. 108]: exchanging, for instance, ξ^1 and ξ^2 also flips \mathbf{n} by 180 degrees. A surface is called *orientable* if no closed curve \mathcal{C} through any point S of the surface exists which causes the sense of \mathbf{n} to change when displacing \mathbf{n} continuously from S along \mathcal{C} back to S . An example of a surface that is not orientable is the *Möbius strip*.

The extrinsic curvature tensor (second fundamental form)

Two surfaces may have the same metric tensor g_{ab} but different curvature properties in \mathbb{R}^3 . In order to describe such properties let us consider a surface Σ of class³ $r \geq 2$ and a curve \mathcal{C} of the same class on Σ with the parametrization $\mathbf{X}(\xi^1(s), \xi^2(s))$ on Σ , where s is the arc length of the curve (see Fig. B.3).

At every point of the curve where its curvature $k > 0$, one may define a moving trihedron $\{\mathbf{t}, \mathbf{p}, \mathbf{b}\}$ where $\mathbf{t} = \dot{\mathbf{X}}$ is the unit tangent vector, $\mathbf{p} = \dot{\mathbf{t}}/|\dot{\mathbf{t}}| = \dot{\mathbf{t}}/k$ is the

³ This means that its parametrization $\mathbf{X}(\xi^1, \xi^2)$ is of class $r \geq 2$.

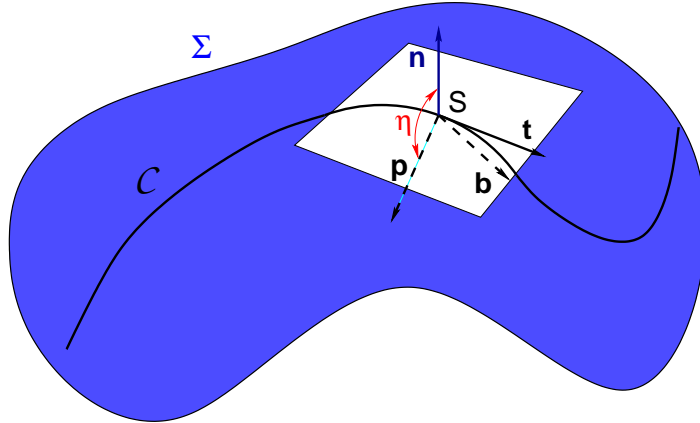


Figure B.3: Curve on a surface

unit principal normal vector, and $\mathbf{b} = \mathbf{t} \times \mathbf{p}$ is the unit binormal vector of the curve.⁴ Furthermore, let η be the angle between the unit normal vector \mathbf{n} of the surface and the unit principal normal vector \mathbf{p} of the curve with $\cos \eta = \mathbf{p} \cdot \mathbf{n}$ (see again Fig. B.3). The curvature k of the curve can then be decomposed into a part which is due to the fact that the *surface* is curved in \mathbb{R}^3 and a part due to the fact that the *curve* itself is curved. The former will be called the normal curvature K_n , the latter the geodesic curvature K_g . One defines:

$$K_n := -\dot{\mathbf{t}} \cdot \mathbf{n} = -k (\mathbf{p} \cdot \mathbf{n}) = -k \cos \eta, \quad \text{and} \quad (\text{B.16})$$

$$K_g := \mathbf{t} \cdot (\dot{\mathbf{t}} \times \mathbf{n}) = k \mathbf{t} \cdot (\mathbf{p} \times \mathbf{n}) = k \sin \eta \operatorname{sign}(\mathbf{n} \cdot \mathbf{b}). \quad (\text{B.17})$$

Here, we are interested in the curvature properties of the surface. Therefore, the normal curvature K_n is the relevant quantity that has to be studied a bit further.⁵ The vector $\dot{\mathbf{t}}$ may be written as

$$\dot{\mathbf{t}} = \ddot{\mathbf{X}} = \frac{d}{ds}(\mathbf{e}_a \dot{\xi}^a) = (\partial_b \mathbf{e}_a) \dot{\xi}^a \dot{\xi}^b + \mathbf{e}_a \ddot{\xi}^a. \quad (\text{B.18})$$

Thus, Eqn. (B.16) turns into

$$K_n = -k \cos \eta = (-\mathbf{n} \cdot \partial_a \mathbf{e}_b) \dot{\xi}^a \dot{\xi}^b, \quad (\text{B.19})$$

where it has been exploited that $\partial_a \mathbf{e}_b = \partial_b \mathbf{e}_a$. The expression in brackets is the *extrinsic curvature tensor* or *second fundamental form*

$$K_{ab} := -\mathbf{n} \cdot \partial_a \mathbf{e}_b = \mathbf{e}_a \cdot \partial_b \mathbf{n}. \quad (\text{B.20})$$

⁴ The dot denotes the derivative with respect to the arc length s .

⁵ The minus sign in the definition of K_n , Eqn. (B.16), is unfortunately a matter of convention and is here chosen in accordance to the literature where the surface stress tensor for fluid membranes has been introduced [CG02b, Guv04a]. A sphere with outward pointing unit normal has a positive normal curvature then. Note that this differs from Ref. [Kre91].

It is a symmetric covariant second rank tensor such as the metric. The second relation in Eqn. (B.20) follows if one differentiates the first equation of (B.4) with respect to ξ^a .

The extrinsic curvature can be written covariantly:

$$K_{ab} := -\mathbf{n} \cdot \nabla_a \mathbf{e}_b . \quad (\text{B.21})$$

This is possible because $\partial_a \mathbf{e}_b$ differs from $\nabla_a \mathbf{e}_b$ only by terms proportional to the tangent vectors \mathbf{e}_c , which vanish when multiplied by \mathbf{n} (see Eqn. (B.14)).

One can easily see from Eqn. (B.20) that K_{ab} has got something to do with curvature: at every point of the surface it measures the change of the normal vector in \mathbb{R}^3 for an infinitesimal displacement in the direction of a coordinate curve.

To learn more about the normal curvature let us consider a reparametrization of the curve \mathcal{C} with the new parameter t . One gets

$$\dot{\xi}^a = \frac{d\xi^a}{dt} \frac{dt}{ds} = \frac{\xi^{a'}}{s'} , \quad (\text{B.22})$$

where $'$ denotes the derivative with respect to t . Equation (B.19) thus takes the form

$$K_n = K_{ab} \dot{\xi}^a \dot{\xi}^b = \frac{K_{ab} \xi^{a'} \xi^{b'}}{(s')^2} \stackrel{(\text{B.6})}{=} \frac{K_{ab} \xi^{a'} \xi^{b'}}{g_{ab} \xi^{a'} \xi^{b'}} = \frac{K_{ab} d\xi^a d\xi^b}{g_{ab} d\xi^a d\xi^b} . \quad (\text{B.23})$$

For a fixed point S , K_{ab} and g_{ab} are fixed as well. The value of K_n then only depends on the direction of the tangent vector \mathbf{t} of the curve. One may search for extremal values of K_n at S by rewriting Eqn. (B.23):

$$(K_{ab} - K_n g_{ab}) \dot{\xi}^a \dot{\xi}^b = 0 . \quad (\text{B.24})$$

A differentiation with respect to $\dot{\xi}^c$ yields the result

$$(K_{ac} - K_n g_{ac}) \dot{\xi}^a = 0 , \quad (\text{B.25})$$

because $dK_n = 0$ is necessary for K_n to be extremal. Through the raising of one index, Eqn. (B.25) becomes an eigenvalue problem for K_a^b . Its eigenvectors are the tangent directions along which the normal curvature is extremal. They are called *principal directions* and are orthogonal to each other [Kre91, p. 129]. The eigenvalues will be called the *principal curvatures* k_1 and k_2 of the surface in point S . All other values of K_n in S in any direction can be calculated via Euler's theorem [Kre91, p. 132]. If the curve follows a principal direction at every point, it is also called a *line of curvature*.

For an arbitrary curve on the surface the symbol K_{\parallel} denotes the normal curvature belonging to the direction the curve is following, whereas K_{\perp} denotes the normal curvature belonging to the direction perpendicular to the curve in every point.

It is useful to define the following two notions: the *total curvature*

$$K := g^{ab}K_{ab} = K_a^a = k_1 + k_2 , \quad (\text{B.26})$$

and the *Gaussian curvature*

$$K_G := |K_a^b| = k_1 k_2 . \quad (\text{B.27})$$

The quantities $|K|$ and K_G are invariant under surface reparametrizations because they only involve the eigenvalues of the extrinsic curvature tensor. They occur, for instance, in the surface Hamiltonian of a fluid membrane (see Eqn. (1.10)). Note that one can rewrite K_G

$$K_G = |K_a^b| = |K_{ac}g^{cb}| = |K_{ac}| |g^{cb}| = \frac{K_{11}K_{22} - K_{12}K_{21}}{g} . \quad (\text{B.28})$$

The equations of Gauss and Weingarten

With the help of the extrinsic curvature it is also possible to find relations for the partial derivatives of the local frame vectors: the normal vector \mathbf{n} is a unit vector (see Eqn. (B.4)) and therefore

$$\mathbf{n} \cdot \partial_a \mathbf{n} = 0 . \quad (\text{B.29})$$

Thus, $\partial_a \mathbf{n}$ is a linear combination of the tangent vectors \mathbf{e}_a . We know that $\partial_a \mathbf{n} \cdot \mathbf{e}_a = K_{ab}$ (see Eqn. (B.20)), which yields the *Weingarten equations*

$$\partial_a \mathbf{n} = \nabla_a \mathbf{n} = K_a^b \mathbf{e}_b . \quad (\text{B.30})$$

For the tangent vector \mathbf{e}_a a decomposition yields

$$\partial_a \mathbf{e}_b = (\mathbf{n} \cdot \partial_a \mathbf{e}_b) \mathbf{n} + (\mathbf{e}^c \cdot \partial_a \mathbf{e}_b) \mathbf{e}_c \stackrel{(\text{B.20}), (\text{B.13})}{=} -K_{ab} \mathbf{n} + \Gamma_{ab}^c \mathbf{e}_c . \quad (\text{B.31})$$

These are the *Gauss equations*, which can be rewritten covariantly:

$$\nabla_a \mathbf{e}_b \stackrel{(\text{B.14})}{=} -K_{ab} \mathbf{n} . \quad (\text{B.32})$$

Intrinsic curvature and integrability conditions

Do the partial differential Eqns. (B.30) and (B.32) have solutions for any chosen g_{ab} and K_{ab} ? The answer is no; certain integrability conditions have to be satisfied. We require the embedding functions \mathbf{X} to be of class $r \geq 3$ and

$$\partial_a \partial_b \mathbf{e}_c = \partial_b \partial_a \mathbf{e}_c . \quad (\text{B.33})$$

From this follows [Kre91, p. 142 et seq.]

$$R^a{}_{bcd} = K_{bd}K_c^a - K_{bc}K_d^a , \quad \text{and} \quad (\text{B.34})$$

$$\nabla_a K_{bc} = \nabla_b K_{ac} , \quad (\text{B.35})$$

where

$$R^a{}_{bcd} := \partial_c \Gamma_{bd}{}^a - \partial_d \Gamma_{bc}{}^a + \Gamma_{bd}{}^e \Gamma_{ec}{}^a - \Gamma_{bc}{}^e \Gamma_{ed}{}^a , \quad (\text{B.36})$$

is called the *mixed Riemann curvature tensor*. It is intrinsic because it does not depend on the normal vector \mathbf{n} . Expression (B.35) is also referred to as the *equation of Mainardi-Codazzi*.

The *Ricci tensor* is defined as the contraction of the Riemann tensor with respect to its first and third index:

$$R_{ab} := R^c{}_{acb} . \quad (\text{B.37})$$

A further contraction of the Ricci tensor yields the intrinsic *scalar curvature* of the surface (Ricci scalar)

$$\mathcal{R} := g^{ab} R_{ab} . \quad (\text{B.38})$$

From Eqn. (B.34) one then obtains

$$R_{ab} = K K_{ab} - K_{ac} K_b{}^c , \quad \text{and} \quad (\text{B.39})$$

$$\mathcal{R} = K^2 - K^{ab} K_{ab} . \quad (\text{B.40})$$

Combining Eqn. (B.28) with the completely covariant form of Eqn. (B.34), one gets after a few calculations:

$$R_{ab} = K_G g_{ab} , \quad \text{and} \quad (\text{B.41})$$

$$\mathcal{R} = 2 K_G . \quad (\text{B.42})$$

These equations confirm Gauss' Theorema Egregium, which states that the Gaussian curvature, even though originally defined in an extrinsic way, in fact only depends on the first fundamental form [Kre91, p. 145] and is thus an intrinsic surface property.

B.2 Gauss-Bonnet theorem

The Gauss-Bonnet theorem for simply connected surfaces

The Gauss-Bonnet theorem states the following [Kre91, p. 169]: Let Σ_0 be a simply connected surface patch of class $r_{\Sigma_0} \geq 3$ with simple closed boundary $\partial\Sigma_0$ of class $r_{\partial\Sigma_0} \geq 3$. Furthermore, let $\mathbf{X}(\xi^1(s), \xi^2(s))$ be the parametrization of the boundary curve, where s is the arc length. Then

$$\int_{\partial\Sigma_0} ds K_g + \int_{\Sigma_0} dA K_G = 2\pi , \quad (\text{B.43})$$

where dA is the infinitesimal area element, K_g is the geodesic curvature of $\partial\Sigma_0$, and K_G is the Gaussian curvature of Σ_0 . Note that the integration along the boundary curve has to be carried out in such a sense that the right-hand rule is satisfied: take

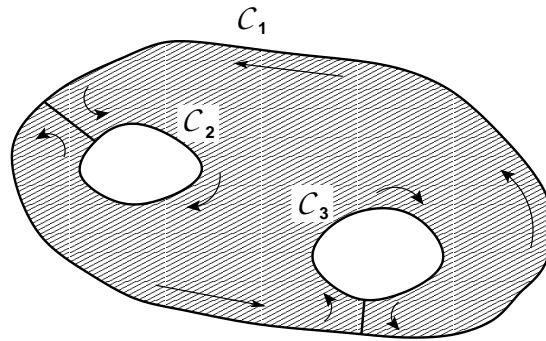


Figure B.4: Integration contour for multiply connected surface patches

your right thumb and point it in the direction of the normal vector \mathbf{n} . If you then curl your fingers, the tips indicate the direction of integration.

One can check the consistency of Eqn. (B.43) easily by considering a flat circle with radius a : Its Gaussian curvature is zero and therefore also the integral over it. The geodesic curvature, however, is equal to $1/a$ in every point of the boundary. Thus, the integral over K_g yields $2\pi a \times 1/a$, which is equal to the right-hand side of Eqn. (B.43).

Generalization to multiply connected surfaces

A generalization of this theorem to multiply connected surfaces is also possible [Kre91, p. 172]: One can cut multiply connected surfaces into simply connected ones. Take, for instance, a surface as in Fig. B.4. The path of integration along the boundary may be chosen as depicted by the arrows. The sections are passed twice in opposite directions; their contributions therefore cancel each other. The end points of every section, however, add a term of π each to the integral $\int ds K_g$. This is due to the rotation the tangent makes at each of these points. Every section therefore contributes 2π to the integral. For the case of Fig. B.4 we thus have an extra term of 4π .

Application to closed surfaces

It is also possible to apply the Gauss-Bonnet theorem to closed surfaces [Kre91, p. 172]. Topologically, any closed orientable surface is homeomorphic⁶ to a sphere with p attached “handles”. This number p is also called *genus* of the surface. Consequently, a sphere has genus 0, a torus genus 1, etc. One then obtains for

⁶ This means that the mapping and its inverse are continuous and bijective.

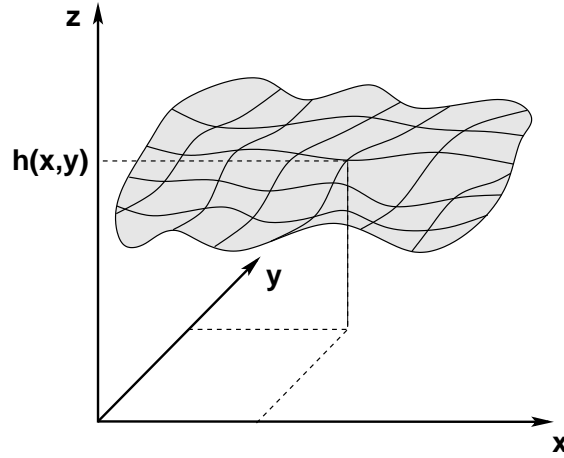


Figure B.5: Monge parametrization

any closed orientable surface Σ of genus p [Kre91, p. 172]:

$$\int_{\Sigma} dA K_G = 4\pi(1 - p) . \quad (\text{B.44})$$

This implies that the integral over the Gaussian curvature is a topological invariant for any closed surface with fixed genus p .

B.3 Monge parametrization

For surfaces with no “overhangs”, it is sufficient to describe their position in terms of a height $h(x, y)$ above the underlying reference plane as a function of the orthonormal coordinates x and y . The direction of the basis vectors $\{\mathbf{x}, \mathbf{y}, \mathbf{z}\} \in \mathbb{R}^3$ is chosen as depicted in Fig. B.5.

The tangent vectors on the surface can then be expressed as $\mathbf{e}_x = (1, 0, h_x)^T$ and $\mathbf{e}_y = (0, 1, h_y)^T$, where $h_i = \partial_i h$ ($i, j \in \{x, y\}$). The metric is equal to

$$g_{ij} = \delta_{ij} + h_i h_j , \quad (\text{B.45})$$

where δ_{ij} is the Kronecker symbol. We also define $\nabla = (\partial_x, \partial_y)^T$. The metric determinant and the infinitesimal surface element can then be written as

$$g = |g_{ij}| = 1 + (\nabla h)^2 \quad \text{and} \quad (\text{B.46})$$

$$dA = \sqrt{g} dx dy . \quad (\text{B.47})$$

The inverse metric is given by

$$g^{ij} = \delta_{ij} - \frac{h_i h_j}{g} . \quad (\text{B.48})$$

Note that Eqns. (B.45) and (B.48) are not tensor equations. The right-hand side gives merely numerical values for the components of the covariant tensors g_{ij} and g^{ij} . The unit normal vector is equal to

$$\mathbf{n} = \frac{1}{\sqrt{g}} \begin{pmatrix} -\nabla h \\ 1 \end{pmatrix} . \quad (\text{B.49})$$

With the help of Eqn. (B.20) the extrinsic curvature tensor can be calculated:

$$K_{ij} = -\frac{h_{ij}}{\sqrt{g}} , \quad (\text{B.50})$$

where $h_{ij} = \partial_i \partial_j h$. Note that Eqn. (B.50) again is not a tensor equation and gives only numerical values for the components of K_{ij} .

Finally, it is also possible to write the total curvature K in Monge parametrization:

$$K = -\nabla \cdot \left(\frac{\nabla h}{\sqrt{g}} \right) . \quad (\text{B.51})$$

In Chaps. 3, 4, and 6 we are interested in surfaces that deviate only weakly from a flat plane. In this situation the gradients h_i are small. Therefore, it is enough to consider only the lowest nontrivial order of a small gradient expansion. K and dA can then be written as

$$K = -\nabla^2 h + \mathcal{O}[(\nabla h)^2] , \quad (\text{B.52})$$

$$dA = \left\{ 1 + \frac{1}{2}(\nabla h)^2 + \mathcal{O}[(\nabla h)^4] \right\} dx dy . \quad (\text{B.53})$$

In Chap. 6 we also need K_{\perp} and K_{\parallel} and, in addition, the derivatives $\nabla_{\perp} K_{\perp}$ and $\nabla_{\perp} K_{\parallel}$ at $x = 0$ (see Fig. 5.1) in Monge parametrization. Due to the chosen orientation, the result in small gradient expansion is simply

$$K_{\perp} = -h_{xx}(0, y) , \quad (\text{B.54a})$$

$$K_{\parallel} = -h_{yy}(0, y) , \quad (\text{B.54b})$$

as well as

$$\nabla_{\perp} K_{\perp} = -h_{xxx}(0, y) , \quad (\text{B.55a})$$

$$\nabla_{\perp} K_{\parallel} = -h_{yyx}(0, y) . \quad (\text{B.55b})$$

C Surface variations

This appendix provides the first order changes of the geometry, *i. e.* g_{ab} , K_{ab} , etc., under a variation of the embedding functions

$$\mathbf{X} \rightarrow \mathbf{X} + \delta\mathbf{X} , \quad (\text{C.1})$$

where $\delta\mathbf{X}$ may be decomposed into a part tangential and a part normal to the surface:

$$\delta\mathbf{X} = \Phi^a \mathbf{e}_a + \Psi \mathbf{n} . \quad (\text{C.2})$$

The following equations and parts of the calculations can be found in [CG02b] and [CGS03].

Let us first consider the tangent vectors \mathbf{e}_a :

$$\begin{aligned} \delta\mathbf{e}_a &\stackrel{(\text{B.2})}{=} \delta(\partial_a \mathbf{X}) = \partial_a(\delta\mathbf{X}) = \nabla_a(\delta\mathbf{X}) \stackrel{(\text{C.2})}{=} \nabla_a(\Phi^a \mathbf{e}_a + \Psi \mathbf{n}) \\ &= (\nabla_a \Phi^b) \mathbf{e}_b - K_{ab} \Phi^b \mathbf{n} + (\nabla_a \Psi) \mathbf{n} + \Psi K_a^b \mathbf{e}_b , \end{aligned} \quad (\text{C.3})$$

where the Weingarten and Gauss equations (B.30) and (B.32) were used in the last step. Note also that δ and ∂_a commute due to their linearity.

Eqn. (C.3) may be decomposed into its tangential and normal parts just by collecting all terms in Φ_a and Ψ , respectively. This is also possible with the following variations.

Variation of the first fundamental form

For the variation of the metric we find

$$\begin{aligned} \delta g_{ab} &\stackrel{(\text{B.5})}{=} \mathbf{e}_a \cdot \delta\mathbf{e}_b + \delta\mathbf{e}_a \cdot \mathbf{e}_b \\ &\stackrel{(\text{C.3})}{=} \nabla_a \Phi_b + \nabla_b \Phi_a + 2K_{ab} \Psi . \end{aligned} \quad (\text{C.4})$$

Varying Eqn. (B.7) yields $g_{ac} \delta g^{cb} + \delta g_{ac} g^{cb} = 0$. From this follows that the variation of the inverse metric is given by

$$\delta g^{ab} = -g^{ac} g^{bd} \delta g_{cd} \stackrel{(\text{C.4})}{=} -\nabla^a \Phi^b - \nabla^b \Phi^a - 2K^{ab} \Psi . \quad (\text{C.5})$$

To proceed, one needs to calculate the derivative of the metric determinant with respect to g_{ab} . For that purpose, consider first quite generally a symmetric $n \times n$

matrix \mathbf{M} . It can be diagonalized with its eigenvalues M_1, \dots, M_n being the diagonal elements: $\mathbf{M} = \mathbf{T}\mathbf{M}_D\mathbf{T}^{-1}$ where \mathbf{M}_D is the diagonal matrix. From this follows:

$$\begin{aligned} \log(\det \mathbf{M}) &= \log[\det(\mathbf{T}\mathbf{M}_D\mathbf{T}^{-1})] = \log(M_1 \cdot M_2 \cdot \dots \cdot M_n) \\ &= \sum_{i=1}^n \log M_i = \text{Tr}(\log \mathbf{M}_D) = \text{Tr}[\log(\mathbf{T}^{-1}\mathbf{M}\mathbf{T})] \\ &= \text{Tr}[\mathbf{T}^{-1} \log(\mathbf{M})\mathbf{T}] = \text{Tr}(\log \mathbf{M}) . \end{aligned} \quad (\text{C.6})$$

Thus,

$$\begin{aligned} \frac{\partial g}{\partial g_{ab}} &= \frac{\partial \det \mathbf{g}}{\partial g_{ab}} = \frac{\partial}{\partial g_{ab}} \left\{ \exp[\log(\det \mathbf{g})] \right\} \stackrel{(\text{C.6})}{=} \frac{\partial}{\partial g_{ab}} \left\{ \exp[\text{Tr}(\log \mathbf{g})] \right\} \\ &= \left\{ \exp[\text{Tr}(\log \mathbf{g})] \right\} \frac{\partial}{\partial g_{ab}} [\text{Tr}(\log \mathbf{g})] = g \text{Tr} \left[\frac{\partial}{\partial g_{ab}} (\log \mathbf{g}) \right] \\ &= g \text{Tr} \left[\mathbf{g}^{-1} \frac{\partial \mathbf{g}}{\partial g_{ab}} \right] = gg^{cd} \frac{\partial g_{dc}}{\partial g_{ab}} = gg^{ab} . \end{aligned} \quad (\text{C.7})$$

The determinant of the metric then changes as follows

$$\delta g = \frac{\partial g}{\partial g_{ab}} \delta g_{ab} = gg^{ab} \delta g_{ab} = 2g(\nabla_a \Phi^a + K\Psi) , \quad (\text{C.8})$$

which yields for \sqrt{g}

$$\delta \sqrt{g} = \frac{1}{2\sqrt{g}} \delta g = \sqrt{g}(\nabla_a \Phi^a + K\Psi) , \quad (\text{C.9})$$

and finally for the infinitesimal area element:

$$\delta(dA) = dA(\nabla_a \Phi^a + K\Psi) . \quad (\text{C.10})$$

Variation of the second fundamental form

The variation of the normal vector \mathbf{n} may be obtained from Eqns. (B.4):

$$\mathbf{e}_a \cdot \delta \mathbf{n} = -\mathbf{n} \cdot \delta \mathbf{e}_a , \quad (\text{C.11})$$

$$\text{and } \mathbf{n} \cdot \delta \mathbf{n} = 0 . \quad (\text{C.12})$$

It follows:

$$\delta \mathbf{n} \stackrel{(\text{C.3})}{=} K_{ab} \Phi^a g^{bc} \mathbf{e}_c - (\nabla_a \Psi) g^{ab} \mathbf{e}_b , \quad (\text{C.13})$$

and

$$\begin{aligned} \delta K_{ab} &\stackrel{(\text{B.21})}{=} -(\delta \mathbf{n}) \cdot \nabla_a \mathbf{e}_b - \mathbf{n} \cdot \nabla_a \delta \mathbf{e}_b \\ &\stackrel{(\text{C.3})}{=} -\mathbf{n} \cdot \nabla_a [(\nabla_b \Phi^c) \mathbf{e}_c - K_{bc} \Phi^c \mathbf{n} + (\nabla_b \Psi) \mathbf{n} + \Psi K_b^c \mathbf{e}_c] \\ &\stackrel{(\text{B.35})}{=} \Phi^c \nabla_c K_{ab} + K_{ac} \nabla_b \Phi^c + K_{bc} \nabla_a \Phi^c - \nabla_a \nabla_b \Psi + K_{ac} K_b^c \Psi . \end{aligned} \quad (\text{C.14})$$

The first term in the first line is equal to zero: $-(\delta\mathbf{n})\cdot\nabla_a\mathbf{e}_b \stackrel{(B.32)}{=} -K_{ab}(\delta\mathbf{n})\cdot\mathbf{n} \stackrel{(C.12)}{=} 0$. Note also that the Weingarten and Gauss equations (B.30) and (B.32) were applied in the last step.

For the total curvature this gives:

$$\begin{aligned} \delta K &\stackrel{(B.26)}{=} \delta g^{ab} K_{ab} + g^{ab} \delta K_{ab} \\ &\stackrel{(C.5),(C.14)}{=} (-\nabla^a\Phi^b - \nabla^b\Phi^a - 2K^{ab}\Psi)K_{ab} \\ &\quad + g^{ab}(\Phi^c\nabla_c K_{ab} + K_{ac}\nabla_b\Phi^c + K_{bc}\nabla_a\Phi^c - \nabla_a\nabla_b\Psi + K_{ac}K_b^c\Psi) \\ &= \Phi^c\nabla_c K - \Delta\Psi - K_{ab}K^{ab}\Psi . \end{aligned} \tag{C.15}$$

Note in particular that for the normal variation this reduces to

$$\delta_\perp K = -(\Delta + K_{ab}K^{ab})\Psi . \tag{C.16}$$

Further variations

The volume of an object (*e.g.* a soap bubble, see Sec. 1.1.2) may be written as a surface integral with help of Gauss' Theorem

$$V = \int_V dV' = \int_V dV' \frac{\nabla\cdot\mathbf{X}}{3} = \frac{1}{3} \int_{\partial V} dA \mathbf{n}\cdot\mathbf{X} . \tag{C.17}$$

To first order, tangential variations only correspond to a reparametrization and therefore cancel (as one can easily check). The variation of the volume yields (see Eqns. (C.2), (C.9) and (C.13))

$$\begin{aligned} \delta V &= \delta_\perp V = \frac{1}{3} \int_{\partial V} d^2\xi [(\delta_\perp\sqrt{g}) \mathbf{n}\cdot\mathbf{X} + \sqrt{g} (\delta_\perp\mathbf{n})\cdot\mathbf{X} + \sqrt{g} \mathbf{n}\cdot(\delta_\perp\mathbf{X})] \\ &= \frac{1}{3} \int_{\partial V} dA [(K\Psi) \mathbf{n}\cdot\mathbf{X} - (\nabla_a\Psi)g^{ab}\mathbf{e}_b\cdot\mathbf{X} + \mathbf{n}\cdot(\Psi\mathbf{n})] . \end{aligned} \tag{C.18}$$

An integration by parts of the second term and use of the Gauss equations (B.32) simplifies Eqn. (C.18):

$$\begin{aligned} \delta V &= \frac{1}{3} \int_{\partial V} dA \{(K\Psi) \mathbf{n}\cdot\mathbf{X} + [-(K\Psi) \mathbf{n}\cdot\mathbf{X} + \underbrace{\Psi g^{ab}\mathbf{e}_b\cdot\nabla_a\mathbf{X}}_{=g^{ab}g_{ba}=2}] + \Psi\} \\ &= \int_{\partial V} dA \Psi . \end{aligned} \tag{C.19}$$

Generally, any scalar function \mathcal{F} defined on the surface varies under a tangential deformation like [CG02b]

$$\delta_\parallel\mathcal{F} = \Phi^a\partial_a\mathcal{F} = \Phi^a\nabla_a\mathcal{F} . \tag{C.20}$$

Application: The formula of Laplace

We want to perform a normal variation of Hamiltonian (1.9) in Sec. 1.1.2:

$$H = \int_{\partial V} dA \sigma - P(V - V_0) . \quad (\text{C.21})$$

Exploiting the results of this appendix, one gets in equilibrium ($\delta_{\perp} H = 0$)

$$\delta_{\perp} H = \int_{\partial V} (\delta_{\perp} dA) \sigma - P \delta_{\perp} V \stackrel{(\text{C.10}), (\text{C.19})}{=} \int_{\partial V} dA \Psi(\sigma K - P) \stackrel{!}{=} 0 \quad (\text{C.22})$$

which yields the *formula of Laplace*

$$P = \sigma K . \quad (\text{C.23})$$

List of Tables

- 1.1 Surface tension for selected substances at room temperature 6
 - (a) against air 6
 - (b) against water 6
- 1.2 Examples of surfactants 8
- 1.3 Self-assembly: structures and appropriate packing parameters 12
- 1.4 Examples of membrane lipids 14

- 2.1 Euler-Lagrange derivative $\mathcal{E}(\mathcal{H})$ and the components of the stress tensor \mathbf{f}^a for several simple scalar surface Hamiltonian densities \mathcal{H} 29

- 4.1 Sign of interaction between two identical colloids depending on inter-face type and colloidal shape 46

List of Figures

| | | |
|-----|--|----|
| 1 | Attraction of two sewing needles on water | 2 |
| 1.1 | Energetics of interfaces | 4 |
| 1.2 | Surface tension | 5 |
| 1.3 | The soap film: a minimum area surface | 7 |
| 1.4 | Structure | 7 |
| | (a) of a soap solution | 7 |
| | (b) of a soap film | 7 |
| 1.5 | The soap bubble: a constant mean curvature surface | 9 |
| 1.6 | Computer simulation of a coarse grained lipid bilayer | 13 |
| 1.7 | The cell membrane | 15 |
| 2.1 | Components of the stress tensor | 18 |
| | (a) in 3D | 18 |
| | (b) in 2D | 18 |
| 2.2 | Curved surface domain | 19 |
| 3.1 | Balance of forces at the three-phase boundary solid/liquid/gas | 32 |
| 3.2 | Geometry of a liquid drop on a flat solid substrate | 33 |
| 3.3 | Sewing needle floating on water | 34 |
| 3.4 | Sphere floating on a liquid | 37 |
| 3.5 | Pinning of the contact line | 39 |
| 3.6 | Sphere adhering to a fluid membrane | 42 |
| 4.1 | Two identical particles bound to an interface | 48 |
| 4.2 | Interaction of two quadrupoles on water | 49 |
| 5.1 | Interface mediated force as a closed line integral of the surface stress tensor | 52 |
| 5.2 | Illustration of the geometry of a symmetric and an antisymmetric two-particle attachment | 53 |
| 5.3 | Two cylinders at opposite interface sides | 55 |
| 6.1 | Coordinates chosen for one quadrupole | 58 |
| 6.2 | Two quadrupoles on a soap film | 59 |

List of Figures

| | | |
|-----|--|----|
| 6.3 | Two cylindrical colloids adhering to a membrane | 61 |
| 6.4 | Contact angles α_A and α_B | 63 |
| 6.5 | Two discoidal inclusions separated by a distance d | 64 |
| 7.1 | Three-body interactions | 68 |
| B.1 | Parametrization of a surface | 76 |
| B.2 | Local frame on the surface | 76 |
| B.3 | Curve on a surface | 79 |
| B.4 | Integration contour for multiply connected surface patches | 83 |
| B.5 | Monge parametrization | 84 |

Acknowledgements

This thesis would not have been possible without the help and encouragement of many other people. First of all, I would like to thank Prof. Kurt Kremer for inviting me to become a member of his group and giving me the possibility to do research in an inspiring and stimulating environment. I am very grateful to my supervisor Markus Deserno who suggested the interesting field of interface mediated interactions for my thesis. He always had time for discussions and encouraged me to follow my own scientific ideas.

He also introduced me to Jemal Guven with whom we worked together. I have to say many thanks for his help: he almost always had an answer whenever formal questions concerning the stress tensor emerged.

Furthermore, I want to thank many of my colleagues: my office mates Pim Schravendijk and Maeng-Eun Lee for cheering me up, also during harder times, and Christian Nowak for enjoying nice tea sessions during the breaks; Ira Cooke and Andrea Corsi for trying to improve my English as far as this was possible. Bernward Mann and Axel Arnold always had time for questions concerning math and computers. Denis Andrienko gave me a kickstart to surface evolver and also provided the very first file that was a good starting point for creating pictures.

Thanks also to the IT team, Torsten Stühn and Harald Bopp, and especially to Timo Schürg who explained me the basics of POV-ray in half a day.

Doris Kirsch, the secretary of our group, was the good heart in the background that helped whenever organisational or problems of different nature arose.

Finally, I would like to thank my family and friends for their support.

Acknowledgements

Bibliography

- [BF03] D. Bartolo and J.-B. Fournier. Elastic interaction between “hard” or “soft” pointwise inclusions on biological membranes. *Eur. Phys. J. E*, 11: pp. 141–146, 2003.
- [BGK03] H.-J. Butt, K. Graf, and M. Kappl. *Physics and Chemistry of Interfaces*. Wiley-VCH, Weinheim, Germany, 2003.
- [BM93] G. Brezesinski and H.-J. Mögel. *Grenzflächen und Kolloide*. Spektrum Akademischer Verlag, Heidelberg, Germany, 1993.
- [Bra04] K. Brakke. The Surface Evolver. <http://www.susqu.edu/facstaff/b/brakke/evolver/evolver.html>, 2004.
- [Can70] P. B. Canham. The Minimum Energy of Bending as a Possible Explanation of the Biconcave Shape of the Human Red Blood Cell. *J. Theoret. Biol.*, 26: pp. 61–81, 1970.
- [CG02a] R. Capovilla and J. Guven. Geometry of lipid vesicle adhesion. *Phys. Rev. E*, 66: 041604, 2002.
- [CG02b] R. Capovilla and J. Guven. Stresses in lipid membranes. *J. Phys. A: Math. Gen.*, 35: pp. 6233–6247, 2002.
- [CGS03] R. Capovilla, J. Guven, and J. A. Santiago. Deformations of the geometry of lipid vesicles. *J. Phys. A: Math. Gen.*, 36: pp. 6281–6295, 2003.
- [DB03] M. Deserno and T. Bickel. Wrapping of a spherical colloid by a fluid membrane. *Europhys. Lett.*, 62(5): pp. 767–773, 2003.
- [Des04] M. Deserno. Elastic deformation of a fluid membrane upon colloid binding. *Phys. Rev. E*, 69: 031903, 2004.
- [DGR02] J. K. G. Dhont, G. Gompper, and D. Richter, editors. *Soft matter*, volume 10 of *Matter and Materials*. Forschungszentrum Jülich GmbH, Jülich, Germany, 2002.

- [DH01] M. Deserno and C. Holm. Cell model and Poisson-Boltzmann theory: A brief introduction. In C. Holm, P. Kékicheff, and R. Podgornik, editors, *Electrostatic Effects in Soft Matter and Biophysics*, volume 46 of *NATO Science Series: II. Mathematics, Physics and Chemistry*. Kluwer Academic Publishers, Dordrecht, The Netherlands, 2001.
- [DPS93] N. Dan, P. Pincus, and S. A. Safran. Membrane-Induced Interactions between Inclusions. *Langmuir*, 9: pp. 2768–2771, 1993.
- [FG97] J.-B. Fournier and P. Galatola. Tubular vesicles and effective fourth-order membrane elastic theories. *Europhys. Lett.*, 39(2): pp. 225–230, July 1997.
- [FG02] J.-B. Fournier and P. Galatola. Anisotropic capillary interactions and jamming of colloidal particles trapped at a liquid-fluid interface. *Phys. Rev. E*, 65: 031601, 2002.
- [GBP93] M. Goulian, R. Bruinsma, and P. Pincus. Long-Range Forces in Heterogeneous Fluid Membranes. *Europhys. Lett.*, 22(2): pp. 145–150, 1993. See also: Erratum in *Europhys. Lett.*, 23(2): p. 155, 1993.
- [GFS03] P. Galatola, J.-B. Fournier, and H. Stark. Interaction and flocculation of spherical colloids wetted by a surface-induced corona of paranematic order. *Phys. Rev. E*, 67: 031404, 2003.
- [GH96] R. Goetz and W. Helfrich. The Egg Carton: Theory of a Periodic Superstructure of Some Lipid Membranes. *J. Phys. II France*, 6: pp. 215–223, February 1996.
- [GKD⁺04] G. Gompper, U. B. Kaupp, J. K. G. Dhont, D. Richter, and R. G. Winkler, editors. *Physics meets Biology*, volume 19 of *Matter and Materials*. Forschungszentrum Jülich GmbH, Jülich, Germany, 2004.
- [GS71] W. A. Gifford and L. E. Scriven. On the attraction of floating particles. *Chem. Eng. Sci.*, 26: pp. 287–297, 1971.
- [Guv04a] J. Guven. Membrane geometry with auxiliary variables and quadratic constraints. *J. Phys. A: Math. Gen.*, 37: L313–L319, 2004.
- [Guv04b] J. Guven. Personal communication, 2004.
- [Hel73] W. Helfrich. Elastic Properties of Lipid Bilayers: Theory and Possible Experiments. *Z. Naturforsch.*, 28 c: pp. 693–703, 1973.
- [Ise92] C. Isenberg. *The science of soap films and soap bubbles*. Dover, Mineola, NY, 1992.

-
- [Isr92] J. N. Israelachvili. *Intermolecular and Surface Forces*. Academic Press, London, U.K. - San Diego, CA, second edition, 1992.
- [Jac75] J. D. Jackson. *Classical Electrodynamics*. John Wiley & Sons, New York, NY, second edition, 1975.
- [KIH98] S. L. Keller, W. H. Pitcher III, W. H. Huestis, and H. M. McConnell. Red Blood Cell Lipids Form Immiscible Liquids. *Phys. Rev. Lett.*, 81(22): pp. 5019–5022, November 1998.
- [KN94] P. A. Kralchevsky and K. Nagayama. Capillary Forces between Colloidal Particles. *Langmuir*, 10: pp. 23–36, 1994.
- [Kre91] E. Kreyszig. *Differential geometry*. Dover, Mineola, NY, 1991.
- [KRS99] I. Koltover, J. O. Rädler, and C. R. Safinya. Membrane Mediated Attraction and Ordered Aggregation of Colloidal Particles Bound to Giant Phospholipid Vesicles. *Phys. Rev. Lett.*, 82(9): pp. 1991–1994, 1999.
- [LFL01] P. Lenz, W. Fenzl, and R. Lipowsky. Wetting of ring-shaped surface domains. *Europhys. Lett.*, 53(5): pp. 618–624, 2001.
- [LL86] L. D. Landau and E. M. Lifschitz. *Theory of Elasticity*. Butterworth-Heinemann, Oxford, U.K., third edition, 1986.
- [MDG04] M. M. Müller, M. Deserno, and J. Guven. Geometry of surface mediated interactions. To appear in: *Europhys. Lett.*, 69(3): pp. 482–488, 2005. See also: *arXiv:cond-mat/0409043*, September 2004.
- [MH01] C. E. Morris and U. Homann. Cell Surface Area Regulation and Membrane Tension. *J. Membrane Biol.*, 179: pp. 79–102, 2001.
- [MM02] V. I. Marchenko and C. Misbah. Elastic interaction of point defects on biological membranes. *Eur. Phys. J. E*, 8: pp. 477–484, 2002.
- [Nic49] M. M. Nicolson. The interaction between floating particles. *Proc. Cambridge Philos. Soc.*, 45: pp. 288–295, 1949.
- [NS03] A. V. Nguyen and H. J. Schulz, editors. *Colloidal Science of Flotation*, volume 118 of *Surfactant Science Series*. Marcel Dekker, New York, NY, 2003.
- [PSLW97] P. Poulin, H. Stark, T. C. Lubensky, and D. A. Weitz. Novel Colloidal Interactions in Anisotropic Fluids. *Science*, 275: pp. 1770–1773, March 1997.

- [RSS89] W. N. Russel, D. A. Saville, and W. R. Schowalter. *Colloidal Dispersions*. Cambridge University Press, Cambridge, U.K., 1989.
- [RW02] J. S. Rowlinson and B. Widom. *Molecular Theory of Capillarity*. Dover, Mineola, NY, 2002.
- [Saf94] S. A. Safran. *Statistical thermodynamics of surfaces, interfaces and membranes*, volume 90 of *Frontiers in physics*. Perseus, Cambridge, MA, first edition, March 1994.
- [SBL91] U. Seifert, K. Berndl, and R. Lipowsky. Shape transformation of vesicles: Phase diagram for spontaneous-curvature and bilayer-coupling models. *Phys. Rev. A*, 44(2): pp. 1182–1202, July 1991.
- [SDJ00] D. Stamou, C. Duschl, and D. Johannsmann. Long-range attraction between colloidal spheres at the air-water interface: The consequence of an irregular meniscus. *Phys. Rev. E*, 62: pp. 5263–5272, 2000.
- [SI97] K. Simons and E. Ikonen. Functional rafts in cell membranes. *Nature*, 387: pp. 569–572, June 1997.
- [VM04] D. Vella and L. Mahadevan. The ‘Cheerios effect’. *arXiv:cond-mat/0411688*, November 2004.
- [Wei03] T. R. Weigl. Indirect interactions of membrane-adsorbed cylinders. *Eur. Phys. J. E*, 12: pp. 265–273, 2003.
- [WKH98] T. R. Weigl, M. M. Kozlov, and W. Helfrich. Interaction of conical membrane inclusions: Effect of lateral tension. *Phys. Rev. E*, 57(6): pp. 6988–6995, 1998.